STUDY OF ENVIRONMENTALLY SENSITIVE POLYMERIC CARRIERS FOR CONTROLLED DRUG DELIVERY

LIU SHAOQIONG

A THESIS SUBMITTED

FOR THE DEGREE OF DOCTOR OF PHILOSOPHY

DEPARTMENT OF CHEMICAL AND BIOMOLECULAR ENGINEERING

NATIONAL UNIVERSITY OF SINGAPORE

2005

ACKNOWLEDGEMENTS

I would like to express my deepest appreciation to my supervisors, Dr. Yang Yi Yan and Dr. Tong Yen Wah, for their guidance and advice I have received from them during the course of my research study.

It is also my pleasure to express my gratitude to all the staff and students in our controlled release group. For their friendship, helps, and encouragement, my heartfelt thanks are due to Ms Wan, J. P., Ms. Shi, M., Ms Wang, L., Ms. Wang, M.Y., Mr. Wang Y., Dr. Soppimath, K. and Dr. Chaw, C. S..

In addition, I would acknowledge National University of Singapore (NUS) for providing me this opportunity to pursue my PhD degree and the research scholarship, and Institute of Bioengineering and Nanotechnology (IBN) of Singapore for providing laboratory space and equipment, which have made this research possible.

I am indebted to my husband and my parents for their support, expectation and encouragement, which are an important part behind the work.

TABLE OF CONTENTS

SUMMARY

Poly(*N*-isopropylacrylamide) (PNIPAAm) is a well-known temperature-sensitive polymer and has a transition temperature (T_{tr}) or lower critical solution temperature (LCST) of about 32°C. PNIPAAm has been widely investigated in biotechnology, medical diagnosis, and drug delivery. However, few degradable or pH-triggered drug delivery systems have been reported. The aim of this study was to design biodegradable and environmentally sensitive microspheres and micelles for controlled delivery of bioactive agents.

Firstly, PNIPAAm-*b*-PLA microspheres containing bovine serum albumin (BSA, as a model protein) were fabricated using a water-in-oil-in-water double emulsion solvent evaporation method. BSA was well entrapped within the microspheres. High encapsulation efficiency (over 80%) was achieved. The *in vitro* degradation behavior of microspheres was investigated. It was found that the microspheres were erodible, and polymer degradation occurred in the PLA block. A PVA concentration of 0.2% (w/v) in the internal aqueous phase yielded microspheres with an inter-connected porous structure, leading to fast matrix erosion and sustained BSA release. BSA release was faster at the temperature below the LCST. In addition, microspheres fabricated with PNIPAAm-*b*-PLA having 1:5 molar ratio of PNIPAAm to PLA and a PVA concentration of 0.2% (w/v) in the internal aqueous phase were able to provide a sustained release of BSA over three weeks in PBS (pH 7.4) at 37ºC.

P(NIPAAm-*co*-DMAAm)-*b*-PLGA with different PLGA contents as well as different LG ratios were synthesized, and used to fabricate micelles for targeted delivery of

doxorubicin (DOX) and paclitaxel using a membrane dialysis method. The micelles prepared from the block copolymer had a very low CAC value in both water and PBS buffer (pH 7.4). Drug loading level depended on the balance between hydrophilic and hydrophobic block. The TEM morphologies showed that micelles were spherical and had a uniform size distribution, which is consistent with the particle size analysis by dynamic light scattering. The LCST of the micelles in PBS was above 37ºC. In particular, it is determined by the shell instead of the core. The micelles were stable in both PBS and PBS containing 10% FBS at 37ºC. Drug release from the micelles was responsive to external temperature changes. Drug release was much faster at a temperature above the LCST than at body temperature. Drug-loaded micelles showed higher cytotoxicity against cancer cells at a temperature above the LCST. The IC_{50} of drug-loaded micelles also depended on the nature of drugs and cells.

In addition, pH-triggered temperature sensitive block copolymer, folate-conjugated poly(NIPAAm-*co*-DMAAm-*co*-MAm)-*b*-PUA was synthesized, and utilized to fabricate micelles for intracellular delivery of anticancer drugs to tumours. The mean diameters of the empty and DOX-loaded micelles were less than 100 nm. The lower critical solution temperature (LCST) of the micelles and *in vitro* drug release were pH-dependent. DOX-loaded folate-conjugated micelles were taken up rapidly by cancer cells *via* endocytosis. DOX-loaded micelles killed cancer cells efficiently. DOX micelles had a longer circulation time in the blood. More importantly, the enhanced accumulation of DOX in tumors using the micelles would lead to higher efficacy for cancer therapy.

List of Tables

LIST OF FIGURES

NOMENCLATURE

Notation

Mw	Molecular weight (weight average)
Mn	Molecular weight (number average)

Abbreviation

AFM	Atomic force microscopy
BSA	Bovine serum albumin
CLSM	Confocal laser scanning microscope
DCM	Dichloromethane
DMF	N,N, -dimethylformamide
DMSO	Dimethyl sulfoxid
DOX	Doxorubicin
DSC	Differential scanning calorimetry
FBS	Fetal bovine serum
FTIR	Fourier transform infrared spectrophotometer
GPC	Gel permeation chromatography
HPLC	High performance liquid chromatography
MTT	3-(4,5-dimethyl-2-thiazolyl)-2,5-diphenyl-2H tetrazolium bromide
PBS	Phosphate buffer solution
PEG	Poly (ethylene glycol)

PLGA	Poly(D,L-lactic-co-glylic acid)
POE	Poly(ortho ester)
PVA	Poly (vinyl alcohol)
SDS-PAGE	Sodium dodecyl sulphate-polyacrylamide gel electrophoresis
SEM	Scanning electron microscope
THF	Tetrahydrofuran
UV	Ultraviolet
XPS	X-ray photoelectron spectroscope

CHAPTER ONE

INTRODUCTION

Many of the pharmacological properties of free drugs can be improved through the use of drug delivery system (DDS) (Allen and Cullis, 2004). It was reported that the world market of advanced drug delivery system is currently valued at $50 billion a year, occupying 12.5% of world total pharmaceutical sales. Some examples of free drugs that can be improved by the use of DDS are listed in Table 1.1 (Allen and Cullis, 2004). There are various types of drug delivery systems, among which polymeric drug delivery systems (PDDS) have been designed to deliver drugs in a predetermined manner (Robinson and Lee, 1990). These systems possess one or more of the following advantages over conventional drug formulations: firstly, it is designed to deliver unstable and/or insoluble drugs with predetermined therapeutic rate for a predefined period of time by maintaining a relatively constant, effective drug level in the body with concomitant minimization of undesirable side effects; secondly, it can localize the drugs to be released by spatial placement of a controlled release system adjacent to or in the diseased tissue or organ; thirdly, it can be designed to target the drug to specific tissues or organs; finally, it is easy to process and its chemical and physical properties is readily controlled *via* molecular synthesis. To date, many PDDS, such as reservoir devices (Lehmann et al., 1979), monolithic devices (Davis and Illum, 1988), polymeric colloidal particles (Yang and Wan et al., 2001; Bittner et al., 1999; Couvreur and Puisieux, 1993; Govender et al., 1999; Lu and Yeh et al., 2004) (microparticles, microspheres and nanoparticles), micelles (Yokoyama and Miyauchi et al., 1990; Toncheva et al., 2003) and polymer-drug conjugate (Yoo and Oh et al., 1999), have been developed and reported. Of these systems, microspheres and micelles are particularly of interest due to their controllable properties.

The use of micropheres involves the encapsulation of a pharmaceutical product within a polymer matrix by microencapsulation techniques (Mathiowitz et al., 1999). They are usually spherical with a size range from 1-250 μm. The polymer can be natural or synthetic, non-degradable or biodegradable. For non-degradable micropsheres, the drug release is diffusion-controlled. However, most research is aimed at investigating biodegradable polymer systems, which degrade into biologically acceptable compounds, often through the process of hydrolysis, and leaving their incorporated drugs in the targeted area. Examples of such polymers include polyester (Li and Vert, 1999), poly(phosphoesters) (Mao et al., 1999) and poly(ortho ester)s (Heller and Gurny, 1999). By varying the polymer composition, microstructure and the rate of matrix degradation, subsequently, drug release can be controlled.

However, a major problem with microspheres is the non-specific uptake by the reticuloendothelial system (RES) (Kwon and Kataoka, 1995). In addition, microspheres could be very large and not suitable for injection. To overcome these problems, polymeric micelles have been proposed. They are only tens of nanometers in diameter and thus avoid the scavenging by the RES. Moreover, they have enhanced vascular permeability and retention (EPR) through tumor tissues compared to healthy tissue (Torchilin, 2001). Micelles self-assembling from amphiphilic polymer in aqueous solution are generally characterized by a core-shell structure (Jones and Leroux, 1999). The core consists of a hydrophobic block and acts as the reservoir for insoluble drugs. The shell consists of a hydrophilic block and is responsible for the micelle stabilization and interaction with plasmatic proteins and cell membranes. Finally, drug release is

achieved *via* diffusion and polymer degradation mechanisms. For example, Kataoka and his co-workers have investigated the use of polymer micelles as a means of delivering doxorubicin (DOX, an anticancer agent). The results showed that the system could effectively deliver the drugs to a solid cancerous tumor *via* EPR effect, showing much stronger activity than the free DOX (Nakanishi et al., 2001). The EPR effect is considered as a passive targeting method, but the drug targeting can be further enhanced by the introduction of an active targeting agent (e.g., environmental stimuli or cell-specific targeting signal) controlled by the polymer design. With such multiple targeting functions, drug release is induced only at a therapeutic site by external stimuli after drug carriers accumulate at a solid tumor site by a passive targeting mechanism utilizing the EPR effect and avoidance of the RES.

The polymer used in these drug delivery systems acts as a carrier and a protective agent for an active drug during the transportation process until the drug is released in the body. Therefore, selecting a suitable polymer is critical for this system. Recently, smart polymers, which respond to small external stimulus changes such as temperature (Yokoyama and Okano et al., 1996), pH (Siegel et al., 1988), electric field (Sawahata et al., 1990) and magnetic field (Kost and Langer, 1991), have been developed for biological applications (Kost and Langer, 1991). The drug release rate of such responsive polymeric systems can be adjusted in response to physiological need. Among these systems, temperature sensitive delivery system based on a temperature sensitive polymer, poly(*N*-isopropylacrylamide) (PNIPAAm), is one of the most promising approaches for controlled drug delivery. PNIPAAm is a well-known thermo-responsive polymer and

shows remarkable hydration-dehydration properties in response to small temperature changes. This transition is referred to as lower critical solution temperature (LCST). The LCST of PNIPAAm is about 32°C (Heskins and Guillet, 1968), but it can be modified by incorporation of hydrophilic or hydrophobic comonomers (Kaneko and Nakamura, 1999). This unique property is very important for practical applications. This is because the body temperature often deviates from normal temperature (37°C) in the physiological presence of pathogens or pyrogens (You and Ick, 1998). This variation during illness as well as external controlled temperature changes can be a useful stimulus that activates the release of therapeutic agents from the temperature responsive drug carriers. Therefore, thermo-responsive carriers play an important role in drug delivery.

However, temperature sensitive micelles may not be easily accessible to deep organs or tumors (Soppimath et al., 2005). An alternative approach to targeting drugs to tumor tissues is to use pH-triggered temperature sensitive carriers. The pH values of disease sites such as tumor tissues are significantly lower (pH 7.0 in the tumor tissue, pH 5.0-6.0 in endosome and pH 4-5 in lysosomes) than under normal physiological conditions (pH 7.4) (Haag, 2004). The polymer carriers remain intact until they have reached tumor tissue or been taken up by a cell, subsequently, these carriers release drug under low pH conditions (Van et al., 2003). Thus, the drug targeting to disease sites can be further improved by combining temperature sensitivity and pH sensitivity.

The purpose of this research was to systematically study biodegradable and environmentally sensitive (temperature sensitive as well as pH-triggered temperature

sensitive) drug carriers and to explore their applications in drug delivery. This objective is implemented by three approaches. Firstly, PNIPAAm-*b*-PLA (poly(*N*-isopropylacrylamide)-*b*-poly(D,L-lactide)) block copolymers were synthesized and used to prepare BSA (Bovine Serum Albumin) -loaded microspheres, the degradation and *in vitro* protein release were investigated. Secondly, P(NIPAAm-*co*-DMAAm)-*b*-PLGA (poly(*N*-isopropylacrylamide-*co*-*N,* *N*-dimethylacrylamide)-*b*-poly(D,L-lactide-*co*-glycolide)) block copolymers with various compositions were synthesized. Model anticancer drugs, doxorubicin (DOX) and paclitaxel were loaded into the micelles using these polymers. Physicochemical properties, *in vitro* drug release as well as cytotoxicity against various cell lines were investigated and compared. Thirdly, a multifunctional polymer, folate-conjugated poly(*N*-isopropylacrylamide-*co*-*N,N*-dimethylacrylamide-*co*-methacrylate)-*b*-poly(10-undecenoic acid) was synthesized, and used to fabricate DOX-loaded micelles for specific and intracellular delivery of anticancer drugs to tumor cells.

The results obtained from this work provided an optimal process for developing biodegradable and environmentally sensitive polymer drug carriers with high encapsulation efficiency. It also provided a clear explanation of degradation mechanism of such drug carriers, which is useful for exploring their potential *in vivo* applications. In addition, *in vitro* drug release and *in vitro* cytotoxicity studies showed that the drug-loaded micelles are environmentally responsive. Furthermore, the enhanced accumulation in tumors and longer circulation of DOX using DOX-loaded micelles made from folate-conjugated poly(*N*-isopropylacrylamide-*co*-*N,* *N*-dimethylacrylamide-*co*-methacrylate)-*b*-poly(10-undecenoic acid) may result in a higher efficacy for cancer

therapy. Finally, the environmentally sensitive drug release from such drug carriers may improve therapeutic efficiency clinically.

The following chapter provides a brief summary of basic properties and the results of some recent research work on polymeric drug delivery system. The polymer properties, some science and technical aspects on drug carriers as well as their applications in protein delivery and anticancer drug delivery will be described.

Table 1.1 Non-ideal properties of drugs and their therapeutic implications

Problem	Implication	Effect of DDS
Poor solubility	A convenient pharmaceutical format is difficult to achieve, as hydrophobic drugs may precipitate in aqueous media. Toxicities are associated with the use of excipients such as cremphor (the solubilizer for paclitaxel in Taxol).	DDS such as lipid micelles or liposomes provide both hydrophilic and hydrophobic environments, enhancing drug solubility.
Tissue damage on extravasation	Inadvertent extravasation of cytotoxic drugs leads to tissue damage, e.g. tissue necrosis with free doxorubicn.	Regulated drug release from the DDS can reduce or eliminate tissue damage on accidental extravasation.
Rapid breakdown of the drug *in vivo*	Loss of activity of the drug follows administration, e.g. loss of activity of camptothecins at physiological pH	DDS protects the drug from premature degradation and functions as a sustained release system. Lower doses of drug are required.
Unfavorable pharmacokinetics	Drug is cleared too rapidly, by the kidney, for example, requiring high doses or continuous infusion.	DDS can substantially alter the pK of the drug and reduce clearance, rapid renal clearance of small molecules is avoided.
Poor biodistribution	Drugs that have widespread distribution in the body can affect normal tissues, resulting in dose-limiting side effects, such as the cardiac toxicity of doxorubicin	The particulate nature of DDS lowers the volume of distribution and helps to reduce side effects in sensitive, nontarget tissues.
Lack of selectivity for target tissues	Distribution of the drug to normal tissues leads to side effects that restrict the amount of drugs that can be administrated. Low concentrations of drugs in target tissues will result in suboptimal therapeutic effects.	DDS can increase drug concentrations in diseased tissues such as tumors by the EPR effect. Ligand-mediated targeting of the DDS can further improve drug specificity.

CHAPTER TWO

LITERATURE REVIEW

Controlled drug delivery systems have an enormous impact on pharmaceutical technology. They greatly improve the performance of many existing drugs and enable the use of entirely new therapies. Such systems are designed to have following functions. Firstly, they attempt to maintain the drug in the desired therapeutic range by a single administration. Secondly, they attempt to preserve drugs from being rapidly destroyed by the body, which is very important for biologically sensitive molecules such as proteins and peptides. Thirdly, they allow localized delivery of the drug to a particular body compartment. Other advantages include the reduced need for follow-up care, increased comfort and improved compliance (Robinson and Lee, 1999).

Among various drug delivery systems, polymer-based drug delivery system (PDDS) is one of the most effective and efficient approaches (Gombotz and Pettie, 1995; Sinha and Khosla, 1998; Langer, 1998). The concept of PDDS is that it consists of a drug and a polymeric carrier capable of delivering the drug to a specific site where the drug is to be released from the carrier. Although other controlled delivery systems have some similar advantages as mentioned above, potential disadvantages do exist. For instance, the materials may be toxic or non-biocompatible, resulting in undesirable side effects. Also, surgery may also be required to implant or remove the system in some cases. Moreover, the higher cost of other controlled release systems may limit their application. In PDDS, a polymer is combined with drugs in a pre-designed manner so that drug delivery can be tailored and controlled (Lisa, 1997). In addition to the advantages as stated above, PDDS are easy to process. In particular, their chemical and physical properties can be easily

controlled *via* molecular synthesis. Furthermore, it allows targeted delivery of the drug to specific tissues or organs.

The type of polymer used for controlled release can be natural or synthetic, biodegradable or non-biodegradable (Leong and Langer, 1998). As drug carriers, these polymers exist in the form of matrices, reservoirs, polymer-drug conjugate, hydrogels, micropsheres, nanoparticles, micelles and so on. They can be administered via parenteral, implantation, oral, insert and transdermal routes (Robinson and Lee, 1999). Polymers used in drug delivery system, controlled release mechanisms, drug carriers and their application in drug delivery will be reviewed as follows.

2.1 Polymers

An appropriate selection of polymers is necessary in order to develop a successful drug delivery system since the polymer is used as a protector for drug during drug transfer in the body until the drug is released. An ideal polymer for drug delivery should meet the following requirements. Firstly, the polymer must be biocompatible and biodegradable. In other words, the polymer should be able to degrade *in vivo* into smaller fragments that can be excreted from the body. The term degradation refers to the process of polymer chain cleavage, which leads to a loss in molecular weight. Degradation induces the subsequent erosion (mass loss) of the materials. Two different erosion mechanisms have been proposed: homogeneous or bulk erosion and heterogeneous or surface erosion (Li and Vert et al., 1995). Bulk eroding polymers degrade all over their cross section because the penetration of water into the polymer bulk is faster than the degradation of

polymer. In contrast, degradation is faster than the penetration of water into bulk for surface eroding polymers. Therefore, these polymers erode mainly from their surface. However, erosion of most polymers exhibits both mechanisms (Winzenburg et al., 2004). If the polymer is non-biodegradable, the molecular weight of the polymer should be small enough to be excreted through the kidneys. Otherwise, it must be surgically removed after drugs are released. Secondly, the degradation products must be non-toxic and not triggering any inflammatory response. Also, they must also have an appropriate physical structure, with minimal undesired aging, and be readily processable. Finally, the degradation of the polymer should occur within a reasonable period of time.

A range of materials has been employed to control the release of drugs and other active agents. The materials that are currently being used or studied for controlled drug delivery include natural and synthetic polymers.

2.1.1 Natural polymers

Natural polymers are always biodegradable and bioabsorbable. These polymers offer many unique and advantageous properties that make them versatile materials. First of all, because they are naturally occurring material, they exhibit high biocompatibility and safety. Chitosan, polysaccharides, albumin and collagen are typical examples of natural polymers (Chourasia and Jain, 2004). Various drug carriers based on these polymers have been reported. In addition, natural polymers can be modified for a specific application. Furthermore, drug release rate from chitosan can be tailored via regulating the degree of crosslinking (Miyazaki et al., 1994). Chitosan also has a number of other good properties, further modification of its amine functional groups can be carried out to

obtain polymers with a range of properties for protein delivery or gene delivery (Dumitriu, 2002).

Since the application of the natural polymers is limited due to their physicohemical limitations, there is significant exploration of synthetic materials which can be readily tailored to offer properties for specific applications (Uhrich et al., 1999). The ability to design biomaterials with specific release, mechanical and processing properties has opened opportunities for synthetic polymers in the area of controlled release.

2.1.2 Synthetic polymers

In broad terms, synthetic polymers may be classified as either biodegradable or non-biodegradable.

2.1.2.1 Biodegradable polymers

Biodegradable polymers have recently captured much attention mainly because their use eliminates the need for removing the implant after the drug has been released. Biodegradable polymers gradually dissolve by hydrolytic or enzymatic cleavage of the polymeric structure by simple dissolution. Hydrophobic biodegradable polymers can be converted to small, water-soluble molecules by backbone cleavage. These breakdown products should be non-toxic. These polymers, for example, polyanhydrides, poly(orthoesters), polyurethanes, polyphophazenes, polyphosphoesters, polyesters (polycaprolactones, PCL, poly(lactic acid), PLA, poly(glycolide), PGA and their copolymers), are suitable as carriers for the administration of drugs to any organs. In the

following subsections, the chemical and physical properties of various biodegradable polymers will be reviewed.

(a) Polyesters

Most of the degradable polymers have hydrolysable groups, such as ester, orthoester, carbonate, amide, anhydride, urea, in their backbone. The ester bond-containing polyesters are the most attractive because of their outstanding biocompatibility and versatility with regards to physical, chemical and biological properties (Li and Vert et al., 1999). Polyesters of lactide and glycolide have been used for more than three decades for a variety of medical applications. Extensive research has been devoted to the use of these polymers as carriers for controlled delivery of a wide range of bioactive agents (Jian and et al., 1999). They have been widely used for delivery of proteins (Yang and Chia et al., 2000), peptides (Yang and Shi et al., 2003) and anticancer drugs (Liggins and Burt, 2001). Injectable formulations containing microspheres of lactide/glycolide polymers have received the most attention in recent years (Jiang and Gupta et al., 2005).

Synthesis

Polyesters are usually synthesized by ring-opening melt polymerization of lactide and glycolide at 140°C-180°C for 2-10h using a tin catalyst. Several mechanisms of this reaction were proposed, including anionic (Kurcok et al., 1992), cationic (Nijenhuis et al., 1992), coordination-inseration (Kohn et al., 1983).

Anionic polymerization: It is generally conducted in solution under comparatively mild reaction conditions compared to other methods. Many initators can be used,

including acetate, carbonate, or octoate salts of calcium, sodium, magnesium, potassium and lithium metals. The active species for chain propagation are alcoholate or carboxylate groups due to the opening of lactide rings by nucleophilic substitution. The ring is opened by cleavage of *O*-acyl bonds when a strong nucleophile attacks the basic alcoholate-type on the carbonyl. This configuation is kept during lactide polymerization. Anionic polymerization is a living process. It leads to polymers with different chain ends such as carboxylic acid group depending on the initation and termination mechanism (Kurcok et al., 1992).

Cationic polymerization: The initiators used in the cationic polymerization of lactides include strong acids, Lewis acids (Nijenhuis et al., 1992) and acylating or alkylating agents. During the initiation step, active species of oxonium or carbocation are formed. These carbocation cycles are unstable. In the absence of other strong nucleophiles (e.g., water and alcohols), the propagation step consists of nucleophilic attack of the active species by the endocyclic oxygen of another monomer molecule. Most of the mechanisms described in literature are based on coinitiation by impurities such as water or lactic acid. Coinitation will lead to polymers with different chain ends depending on the coinitator.

Coordination-inseration: This mechanism was proposed for a class of initiators derived from transition metals such as Zn, Al, Ti and Sn (Dubois et al., 1991). It was regarded as the most versatile and efficient method to prepare PLA, PLG, PCL and

various copolymers. With this method, high Mw and high conversion ratio can be easily achieved.

The common polymerization catalysts are tin compounds such as tin octoate or tin hexanoate. A hypothetical mechanism of the ring opening polymerization of lactide with tin as catalyst was suggested by Kissel (Kissel and Brich, 1991) (Figure 2.1). In this mechanism, the Lewis acid property of the tin catalyst activates the ester carbonyl group in the dilactone. The activated species react with the alcohol initiator to form an unstable intermediate that opens to become the ester alcohol.

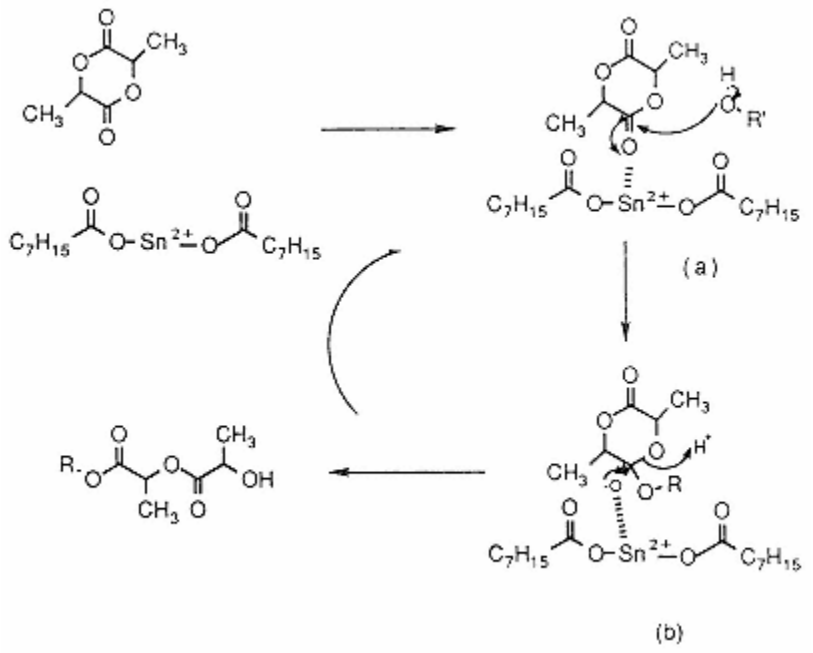

Figure 2.1 Mechanism of ring opening polymerization using tin octoate as catalyst

As discussed above, many initiators and catalysts have been reported. Among them, stannous octoate is used widely. Also, it has been approved by the U.S. FDA for surgical

and pharmacological applications. Stannous octoate thus are used as catalysis in this study for polymer synthesis. The variety of synthetic pathways provides a means to modify the molecular characteristics of polymers such as molecular weight (Mw) and polydispersity, end group nature and chain structure. These characteristics greatly determine the physicochemical properties, especially that of degradability.

Polymer properties

The polymer characteristics are affected by comonomer composition, crytallinity and molecular weight. Lactic acid contains an asymmetric α-carbon, which is typically described as the D- or L- form in stereochemistry. They form homopolymers poly(D-lactide) (PDLA) and poly(L-lactide) (PLLA), respectively. The physicochemical properties of PDLA and PLLA are similar. However, the poly(D, L-lactide) is less crystalline than the D or L-lactide homopolymers. PLA and its copolymers with less than 50% glycolic acid content are soluble in common solvents such as $CHCl_3$, DCM, THF and ethyl acetate. PGA is insoluble in common solvents but soluble in hexafluoroisopropanol.

Factors influencing polymer degradation

Polyester hydrolyzes by random chain scission (bulk erosion) through hydrolytic cleavage of ester groups (Figure 2.2), resulting in a continuing decline of Mw without significant loss of weight compared to the polymer in the beginning. When the Mw reaches about 5K, the cleavage of the chain is accompanied by a loss of weight due to the diffusion of small polymeric fragments from the matrix. Various factors can affect the

degradation of polyesters, including chemical structure, molecular weight and distribution, crystallinity, size of the matrix, porosity, drug load and drug/polymer interactions, physical factors and degradation conditions such as buffer concentration, enzyme and temperature.

Effect of composition: The composition of polymer chains, such as the contents of L-LA, D-LA and GA units, greatly affect the degradation rate of PLGA polymers. This is because the composition of polymers determines the hydrophilicity of the matrix. GA units are more hydrophilic than LA ones. Accordingly, they are more inclined to hydrolysis. In a degradation study (Wu and Wang, 2001), a series of polymers having similar molecular weights but different compositions (PLGA 50/50, 65/35, 75/25, 85/15) were used and compared. The degradation rate increases with the increasing glycolic acid content, which varies from 0.0222 to 0.0544 day^{-1} for PLLA to PLGA50/50 (Wu and Wang, 2001). Based on these results, the degradation rates can be tailored by varying the proportion of LA to GA.

Effect of molecular weight and distribution: Hydrolytically degraded ester bond produce one carboxyl and one hydroxyl end group (Figure 2.2). Polyester with low Mw will yield relatively high concentration of end groups over entire polymer samples. However, in high Mw polyesters, relatively low number of carboxylic acid end groups may slow down the degradation process.

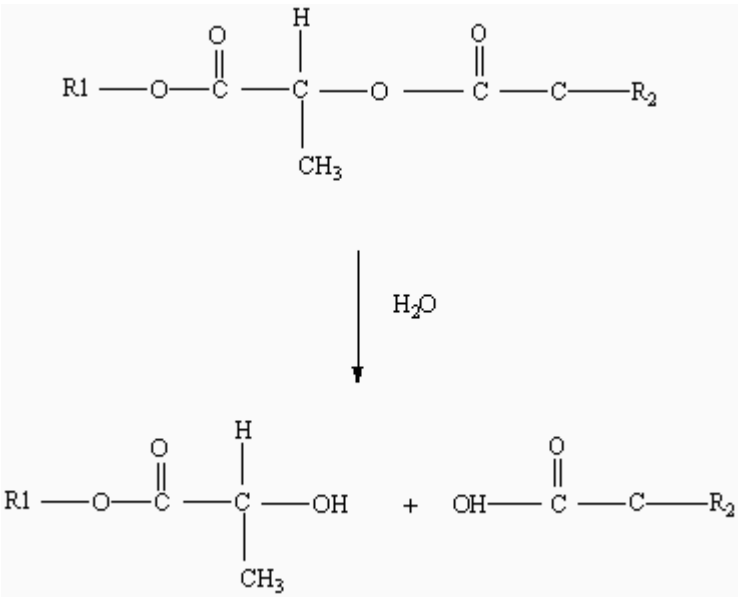

Figure 2.2 Hydrolytically degraded ester bond

Crystallinity: The degree of crystallinity (amorphousness or semicrystallinity) plays a critical role in both the enzymatic and non-enzymatic degradation processes. The degradation of semicrystalline polyester in aqueous media occurs in two stages. Firstly, water diffuses into the amorphous regions with random hydrolytic attack of ester bond. After most of the amorphous regions on the edges have been degraded, hydrolytic attacks move towards the center of crystallites. For example, fast cured PGA (lower crystallinity) showed an *in vivo* half life of 0.85 month, while slow-cured PGA (higher crystallinity) degraded much slower, with an *in vivo* half life of 5 month. This was caused by the crystallinity difference (Miller et al., 1977). Additionally, morphologies can affect degradation rate even with similar crystallinity. For instance, the degradation rate of PGA pellets was found to be much faster than that of fibers due to the presence of long-range order in fibers. Thus, chain orientation could also play an important role in the hydrolytic degradation (Ginde and Gupta, 1987).

(b)Polyanhydrides

Polyanhydrides are prepared by melt condensation polymerization. Starting with a dicarboxylic acid monomer, a prepolymer of a mixed anhydride is formed with acetic anhydride. The final polymer is obtained by heating the prepolymer under vacuum to remove the acetic anhydride byproduct. The most frequently investigated poly(anhydrides) are based on sebacic acid (SA) and *p*-(carboxyphenoxy) propane (Einmahal et al., 1999). Aliphatic polyanhydrides are used as biomaterials due to their hydrolytic instability. They hydrolyze rapidly due to the lability of the anhydride links (Domb and Nudelman, 1995). Thus, the main application of aliphatic polyanhydride is in short-term controlled delivery of bioactive agents. Polyanhydride undergoes surface erosion, which enables a zero order kinetic profile and a good control over the rate and the duration of the release. By varying the monomer ratios in polyanhydride copolymers, degradation can last from one week to several years (Kumar and Langer et al., 2002).

(c) Polyorthoesters

Since the late 1970s, four generations of poly (ortho esters) (POEs) have been synthesized to produce biodegradable carriers for drug delivery (Figure 2.3). Because POEs are extremely hydrophobic material, the amount of water available to react with the hydrolytically labile ortho ester bond is limited. They undergo predominantly surface erosion, allowing the release of drugs to be controlled by surface erosion (Heller and Barr, 2002). Since ortho ester bonds are acid labile, one way of controlling polymer erosion rates is to lower the pH at the polymer-water interface. A considerable amount of work has been done in attempts to achieve control of erosion rates *via* acid sensitivity

(Heller and Barr, 2004). Yang et al. (2003) reported novel POE/PLGA double walled micropsheres, where, the degradation of the POE core was accelerated due to the acidic microenvironment produced by the hydrolysis of the outer PLGA layer. Further, POE IV, a self catalyzed polymer, is a modification of POE II, allowing control over erosion rates without the need to add acidic excipients (Ng et al., 1997). POE has been widely used in drug delivery (Heller and Barr, 2004).

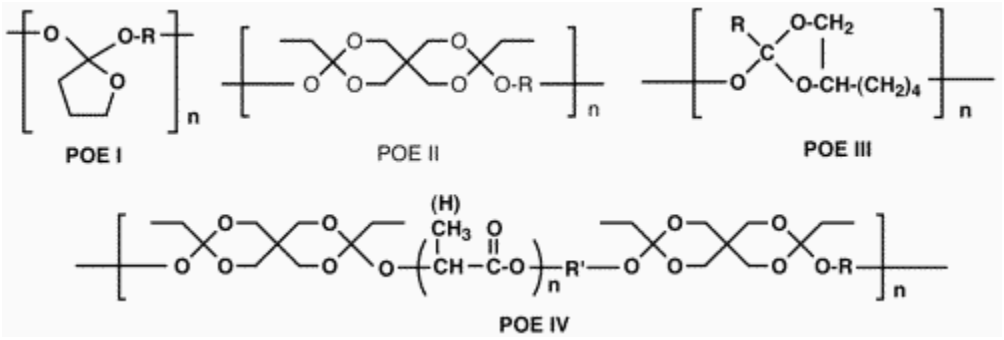

Figure 2.3 Four generations of poly (ortho esters)

2.1.2.2 Nonbiodegradable polymers

Some of the synthetic nonbiodegradable polymers materials that are currently being used or studied for controlled drug delivery include poly(ethylene oxide) (PEO), Poly(ethylene-*co*-vinyl acetate), poly(2-hydroxy ethyl methacrylate), poly(*N*-vinyl pyrrolidone), poly(methyl methacrylate), poly(vinyl alcohol), poly(acrylic acid), polyacrylamide and poly(methacrylic acid) (Peppas, 1997). A number of controlled release systems using such polymers are under study (Edelman and Langer, 1993; Chen and Hoffman, 1995).

(a) Poly(ethylene oxide) (PEO)

PEO and PEG are polymers containing the repeating unit [-CH_2CH_2-O-]. PEG is a subspecies of PEO that contains a hydroxyl group on each end of the chain. PEO is an outstanding biocompatible, non-toxic, non-immunogenic and water-soluble material (Abuchowski et al., 1977). PEO is usually synthesized by the aqueous anionic polymerization of ethylene oxide. Initiators for polymerization of ethylene oxide can be anhydrous alkanols such as methanol or derivatives such as methoxyethoxy ethanol to produce a monoalkyl capped PEO (Greenwald et al., 2003). The polymerization reaction can be modulated and a range of Mw (1000-50,000) can be obtained. PEO has been widely used in both medicine and biotechnology. It has also been successfully applied in different drug delivery systems to enhance their systematic characteristics. One of the applications of PEG is PEG-protein conjugate for controlled release system (Nucci et al., 1991). Such conjugates have significantly increased circulation time and reduced immunogenicity and antigenicity, and allows for the retention of a large portion of the bioactivity of proteins. It has been postulated that these effects are due to a shell of PEG molecules around the protein that sterically hinders the proteins from reacting with immune cells and protects proteins from proteolytic inactivation. PEG has also been conjugated to small organic molecules such as anticancer drugs doxorubicin and paclitaxel to improve drug solubility. For example, mPEG paclitaxel 7- carbonates has much higher solubility than paclitaxel and thus increasing the possibility of more effective drug delivery (Greenwald et al., 1996).

Another important feature of PEG is that PEG can be made with a range of terminal functional groups, which allows it to be easily incorporated into block copolymer systems. There are many examples of amphiphilic block copolymers incorporating PEG, including polystyrene-block-poly(ethylene oxide), poly(ethylene oxide)-block-poly(propylene oxide)-block-poly(ethylene oxide) and the diblock or multiblock of polyesters (PLLA, PDLLA, PLGA, PCL and their copolymers) with poly(ethylene oxide). These polyester-block-poly(ethylene oxide) copolymers have been widely used to prepare microspheres (Kissel and Li et al., 1996), nanoparticles (Li and Pei et al., 2001) and micelles (Jette et al., 2004).

To date, controlled released systems for maintaining constant drug release rate have been extensively studied and tested. However, there are a number of clinical situations where such an approach may not be sufficient. These include the delivery of proteins such as insulin for patients with diabetes mellitus (Brownlee and Cerami, 1979) as well as cancer chemotherapy (Yokoyama and Okano, 1996). Thus, drug delivery patterns can be further improved by responsive delivery, which is the adjustment of drug delivery to match biological rhythms.

(b) Responsive polymers

In recent years, several research groups have been developing responsive systems that would more closely resemble the normal physiological process in which the amount of drug released can be changed according to physiological needs. Drug release rates can be activated by an external stimuli such as magnetism (Hsieh et al., 1981), ultrasound

(Mitragotri et al., 1995), light (Suzuki and Tanaka, 1990), temperature changes (Chung et al., 1999) and electrical effects (Wong et al., 1994) or self regulated stimuli such as pH sensitive polymers (Lee and Na et al., 2003), ionic strength (Kristein et al., 1985) and glucose concentration (Ito et al., 1989). Among these responsive carriers, thermo-responsive delivery system based on poly(*N*-isopropylacrylamide) (PNIPAAm), has been of interest in the field of controlled drug delivery.

Temperature responsive polymers

Temperature responsible polymers possess temperature-dependent solubility in water. They are insoluble above or below a certain temperature, called the lower or upper critical solution temperature (LCST or UCST). In general, most drug delivery applications utilize LCST systems. When the temperature is below the LCST, water molecules surround hydrophobic group of polymers to make polymer soluble. Once LCST is reached, ordered water cages break and expose hydrophobic groups, hydrophobic association occurs. Thermodynamically, polymers that phase separate from water on increasing temperature are driven by entropy changes. This is because the entropy of the two-phase polymer and water systems (random water molecules structure) is greater than that of polymer solution (ordered water molecules structure). Thus, hydrophobic association is favorable at a temperature above the LCST.

Among the temperature responsive polymer, poly(*N*-isopropylacrylamide) (PNIPAAm) is the most well-known one and demonstrates a transition temperature (T_{tr}) or lower critical solution temperature (LCST) of about 32^{o}C (Heskin and Guillet, 1968). PNIPAAm in an aqueous solution has reversible solubility and exhibits a remarkable hydration-dehydration change in response to temperature (Chen and Yang et al., 1990). Below the

LCST, PNIPAAm is well soluble in water. However, as the temperature is increased above the LCST, it becomes hydrophobic and precipitates out from the aqueous solution. The abrupt shrinking and the resulting insolubility of LCST systems when the environmental temperature is above the LCST allows the copolymer of the invention to leave the aqueous phase and assume a hydrophobic phase, thereby facilitating interaction with cell membranes. Furthermore, temperature sensitive monomeric units can be co-polymerized with hydrophilic co-monomers such as acrylamide (AAm), or other types of modified co-monomers to achieve a higher or lower LCST (Yoshida et al., 1994). This unique property is very important for its applications in drug delivery. Such copolymers can be applied as a functional drug delivery material for controlling drug release rate.

pH responsive polymers

Studies have been performed by several groups on polymers containing weak acidic or basic groups in the polymeric chain. Some examples of these polymers include, poly(acrylic acid) (Ito et al., 1989), poly(L-histidine) (Lee and Na et al., 2003). The charge density of these polymers depends on the pH or ionic composition of the medium. Altering the pH will cause the changes in solubility or other properties of the polymer. For polyacidic polymers, acidic groups will be protonated at low pH and hence deionized. Thus it will become more hydrophobic. With increasing pH, acidic groups will be ionized and hence the solubility will increase.

2.2 Mechanisms of controlled drug release

Drug release mechanisms can be physical or chemical in nature. Diffusion is always involved in drug release from non-biodegradable matrix and membrane devices. Release

by diffusion is driven by concentration gradient, osmotic pressure and matrix swelling. However, for matrices that are biodegradable or contain drug conjugate, release can also be controlled by hydrolytic or enzymatic cleavage of relevant chemical bonds. Accordingly, mechanisms of drug release have been classified into diffusion, swelling and degradation controlled (Narasimhan et al., 1999).

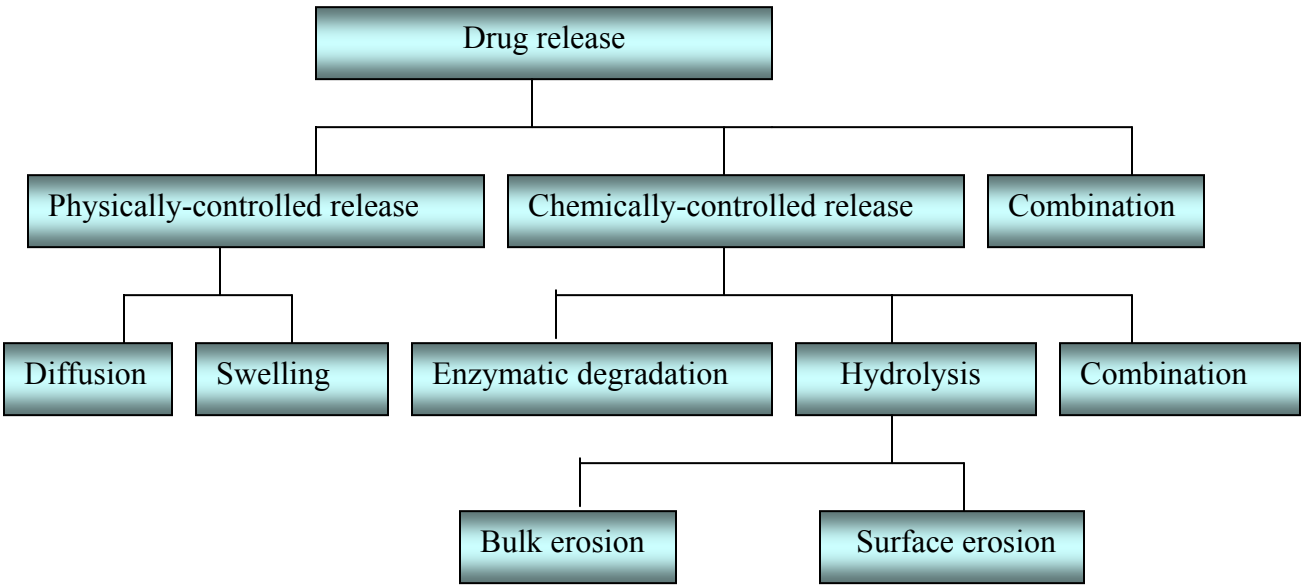

Figure 2.4 A diagram of drug release mechanisms

As shown in Figure 2.4, the continuous release of drugs can occur either by diffusion of the drug from the polymer matrix, by matrix swelling or by the erosion of the polymer due to degradation or by a combination of these three mechanisms.

2.2.1 Physically-controlled release mechanism

Under this category, the release mechanisms may be further classified into drug diffusion or swelling.

2.2.1.1 Diffusion

A device is considered diffusion-controlled when the diffusion of active agent through any part of the device controls the release rate. The polymer forming the device remains relatively unaffected by the polymer-environmental fluid interaction. There are two types of diffusion-controlled systems: reservoirs and matrices. For the former case, the drug reservoir is surrounded by a polymeric membrane. The drug core can be in either solid or liquid form, and the membrane can be microporous or nonporous. If the drug core is maintained in a saturated state, the transport of drug molecules across the membrane will be kept constant (zero-order release), as the driving force is unchanged. However, the saturated state would be difficult to maintain if the drug has high water solubility.

The most widely used devices are the matrix systems in which the drug is dissolved or dispersed in the polymer. One characteristic of these systems is that the release rate decreases with time as a result of increasing diffusion distance for the drug solutes to travel from the core to the surface. The amount of drug released is often proportional to the square root of elapsed time. In addition to permeation through the polymer phase, the drug molecules can also diffuse through channels created by dissolution of the drug phase. Release of macromolecules with low permeability generally occurs *via* these pores. Since the extent and size of the pores and channels created are determined by the

drug incorporated, the loading level and particle size of the drug solutes have a profound influence on release kinetics. Below a critical loading level, some of the isolated drug particles may be trapped inside the matrix.

The release behavior of these diffusion-controlled systems is highly dependent on the physical properties of the drug. In addition to loading level and particle size of the solutes, the drug solubility in the polymer and drug diffusivity in the polymer phase are also important parameters. The shape of the device, which determines the surface area available and the path length for diffusion, is also critical.

2.2.1.2 Swelling

Swelling-controlled release systems are formed by dissolving or dispersing the active agent in a polymeric matrix which is initially dry. However, when this matrix is placed in an environmental fluid thermodynamically compatible with the polymer, the fluid is absorbed into the polymer, causing it to swell. The swelling increases the aqueous solvent content in the formulation as well as the polymer mesh size, allowing the drug to diffuse through the swollen network to the external environment. The release rate is therefore mainly related to the swelling phenomenon. Most of the materials used in swelling-controlled release systems are hydrogels, e.g. poly(hydroxy methyl methacrylate), polyacrylamide, and poly(ethylene glycols). The size of the pores located within the network, which is related to the extent of crosslinking and the degree of swelling, determines the protein release rate. The rate at which protein is released from the hydrogel network can be modified by varying the degree of physical entanglement

within the gel, by altering the chemical crosslink density or by altering the interactions between the polymer matrix and the molecules of interest.

2.2.2 Chemically-controlled release mechanism

Chemical reaction controlled release systems are delivery systems in which the polymer is not merely a passive carrier but an active participant in the release process. Two common chemically-controlled systems are biodegradable matrix in which the drug is dispersed, and polymer-drug conjugate in which the drug molecules are chemically bonded to the side chains of the polymer.

2.2.2.1 Polymer degradation

The active agent in erosion-controlled devices is physically immobilized in the polymer and is released by the erosion of the polymer. While these devices can be made in both the reservoir and monolithic forms, the latter is more suitable for the purpose of drug delivery. In an ideal system, the polymeric carrier would undergo surface erosion, releasing the active agent at a rate proportional to the erosion rate. Systems with constant erosion rate and symmetric matrix geometry would produce zero-order (constant) release rates. However, erosion in practical systems is seldom solely from the surface inwards. Bulk erosion leading to a loss of physical integrity of the matrix and its eventual collapse, is frequently observed. Moreover, drug molecules can also diffuse through the matrix. The release is commonly intermediate between zero-order and first order kinetics. Various polymers have been utilized in forming erodible devices, including copolymers

of lactic and glycolic acid. It has also been reported that polyanhydrides and POE undergo surface erosion. Bioerodible polymer remains a very actively researched area.

2.2.2.2 Polymer-drug conjugates

In polymer-drug conjugates, the active agent itself is chemically bound to the polymeric backbone. Release occurs by hydrolytic or enzymatic cleavage of this bond. The polymer itself may be degradable in these systems. The release rate of the polymer-drug conjugate depends on the rate of cleavage of the polymer-drug bond. If the drug is attached to the polymer *via* a spacer, the hydrolysis of both the polymer-spacer and the spacer-drug bonds is relevant.

In general, many degradation systems use a combination of these mechanisms.

2.2.3 Responsive drug release

In addition to the mechanisms discussed above, another method of controlled release is responsive drug delivery in which the drug is released in a pulsatile manner only when required by the body. As described earlier, responsive systems based on thermo responsive or pH responsive polymers have been widely investigated. It would be desirable that polymeric systems could be designed to release increased levels of drug when needed, mimicking the body's physiological processes (Kost and Langer, 2001). In general, responsive drug delivery systems have two components: a sensor that detects the environmental conditions that stimulates drug release and a delivery device that releases the drug (Uhrich et al., 1999). Drug release can be activated by an external stimulus

(such as magnetism, ultrasound, temperature changes and electrical effects) or self regulated stimuli (such as pH sensitive polymers, pH sensitive drug solubility and enzyme-substrate reactions). The concept of responsive drug release can be used for any drug therapy in which a sensor and delivery device can be coupled. Signals that have been employed to trigger drug release include: temperature in which thermosensitive hydrogels swell and collapse in response to temperature variations; pH in which ionizable groups within the polymer control polymer interactions. For diabetes treatment, responsive drug delivery systems have been proposed, using the enzyme glucose oxidase as the sensor. When blood sugar levels rise, glucose oxidase converts glucose to gluconic acid, resulting in lowered pH. This pH decrease is then used as signal for insulin release (Kost and Horbett et al., 1985). The drug is released by using pH sensitive polymers that either swell or degrade in acidic environment.

2.3 Drug delivery systems

Various delivery systems for controlled drug delivery have been developed in recent years. These include monolithic devices, reservoir devices, polymer-drug conjugate, hydrogels, lipsomes, polymeric colloidal particles (microparticles, microspheres or nanoparticles) and micelles.

2.3.1 Monolithic devices

Monolithic devices are possibly the most commonly used drug delivery systems. In such a device, the drug is uniformly dispersed within the polymer matrix. Monolithic devices

are normally formed by the compression of the polymer/drug mixture or by dissolution or melting.

2.3.2 Reservoir devices

In reservoir devices, the drug is encapsulated by a film or membrane made of a rate-controlling material. The only structure effectively limiting the release of the drug is the polymer layer surrounding the reservoir. Since this polymer coating is essentially uniform and of fixed thickness, the diffusion rate of the active agent can be kept fairly stable throughout the lifetime of the delivery system if the drug is in a saturated state (Stannett et al., 1979). Otherwise, the drug release rate of the drug decreases with time as the drug concentration decreases. To design reservoir devices with desired properties, various factors such as additives, polymer functionality, porosity and film casting conditions that can affect the diffusion process should be optimized. However, there are some difficulties with regards to protein delivery using reservoir devices. Large molecules such as proteins diffuse very slowly through polymer films. Moreover, unforeseen membrane failure may occur, resulting in massive release of entrapped drugs.

2.3.3 Hydrogel

Hydrogel is defined as soft solid like material that can absorb a substantial amount of water while maintaining a distinct three-dimensional structure (Brornberg and Ron, 1998). One of the most useful features of hydrogen's swelling ability is that swelling can be triggered by a change in the environment surrounding the delivery system. Depending upon the polymer, the environmental change can involve temperature, pH, or ionic

strength, and the system can either shrink or swell upon a change in any of these environmental factors. For most of these polymers, the structural changes are reversible and repeatable upon additional changes in the external environment. One example is temperature sensitive PNIPAAm hydrogel. PNIPAAm hydrogel possesses a three-dimensional network structure, which is insoluble but has characteristics of reversible swelling. The polymer chains undergo a coil (soluble)-globule (insoluble) transition when the external temperature cycles across the LCST at about 33^{o}C (Zhang and Yang et al., 2001). Thus, at the temperature below the LCST, PNIPAAm hydrogel absorbs water and exists in a swollen state. But it turns to shrink and displays an abrupt volume decrease as the environmental temperature is higher than the LCST.

Generally, the main reason for this distinctive property of the PNIPAAm hydrogel has been attributed to its uniquely rapid alteration in hydrophilicity and hydrophobicity (Feil et al., 1993; Inomata et al., 1990; Tokuhiro et al., 1991). When the hydrophilic groups in the side chains of the PNIPAAm hydrogel connect with water molecules through hydrogen bonds, these hydrogen bonds act cooperatively to form a stable hydration shell around the hydrophobic groups, which leads to the great water-uptake of the PNIPAAm hydrogel at temperatures below the LCST. However, as the external temperature increases, the hydrogen bonding interactions become weakened or destroyed, thus the hydrophobic interactions among the hydrophobic groups grow to be stronger which induces the freeing of the entrapped water molecules from the network. When the temperature reaches or is above the LCST, the hydrophobic interactions become fully dominant. With a rapid water release, the polymer chains contract or collapse abruptly

and the phase separation of the PNIPAAm hydrogel system occurs. This phase separation is thermoreversible, which makes this hydrogel especially useful for drug delivery applications. A lot of work has been done on the application of PNIPAAm hydrogel for protein delivery. For example, Braxel and Peppas (1996) reported pulsatile delivery of streptokinase (a fibrinolytic enzyme used to treat coronary thrombosis) using poly(*N*-isopropylacrylamide-*co*-methacrylic acid) hydrogel. However, PNIPAAm-based hydrogels are not degradable and their monomers and cross-linkers may be toxic. Recently, biocompatible and/or degradable gels, based on poly(lactide-co-glycolide)-poly(ethylene glycol)-poly(lactide-*co*-glycolide) (PLGA-PEG-PLGA) and poly(ethylene oxide) (PEO)-poly(propylene oxide) PPO-PEO, have been developed (Jeong et al., 2000).

2.3.4 Polymer-drug conjugate

Drugs can be attached to soluble synthetic polymers such as PEG *via* degradable linkages. This process alters the drug's size and solubility, resulting in different pharmacokinetics and biodistribution. One example involves covalent attachment of mPEG to proteins (PEGylation). α-interferon, with a Mw of 19 kDa, used for treatment of hepatitis C, is cleared rapidly from the blood plasma of human body. However, PEGylated α-interferon has a half-life about eight times that of native α-interferon *in vivo*, allowing weekly subcutaneous dosage of the conjugated protein. The continued presence of circulating α-interferon activity allows for increased antiviral efficacy compared to unmodified protein (Greenwald et al., 2003). The current size of the PEGylated protein market is about $1.0 billion per year. It is expected that this market will grow to over $6.0 billion by 2008 (Sinha and Trehan, 2003).

2.3.5 Microspheres

Microspheres are attractive drug carriers because they can be used to protect drugs against degradation and can be administered *via* injection, avoiding the need for surgery (Baldwin and Saltzman, 1998). Micropsheres are also able to control drug release from the site of administration and in some particular cases to improve their passage through biological barriers. Microspheres can be composed of biodegradable or non-biodegradable polymers. They can be produced in a wide range of sizes (1-100μm). Drugs may be dispersed in microspheres in either macroscopic (particulates) or molecular (dissolution) form.

2.3.5.1 Micropsheres fabrication

Generally, microspheres can be fabricated by either emulsion solvent-evaporation/extraction or spray drying methods. One of the most common methods of preparing microspheres is the oil-in-water (O/W) solvent evaporation method (Johnson et al., 1991). It involves the dispersion of an organic solution of the polymer and the drug into a continuous aqueous phase. Hydrophobic drugs are successfully encapsulated in microspheres using this method. However, poor encapsulation efficiency was observed for hydrophilic drugs. A typical emulsion method for hydrophilic drugs is based on the water-in-oil-in-water double emulsion (w/o/w) process (Alonso et al., 1993). First, the drug is dissolved or suspended in an aqueous solution and the polymer is dissolved in an organic solvent, and the two solutions are sonicated to form a first emulsion. DCM is considered as one of the most suitable solvents for the preparation of micropsheres as it is highly volatile and readily dissolves a range of polymers. The first emulsion is then

poured into an aqueous medium and stirred to form a double emulsion. The first emulsion droplets are hardened by solvent evaporation or extraction, yielding microspheres. The size of microspheres can be controlled by varying fabrication conditions, including stirring rate, polymer concentration, surfactant and internal water volume (Yang et al., 2000).

When an A-B block copolymer (A: hydrophobic, B: hydrophilic) is used in the double emulsion process, the hydrophilic B block intends to migrate to the external aqueous phase and yields core-shell structured particles. Gref et al. (1994) reported that poly(ethylene glycol)-poly(lactide-*co*-glycolide) nanoparticles of 150 nm were obtained by this method. The emulsion method is suitable to encapsulate both hydrophilic and hydrophobic drugs.

2.3.5.2 Microspheres for protein delivery

Proteins form an integral part of the body as they carry out all important physiological and biological processes. For example, proteins can act as ligands for signalling, enzymes for facilitating metabolic activities, antibodies in immune system interactions and carry out transcription and translation of DNA (Sinha and Trehan, 2003). Protein drugs are becoming very important therapeutic agents due to our understanding of their roles in physiology and pathology as well as the rapid growing biotechnology/genetic engineering. The development of DNA-recombination techniques has allowed the discovery of many new proteins (Lee, 1991). Moreover, it allows proteins to be made available in a large scale.

Several hundred protein drugs including insulin, hormones, growth factors, monoclonal antibodies and proteins for curing various diseases are currently undergoing clinical trials (Talmadse, 1993). However, all proteins have a short biological half-life. They are difficult to administer orally because they are unstable and are easily degraded by enzymes. Most proteins can not easily pass through biological barriers because of their poor diffusivity and low partition coefficient. To resolve these problems, the entrapment of proteins within microparticles, especially microspheres, has been investigated extensively (Couvreur et al., 1997). This is because microspheres are able to protect proteins against degradation and control their release from the site of administration. For example, insulin was encapsulated in blends of PEG with PLA and PLGA using w/o/w techniques. The encapsulation efficiency was 48% and 56%, respectively. Such microspheres were capable of controlling the release of insulin for 28 days (Sinha and Trehan, 2003). PLGA/PEG microspheres exhibited more extensive degradation over 4 weeks as compared to PLA/PEG. PLA/PEG microspheres thus resulted in more stable particle morphology along with reduced fragmentation and aggregation of associated insulin. Microspheres have also been used to deliver proteins to local tissue sites. When microspheres are implanted in a tissue, released proteins accumulate at the delivery site. It is possible to achieve the desired release rate and let proteins accumulate within the tissue by designing microspheres of proper size, composition and microstructure (Baldwin et al., 1998). Another advantage of using microspheres for protein delivery is that they can improve protein passage through biological barriers in some particular cases (Krewson et al., 1996).

As mentioned before, since certain therapy requires fluctuating protein levels, polymer-based responsive delivery systems using microspheres have thus been investigated. Lynn and Amiji et al. proposed novel micropsheres composed of poly(*β*-amino ester), whose solubility is influenced by solution pH (Lynn and Amiji et al., 2001). The polymer was insoluble in aqueous media in the pH range 7.0 to 7.4, and the transition between solubility and insolubility occurred at pH near 6.5. Based on the difference between extracellular and endosomal/lysosomal pH (7.4 and 5.0-6.5, respectively), these microspheres were designed to release drugs in the intracellular pH range. *In vitro* release experiments showed that the microspheres dissolved rapidly in buffer with pH 5.1, leading to instantaneous release of drug from microspheres (80% was released over 1 h). In contrast, less than 20% of the drug molecules were released for microspheres incubated at PBS (pH 7.4) over 60 h. CLSM results suggested that these microspheres could be internalized and digested by macrophages. Therefore, poly(β-amino ester) microspheres retained the drug at extracellular or cytoplasmic pH value and released the drug in the range of endosomal/lysosomal pH value.

Despite many attractive features provided by microspheres, there are still problems associated with protein delivery. The most important factor affecting effectiveness of microspheres in protein delivery is the complexity of protein structure. Proteins must maintain specific, folded, three-dimensional structure (conformation) during the encapsulation process to allow delivery of biologically active native protein upon administration. Studies have shown that the fabrication process may cause degradation of proteins. Furthermore, when encapsulated proteins remain in the body for a long time,

they may denature or aggregate as a result of exposure to moisture at 37°C. This will lead to loss of biological activity and possibly produce an immune response. However, if the protein is recognized as self-protein, the probability of immune response is reduced. It is therefore essential to keep the protein in its native conformation in both the fabrication and the release process.

BSA is a commonly used model protein in the development of controlled release system (Yang and Chia et al., 2000). The surface-active property of BSA makes it stable in the first emulsion process. Therefore, BSA, with a molecular weight of 58 kDa, was used as the model protein to explore the possibility of using thermo-responsive polymer microspheres for protein delivery in this study.

Microspheres (1-250 μm) are considered the first generation colloidal carriers, which are able to control drug release. Despite promising results with microspheres, their usefulness is limited by their distribution and in particular by their recognition by the mononuclear phagocyte system. Recently, much interest has been directed towards the development of second generation drug carriers, nanoparticles (<1μm) (Barrat et al., 2002). Such carriers can deliver drugs directly to the target site (Langer, 1998).

2.3.6 Nanoparticles

Nanoparticles, usually smaller than 1μm, can be made by polymers (Feng et al., 2004) polymer-drug complex or lipsomes (Guo et al., 2003). Nanoparticles have special properties that can be exploited to improve drug delivery. Nanoparticles are often taken

up by cells due to their fine size. According to the process used for the preparation of the nanoparticles, they are classified into nanospheres and nanocapsules. Nanospheres are matrix systems in which drugs are dispersed throughout the particles. They are usually prepared by O/W or W/O/W method (Brigger et al., 2002). Unlike nanospheres, nanocapsules are vesicular systems in which the drug is confined to an aqueous or oily cavity surrounded by a single polymeric membrane. With appropriate design, drugs such as peptides, proteins and anticancer drugs can be loaded into nanoparticles that are not recognized by the immune system and can be targeted to particular tissue types. A lot of research has been done on using nanoparticles as drug carriers. For example, Feng's group has investigated PLGA nanopaticles for controlled release of paclitaxel. Paclitaxel-loaded PLGA nanoparticles were prepared using O/W emulsion method. Drug release profile was determined by the polymer type and its molecular weight, the ratio of the copolymers, the emulsifier used, the ratio of the oil to water in the encapsulation process, the drug properties, the drug loading level, and other preparation parameters. The release profiles were thus adjustable by varying these parameters (Feng and Chien, 2003). However, it is still possible that these hydrophobic nanoparticles be captured by the macrophages of the mononuclear phagocytes system (MPS) after intravenous administration. Recently, a great deal of work has been devoted to developing stealth nanoparticles (Gref et al., 1994). By introducing hydrophilic polymers such as PEG on the surface, nanospheres will have a prolonged half-life in the blood. This allows them to selectively target inflamed regions with a leaky vasculature. There are two ways of introducing hydrophilic polymers either by adsorption of surfactants or by formation of block copolymers such as PEG-PLGA.

2.3.7 Micelles

Polymeric micelles were first proposed as drug carriers in 1984 (Bader et al., 1984). Polymeric micelles are self-assembled from amphiphilic block or random copolymers. Here, a block copolymer is composed of one segment of an A homopolymer with a B homopolymer (A-B), while random copolymers have randomly arranged repeat units in their backbone (A-B-A-B or A-A-A-B-B-A-B and so on) (Kumar and Ravikumar et al., 2001). Normally, the size of polymeric micelles is less than 200 nm. Two forces are involved in the formation of micelles. One is the attractive force, leading to the assembly of molecules. The other is the repulsive force, preventing unlimited growth of the micelles. Amphiphilic copolymers tend to self assemble when put in a solvent in which either the hydrophilic or the hydrophobic segment is soluble. When the solvent is an aqueous phase, micelles are formed with a hydrophilic shell and a hydrophobic core at a polymer concentration above the critical association concentration (CAC). With the core-shell structure, polymeric micelles can solubilize insoluble drugs in the core while the outer shell is responsible for interactions with biocomponents. In addition, the hydrophilic shell can prevent unwanted interactions between the particles and the reticuloendothelial system (RES). It was reported that drug-loaded polymeric micelles might accumulate to a greater extent than free drug in tumor tissues as compared to healthy tissues due to an increased vascular permeability and impaired lymphatic drainage (Jones and Leroux, 1999). This is referred to as the enhanced permeability and retention effect (EPR) (Matsumura and Maeda, 1986). The EPR effect is considered as a passive targeting method, but the drug targeting could be further enhanced by the introduction of an environment-responsive polymer segment or a signal on the surface of

the micelles which can recognize tumor cells (Jones and Leroux, 1999). This is known as active targeting method. Nowadays, polymeric micelles are regarded as one of the most suitable carriers for delivering anticancer drugs. The use of these micelles for anticancer drug delivery requires the determination of several important parameters such as particle size, critical association concentration (CAC), drug loading capacity, physical stability and drug release. Since these parameters strongly depend on the procedure used in the preparation of micelles, micellar shell and the micellar core, these factors as well as the applications of the micelles in anticancer drug delivery will be reviewed in the following subsections.

2.3.7.1 Fabrication of micelles

There are two methods used for the preparation of drug-loaded micelles, dialysis method and direct dissolution method (Allen and Cullis, 1999). The selection of the method to be used depends on the solubility of the block or copolymer in water. In the case of direct dissolution, polymer is simply dissolved in an aqueous medium. This method is used for micelles preparation from pluronics and polymers with a good solubility in water. The dialysis method is most often used to prepare micelles using poorly soluble polymers. In the dialysis method, the drug and polymer are added to an organic solvent, and then the solution is dialyzed against water. During the process of dialysis, micelles are formed and the drug is loaded into the core as the organic solvent is removed. Some studies have reported that the micelle size and drug loading capacity depend on the organic solvent used (Kim and Shin et al., 1998). In a study reported by Lee and Kim (2003), the use of THF as the organic solvent gave rise to the micelles with a drug loading

content of 0.5%. In contrast, when acetonitrile was used, the micelles obtained had a much higher loading content of 2.4%. In addition, Chung (Chung et al., 1999) reported that the dialysis temperature had a great effect on the particle size and drug loading. It was found that the optimum temperature for forming PNIPAAm-*b*-PBMA micelles with efficient drug incorporation and small particle size was 20°C. This is because a thermo-responsive polymer was used in the experiment, and it would precipitate above the LCST, leading to lower drug loading level. According to these studies, the size and drug loading capacity of the micelles can be modulated by varying fabrication conditions.

2.3.7.2 Shell of micelles

The micellar shell acts as a stabilizing interface between the hydrophobic micelle core and the external medium. In most cases, PEG/PEO with molecular weight ranging from 1000 to 12000 is used as the hydrophilic block to form the shell of the micelles. The outer PEG shell of micelles can inhibit the surface adsorption of biological components such as proteins and protect the core through steric stabilization. It has been demonstrated that PEO prevented the adsorption of proteins (Deng et al., 1996) and thus formed a biocompatible polymeric shell. Also, it can influence the extent to which primary micelles aggregate to form large secondary clusters. Additionally, the surface density of PEG and the thickness of the PEG shell can influence the stability of micelles. Usually, the density of PEG at the surface of micelles is determined by aggregation number. The larger the aggregation number, the more PEG blocks on the surface of micelles. The surface properties of the micelles such as charge, hydrophilicity and steric stability have a great effect on the biodistribution of the drug-loaded micelles. The high PEO surface

density of the 1.5:2 PEG-PLA micelles led to an improved biodistribution with reduced liver uptake compared to that of 2:5 PEG-PLA micelles (Hagan and Coombes et al., 1996).

As described in the previous paragraphs, drug targeting can be improved by the introduction of a signal on the surface the micelles, which can recognize tumor cells or an environment-responsive polymer segment. Block copolymers with a functional group at one end of the PEG chain were used to introduce the targeting signal on the outer shell of the micelles. The specificity results from a receptor-ligand interaction. Specific ligands will bind to receptors on the plasma membrane of the target tissue. It was reported that micelles prepared from PEG-distearyl phosphoethanolamine (PEG-PE) were convalently modified with the nucleosome-specific monoclonal antibody 2C5 (Gao and Lukyanov et al., 2003). These antibody conjugated paclitaxel-loaded micelles recognized specific tumor cells and showed enhanced cytotoxicity compared to normal paclitaxel-loaded micelles. Another widely used signal is folic acid. Folic acid constitutes an attachable ligand with high affinity for a receptor that is commonly over expressed on ovarian, breast carcinomas and other cancers (Lu and Low, 2003).

Other than PEG, several other hydrophilic polymers such as PNIPAAm, poly(acrylic acid) (PAAc) have been used as the shell of micelles. As stated earlier, PNIPAAm is a temperature-sensitive polymer with LCST of 32^{o}C. The LCST can be modified by the incorporation of hydrophilic or hydrophobic comonomer. This unique property is very important for active targeting. Okano's group tested a series of DOX-loaded thermo-responsive micelles with PNIPAAm shells (Chung et al., 1999; Kohori et al., 1999). It

was found that these micelles exhibited reversible structural changes upon heating or cooling across the LCST (32^{o}C). Such DOX-loaded micelles showed a dramatic thermo-responsive on/off switching behavior for both drug release and *in vitro* cytotoxicity based on the temperature responsive structural changes.

2.3.7.3 Core of micelles

As mentioned above, the core of micelles, which consists of hydrophobic polymer, serves as a reservoir for drugs. The hydrophobic core generally consists of biodegradable polymers such as PLA, PLGA or non-biodegradable polymers such as alkyl chain, polystyrene (PSt) and poly(methyl methacrylate) (PMMA). Usually, the core exists in two states: one is a liquid-like core; another is a solid-like core (Allen and Eisenberg, 1999). Whether it is liquid-like or solid-like, it has a large influence on the drug loading, physical stability and drug release of the thermo-responsive micelles. The physical state of the core under normal physiological conditions (37°C) depends on the glass transition temperature (Tg) of the core-forming block. The polymer is liquid above the Tg, while it is solid below the Tg. Several studies have described the use of polymers such as polystyrene (PSt) (Zhang and Eisenberg, 1995) or poly(methyl methacrylate) (PMMA) (Inouse and Chen, 1998) as constituents of the micellar core. These polymers have solid-like core, which exhibited low drug loading capacity (5.0%) but remarkable stability. In contrast, the liquid-like core composed of poly(butylmethylacrylate) (PBMA) offered high drug loading capacity (9.6%), but the stability of these micelles is not good (Chung et al., 1999). Furthermore, the state of the micelle core has a significant effect on the rate of drug release from the thermo-responsive micelles. Chung et al. (1999)

compared the anticancer drug (DOX) release between PNIPAAm-*b*-Pst and PNIPAAm-*b*-PBMA micelles. It was found that drug release from the PNIPAAm-*b*-PBMA was initiated by increasing the temperature above the LCST (over 80% was released), while it was suppressed below the LCST (about 10% was released). This is because PNIPAAm shell collapsed above the LCST, inducing the deformation of the micellar structure, leading to faster drug release (Chung et al., 2000). However, the drug release from the PNIPAAm-*b*-PSt was suppressed at temperatures both above and below the LCST. This can be explained by the fact that the PSt core possessing a much higher Tg (100°C), retained its structure regardless of outer shell (PNIPAAm) changes. Thus, the movement of the drug out of a solid core was slower.

In addition to affecting drug loading and drug release, micellar core is also sensitive to physicological environment such as pH value in some cases (Lee and Na et al., 2003). Micelles composed of pH responsive components offered pH sensitivity that responds reversibly or irreversibly to changes in solution pH. As mentioned earlier, pH sensitivity allows the delivery system to be self-regulated. This is because the tumor extracellular pH is different from surrounding normal tissues. The measured pH values of most tumors are below 7.2. Moreover, there is a significant drop in the pH value intracellularly from pH 5.0-6.0 in endosomes to around pH 4.0-5.0 in primary and secondary lysosomes. Furthermore, a large number of lysosomal enzymes such as phosphatases and nucleases became active in the acidic environment of these vesicles. Therefore, the low pH values in extracellular tumor tissues, intracellular properties as well as the presence of lysosomal enzymes can be used for the development of new

polymeric nanocarriers which release drugs from pH sensitive micelles in specific tumor cells (Haag, 2004). Lee et al. (2003) reported pH sensitive micelles PEG-poly(L-histidine), where poly(L-histidine) acted as pH sensitive polymer. Mixed micelles prepared from poly(L-histidine) and PEG-PLA were destabilized in the pH range of 7.2-6.6, leading to accelerated DOX release.

2.3.7.4 Micelles for delivery of anticancer drugs

There are hundreds of anticancer drugs currently available for clinical application. Doxorubicin (DOX) and paclitaxel are most commonly used ones. However, since they are toxic to both tumor and normal cells, the efficacy of chemotherapy is limited by the serious side effects (Brigger and Dubernet, 2002). Because polymeric micelles offer a lot of advantages as discussed earlier, they seem to be one of the most promising carriers for the delivery of anticancer drugs.

Doxorubicin (DOX)

DOX is an anthracycline antibiotic that exerts its effects on cancer cells *via* inhibiting the synthesis of DNA as well as DNA transcription (Yoo and Park, 2000). DOX has undesirable side effects such as cardiotoxicity and myelosupression, which lead to a limited therapeutic efficacy. A number of studies have been conducted to target DOX delivery to cancer tissues using polymeric micelles. Kataoka's research team reported a novel amphiphilic block copolymer PEG-poly(β-benzyl-L-aspartate) (PEG-PBLA) synthesized from the ring-opening polymerization of (β-benzyl-L-aspartate *N*-carboxy-anhydride (BLA-NCA) (Nakanishi et al., 2001). DOX was physically loaded into PEG-

PBLA micelles, which was proved via GPC. It is noteworthy that DOX entrapped in micelles interacted only slightly with serum, making them stable in body. However, free DOX readily interacted with serum in aqueous solutions. Kataoka's research team also developed pH-sensitive micelles based on PEG-Pasp (poly(aspartate-hydraxzone-adriamycin) block copolymer for DOX delivery. DOX was conjugated with PEO-*b*-PAsp through an acid-labile hydrazone linker (Bae et al., 2003). Release kinetics demonstrated the effective cleavage of the hydrazone bonds at pH $\leq$ 5 with release of DOX. The released DOX molecules accumulated in the cell nuclei and effectively suppressed the growth of cancer cells. However, the release was negligible under physiological conditions in the cell culture medium (pH 7.4). Compared to the chemical conjugated approach, physical entrapment of drugs offer more advantages including easy preparation and enhanced drug bioavailability. For example, DOX was physical loaded into micelles prepared from PEG-PBLA with a high drug loading level of 15% and particle size of 50-70 nm. Blood circulation of DOX was greatly improved by use of PEG-PBLA micelles as carrier. Most of all, DOX loaded micelles showed a considerably higher antitumor activity compared to free DOX against mouse C26 tumor by intravenous injection (Kaotaoka and Matsumot et al., 2000). Recently, Okano's group have developed thermo-responsive micelles from poly(*N*- isopropylacrylamide) with various cores. In a study by his group, temperature responsive micelles prepared from PNIPAAm-PBMA were developed (Chung et al., 1999). Both blank micelles and DOX loaded micelles showed a dramatic thermo-responsive on/off switch behavior for both drug release and *in vitro* cytotoxicity, resulting from temperature responsive structural changes of a micellar shell. Furthermore, the properties of micelles also depended on the core block, which was

presented in Section 2.3.7.3. The micelles self-assembled from PEG-PCL block copolymers were also studied for DOX delivery (Shuai and Ai et al., 2004). The micelles size was greatly affected by PLC length. The micelle diameter increased from 22.9 nm to 104.9 nm with an increased PCL length in the copolymer composition. No hemolysis observed with DOX-loaded PEG-PCL micelles, indicating they were very stable in the blood. More recently, an effective ligand (cRGDfK) was conjugated to the surface of DOX-loaded PEG-PCL micelles for active targeting (Nasongkla et al., 2004). A remarkable increase in the uptake of ligand-conjugated micelles in the cells was observed. A higher density of ligand molecules led to a higher level of cellular internalization of these micelles *via* receptor-mediated endocytosis.

Paclitaxel

Paclitaxel is a unique antimicrotubule agent that promotes polymerization of tubululin, leading to cell death by disrupting the dynamics necessary for cell division. It is a promising anticancer drug with special effects against breast and ovarian cancers, colon and non-small cell lung cancers. One major limitation of paclitaxel is its difficulty in clinical administration. Paclitaxel is highly hydrophobic with water solubility less than 0.5ppm. Paclitaxel is thus formulated in a 50:50 mixture of Cremophor EL (polyoxyethylated castor oil) and dehydrated alcohol. However, Cremophor EL is very toxic and shows side effects such as hypersensitivity reactions, nephrotoxicity and neurotoxicity. Formulation strategies based on polymeric micelles have been studied. Several reports have showed controllable encapsulation and high antitumor of paclitaxel-loaded micelles based on biodegradable block copolymers such as PEG-PLA and PEG-

PCL. It was reported that up to 25% of paclitaxel was successfully loaded into PEG-PLA micelles (Zhang and Jackson et al., 1996). It is demonstrated that the solubilization of paclitaxel in the core of micelles did not alter the chemical nature of drugs. PCL is another interesting core forming block. PEG-PCL micelles with high drug loading (20%) and narrow size distribution were obtained. In addition, these blank micelles showed low *in vivo* toxicity using male ICR mice (Kim and Lee, 2001). To further enhance stability of micelles, PEG-PCL micelles were cross-linked by radical polymerization of the double bonds introduced into the PCL blocks. Both encapsulation efficiency and stability increased markedly (Shuai and Merdan et al., 2004). Additionally, efficient cellular internalization of fluorescence-labeled paclitaxel encapsulated in these cross-linked micelles was observed. In addition to polyester, lipid was used as hydrophobic blocks, which can provide additional advantages for enhancing micelles stability. A series of PEG-phosphatidylethanolamine (PEG-PE) conjugates was synthesized using egg PE (transphosphotidylated) and *N*-hydroxysuccinimide esters of methoxy-PEG succinates (Torchilin, 2001). Paclitaxel can be efficiently loaded into PEG-PE micelles. In addition, it was found that they can accumulate in certain tumors *via* the EPR effect more efficiently compared to other carriers because of their small size (Gao and Lukyanov et al., 2002). Another important finding is a novel formulation of PEG-PE/ePC mixed micelles loaded with paclitaxel and conjugated with 2C5 antibody. These micelles could recognize a variety of tumor cells *in vitro* and showed a dramatically enhanced cytotoxicity against tumor cells.

Various other examples of polymeric micelles for anticancer drug delivery can be found in literature. Because of their superior advantages including small size, high solubility, simple sterilization and controlled release of drugs, polymeric micelles are expected to be an ideal carrier for chemotherapy with the best efficacy and the least side effects in near future.

2.4 Motivation and research objectives

As reviewed in this chapter, polymeric controlled drug delivery systems offer sustained drug delivery in a constant release rate. However, such an approach may not be sufficient in some therapy situations. These include the delivery of proteins and cancer chemotherapy. It would be desirable that polymer systems could be further optimized to release increased levels of drugs when needed. Several research groups have been developing responsive systems in which drug release can be tailored according to physicological needs.

Temperature sensitive carriers have been widely used in drug delivery area such as protein delivery and anticancer drug delivery. Previous studies have used PNIPAAm-based hydrogels for protein delivery, and it has been proven that protein release has responded to the temperature changes. However, PNIPAAm hydrogels are not degradable and their monomers and cross-linkers may be toxic. Another major limitation of hydrogels is that surgery may be required to implant or remove the system. As reviewed in the previous section, polymeric microspheres are an attractive carrier for protein delivery because they can be used to protect protein against degradation and

administered *via* injection, avoiding the use of surgery. However, there is a big problem facing protein delivery from PNIPAAm microspheres. Since PNIPAAm is a highly hydrophilic polymer, PNIPAAm microspheres can only be fabricated with the inverse emulsion method. This method uses an organic solvent as a medium, leading to the inactivity of the protein during fabrication. To overcome this problem, a hydrophobic polymer poly(lactide-*co*-glycolide) (PLGA, the most widely used polymer with superior biocompatibility and biodegradability) or polylactide (PLA) (Rahman and Mathiowitz, 2004) is built into the PNIPAAm chain. By doing so, a block copolymer can be formed and this copolymer is more hydrophobic than PNIPAAm alone. Therefore, we can use double emulsion instead of inverse emulsion to fabricate thermo-responsive microspheres. Unlike the inverse emulsion method, the double emulsion requires a mild environment, which may stabilize the protein and enhance protein encapsulation efficiency.

It was also shown in the previous section that thermo-responsive micelles have been used to deliver anticancer drugs. An *in vitro* study on DOX-loaded PNIPAAm-*b*-PBMA micelles showed that the release rate of DOX from the micelles was much higher when the temperature was above the LCST than below the LCST. Due to enhanced drug release and increased interaction between micelles and the cells, the micelles expressed high cytotoxicity against tumor cells above the LCST (Chung et al., 2000). However, so far, most cores reported for the thermo-responsive micelles are all non-degradable. In order to be considered as clinically relevant drug carriers, the core must be both biocompatible and biodegradable. Hence, it is desirable to develop temperature sensitive

micelles with biodegradable cores. Kohori et al. (1999) used poly(D,L-lactide) as the core-forming segment, which is biodegradable. Nevertheless, the encapsulated doxorubicin (DOX) release was very slow at temperatures both below and above the LCST. It might be due to the high hydrophobicity of the inner core of the micelles. It is desirable that the properties of the core-forming block can be tailored to achieve desired release profiles.

In addition, temperature responsiveness of micelles can be triggered by pH change in the environment without external heating via a pH sensitive core-forming block (Soppimath et al., 2005).

The objective of this study is to systematically study two biodegradable thermo-responsive drug carriers and explore their applications in controlled delivery of proteins and anticancer drugs. The specific objectives of this study are:

1. To synthesize and characterize thermo-responsive PNIPAAm-*b*-PLA and P(NIPAAm-*co*-DMAAm)-*b*-PLGA block copolymers.
2. To prepare bovine serum albumin (BSA, a model hydrophilic protein)-loaded microspheres using the PNIPAAm-*b*-PLA block copolymer by the double emulsion method, and to study the degradation of the microspheres and *in vitro* protein release from microspheres.
3. To fabricate the anticancer drug (DOX) and paclitaxel-loaded micelles using the P(NIPAAm-*co*-DMAAm)-*b*-PLGA block copolymer by the dialysis method, to investigate the stability of the micelles under physiological

conditions and to examine the effect of hydrophobic content on the drug loading, morphology of micelles, *in vitro* anticancer drug release and to study cytotoxicity of drug-loaded micelles against various animal and human cancer cells at different temperatures as well as cellular uptake of doxorubicin-loaded micelles.

4. To synthesize a multifunctional polymer, folate conjugated poly(*N*-isopropylacrylamide-*co*-*N,N*-dimethylacrylamide-*co*-methacrylate)-*b*-poly(10-undecenoic acid) and to fabricate DOX-loaded micelles for specific and intracellular delivery of anticancer drugs to tumor cells, to examine *in vivo* DOX biodistribution using a nude mice xenograft model.

CHAPTER THREE

MATERIALS AND METHODS

The materials and methodology employed in the course of the research project are presented as follows. Included are the methods for polymer synthesis, microspheres and micelles fabrication as well as analyses.

3.1 Materials

N-isopropylacrylamide (NIPAAm, purchased from Sigma-Aldrich) was purified by re-crystallization from n-hexane. *N, N*-dimethylacrylamide and 10-undecenoic acid (98%) was purchased from sigma and pre-vacuum distilled before use. D, L-lactide was bought from Sigma-Aldrich and purified by re-crystallization from ethyl acetate. Poly(D,L-lactide) (PLA) and glycolide (99.0%) was purchased from Polyscience. Bovine serum albumin (BSA) (fraction V, 58 kDa), poly(vinyl alcohol) (PVA, 87-89 mol % hydrolyzed, Mw 31,000-50,000), fetal serum albumin (FBS) were supplied from Invitrogen Corporation. Doxorubicin hydrochloride (DOX), paclitaxel, pyrene, 2-hydroxyethanethiol, 3-mercaptopropionic acid (MPA), 2-aminoethyl methacrylate hydrochloride (90%), 2-hydroxyethanethiol, 2-aminoethanethiol (AET), *N*-hydroxysuccinimaide (NHS), dicyclohexylcarbodiimide (DCC), tin(II)2-ethylhexanoate, 3-[4,5-dimethylthiazolyl-2]-2,5-diphenyl tetrazolium bromide (MTT), L-glutamine, acetonitrile (HPLC grade), anhydrous dichloromethane (DCM), anhydrous dimethyl sulfoxide (DMSO), *N*, *N*-dimethylacetamide (DMAc), methanol(HPLC grade), dichloromethane (DCM) and dimethylformamide (DMF) were purchased from Sigma-Aldrich, and used as received. Ammonium persulphate (APS) was purchased from Bio-Rad Laboratories. Tetrahydrofuran (THF) and toluene were purchased from Merck, and dried over sodium. 4T1 (mouse breast cancer cell line) were purchased from ATCC.

MDA-MB-435S (human breast carcinoma cell line) was purchased from Interlab Cell Line Collection (Italy). All other chemicals were of analytical grade, and used as received.

3.2 Polymer synthesis

3.2.1 Synthesis of poly(*N*-isopropylacrylamide-*co*-*N, N*-dimethylacrylamide)-*b*-poly(D,L-lactide-*co*-glycolide) ((P(NIPAAm-*co*-DMAAm)-*b*-PLGA)

The diblock copolymers with different contents and compositions of PLGA were synthesized (Figure 3.1) according to the method reported previously (Kohori et al., 1998; Liu and Yang, 2003). Briefly, hydroxyl-terminated poly(*N*-isopropylacrylamide-*co*-*N, N*-dimethylacrylamide) precursor polymer was prepared by the radical copolymerization using benzoyl peroxide (BPO) as an initiator and 2-hydroxyethanethiol as a chain transfer agent (CTA). For instance, *N*-isopropylacrylamide (20.0 g, 176.9 mmol), *N, N*-dimethylacrylamide (4.37 g, 44.2 mmol), 2-hydroxyethanethiol (172.5 mg, 2.21 mmol) and BPO (89.2 mg, 0.295 mmol) were dissolved in 30 mL THF. The solution was degassed by bubbling with nitrogen for 20 minutes. The reaction mixture was refluxed for 8 hours under nitrogen. Upon completion, the product was precipitated out by the addition of diethyl ether. The products were purified by re-precipitation twice from dichloromethane-diethyl ether using a slow liquid-liquid diffusion method. The diblock copolymers of P(NIPAAm-*co*-DMAAm)-*b*-PLGA were synthesized by the ring-opening esterification polymerization of D,L-lactide (LA) and glycolide (GA) with the hydroxy-terminated precursor in toluene using tin(II) 2-ethylhexanoate as the catalyst. It should be noted that all monomers and precursor polymer should be dried at vacuum oven before reaction. The reaction mixture was refluxed at 120°C for 24 hours under

nitrogen. The reaction mixture was refluxed at 120°C for 24 h under nitrogen (Figure 3.1). The ^{1}H-NMR spectra of the polymers were recorded using a Bruker Avance 400 spectrometer (400 MHz), and chloroform-d ($CDCl_3$) was used as the solvent. Chemical shifts were expressed in parts per million (δ) using residual protons in the indicated solvents as the internal standards. The IR spectra were recorded on a Fourier transform infrared spectrometer (Perkin-Elmer Spectrum 2000, KBr). The molecular weight was determined by gel permeation chromatography (GPC, Waters, polystyrene standards) in THF (elution rate: 1ml/min) at 25°C. Optical transmittance of aqueous polymer solution (5 mg/mL) at various temperatures was measured at 500 nm with a UV–VIS spectrometer (Shimadzu, UV-2501PC, Japan). Sample cells were thermostated with a temperature-controller (Shimadzu, TCC-240A, Japan). Heating rate was 0.1°C/min. The LCST values of polymer solutions were determined at the temperatures showing an optical transmittance of 50%. The properties of the precursor polymers and the resulting block copolymers are listed in Tables 4.1.

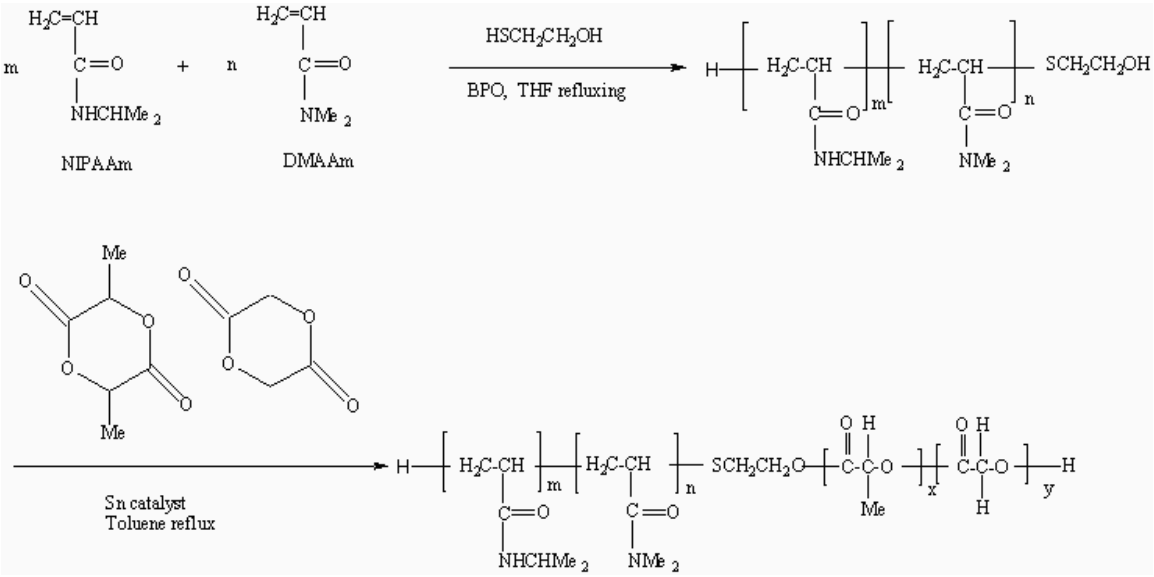

Figure 3.1 Synthesis route of P(NIPAAm-*co*-DMAAm)-*b*-PLGA

3.2.2 Synthesis of folate-conjugated poly(*N*-isopropylacrylamide-*co*- *N, N*-dimethylacrylamid-*co*-methacrylate)-*b*-PUA (Poly(NIPAAm-*co*-DMAAm-*co*-MAm)-*b*-PUA)

3.2.2.1 Synthesis of Poly(NIPAAm-*co*-DMAAm-*co*-MAm)-COOH

Carboxylic acid-terminated poly(*N*-isopropylacrylamide-*co*- *N, N*-dimethylacrylamide) precursor polymer was prepared by the radical copolymerization using benzoyl peroxide (BPO) as an initiator and 3-mercaptopropionic acid as a chain transfer agent. For instance, *N*-isopropylacrylamide (20.0 g, 176.9 mmol), *N, N*-dimethylacrylamide (3.50 g, 35.38 mmol), 2-aminoethyl methacrylate hydrochloride (90%) (158.4mg, 0.86 mmol), MPA (269mg, 2.54mmol) and BPO (85.6 mg, 0.35 mmol) were dissolved in 30 mL THF (Figure 3.2). The solution was degassed by bubbling with nitrogen for 20 minutes. The reaction mixture was refluxed for 8 h under nitrogen at 85°C. Upon completion, the product was precipitated out by the addition of diethyl ether. The products were purified by re-precipitation three times from THF-diethyl ether using a slow liquid-liquid diffusion method and then vacuum dried. Then, it was placed in a dialysis membrane (Spectra/Por 7, MWCO 2000, Spectrum Laboratories Inc.) and dialyzed against distilled water for 1 week. The dialyzed solution was freeze-dried.

3.2.2.2 Synthesis of folate-conjugated Poly(NIPAAm-*co*-DMAAm-*co*-MAm)-COOH

The carboxylic acid group of folic acid (1.0g, 2mmol) dissolved in 20 ml DMSO was pre-activated with DCC (0.495g, 2.4mmol) and NHS (0.463g 4mmol) at room temperature (Figure 3.3 (a)). In the reaction, dicyclohexylurea (DCU) was formed and removed by filtration. The vacuum-dried precursor polymer was added to the reaction solution (Figure 3.3(b)). The reaction was kept at room temperature for 48 h. The

resulting solution was placed in a dialysis membrane (Spectra/Por 7, MWCO 2000, Spectrum Laboratories Inc.) and dialyzed against distilled water for 1 week. The dialyzed solution was then freeze-dried.

3.2.2.3 Synthesis of poly(10-undecenoic acid)-NH_2

Amine group-terminated poly(10-undecenoic acid) precursor polymer was prepared by the radical copolymerization using the redox agent ammonium persulfate (APS) as an initiator and 2-aminoethanethiol as a chain transfer agent. Briefly, 10-undecenoic acid (40.0 g, 217.0mmol) was first converted into sodium salt by reacting with sodium hydroxide solution (0.1M), the pH of the solution was adjust to 8.0. The solution was bubbled with N_2 for overnight. Then, AET (2.0%-2.5% molar ratio) and APS (4% mass ratio) were added to the solution with stirring (Figure 3.4). The reaction was kept at 70°C for 48 h. Upon completion, the crude product was precipitated by the addition of cold ethanol. The pale yellow power was obtained after filtration. It was re-dispersed three times in ethanol to remove un-reacted monomer. The product was dialyzed against distilled water (Spectra/Por® C E, MWCO 1000, Spectrum Laboratories Inc.) to remove salt. The final white product was obtained by freeze-drying.

3.2.2.4 Conjugation of poly(10-undecenoic acid)-NH_2 to folate-conjugated poly(NIPAAm-*co*-DMAAm-*co*-MAm)-COOH

The carboxylic acid group of folate-conjugated poly(NIPAAm-*co*-DMAAm-*co*-MAm)-COOH (1 mmol) was activated using DCC (1.2 mmol) and NHS (2 mmol) in DCM. DCU was removed by filtration and excess diethyl ether was added to precipitate the activated folate-conjugated poly(NIPAAm-*co*-DMAAm-*co*-MAm)-COOH. The vacuum dried products and an excess amount of poly(10-undecenoic acid)-NH_2 were dissolved in

DMSO and stirred at room temperature for 48 h (Figure 3.5). The un-reacted poly(10-undecenoic acid)-NH_2 was removed by dialysis against DMSO for 1 week (DMSO was replenished daily, dialysis membrane with a Mw cut-off of 3,500 Da). The solution in the dialysis tubing was further dialyzed against de-ionized (DI) water for another week. The final yellowish product was obtained by freeze-drying. The final product was characterized by GPC, ^{1}H-NMR, FTIR and titration.

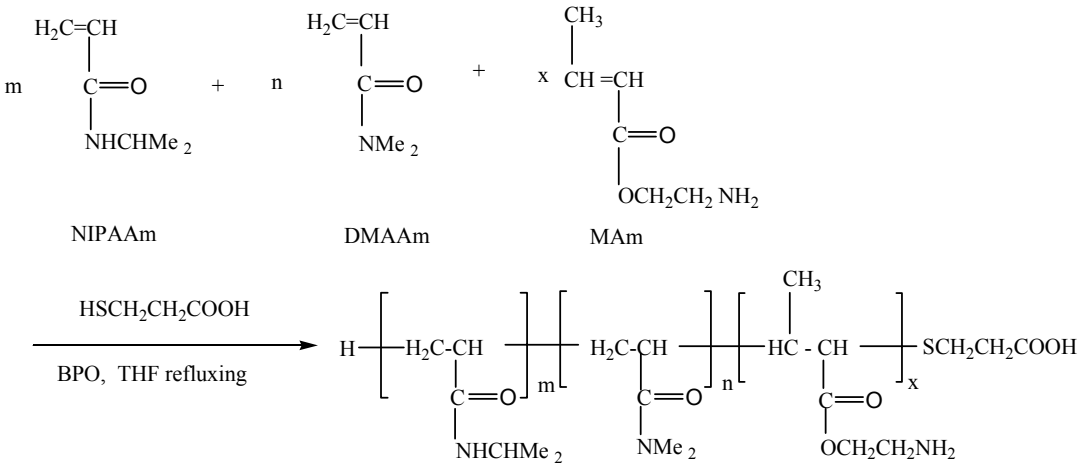

Figure 3.2 Synthesis poly(*N*-isopropylacrylamide-*co*- *N, N*-dimethylacrylamid-*co*-methacrylate)-COOH

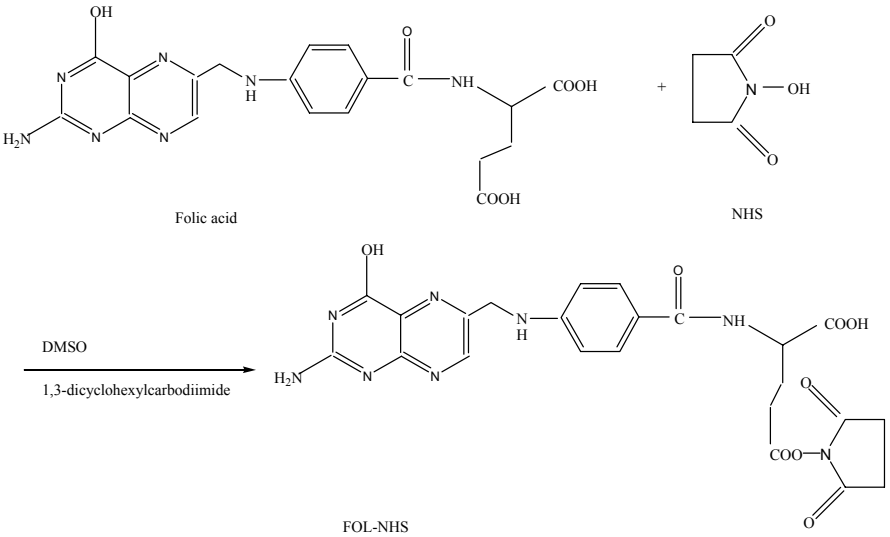

(a)

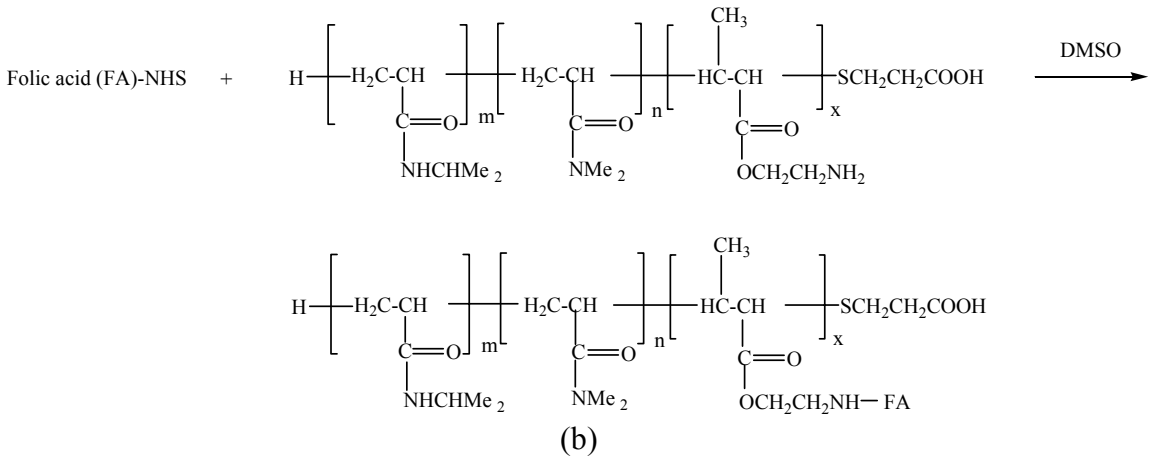

(b)

Figure 3.3 Synthesis folate-conjugated Poly(NIPAAm-*co*-DMAAm-*co*-MAm)-COOH. (a) activation of folic acid; (b) conjugation of folic acid to Poly(NIPAAm-*co*-DMAAm-*co*-MAm)-COOH

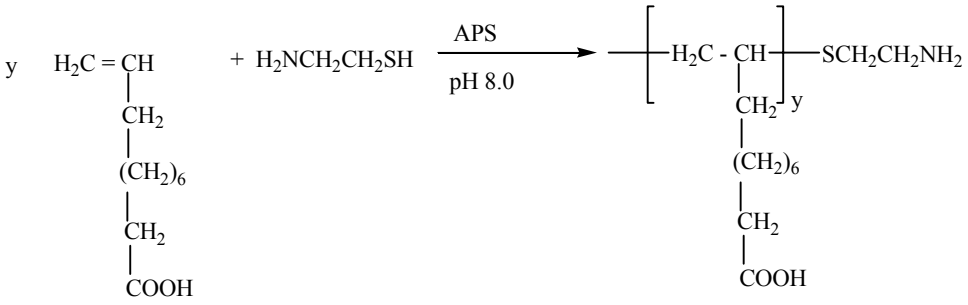

Figure 3.4 Synthesis of poly(10-undecenoic acid)-NH_2

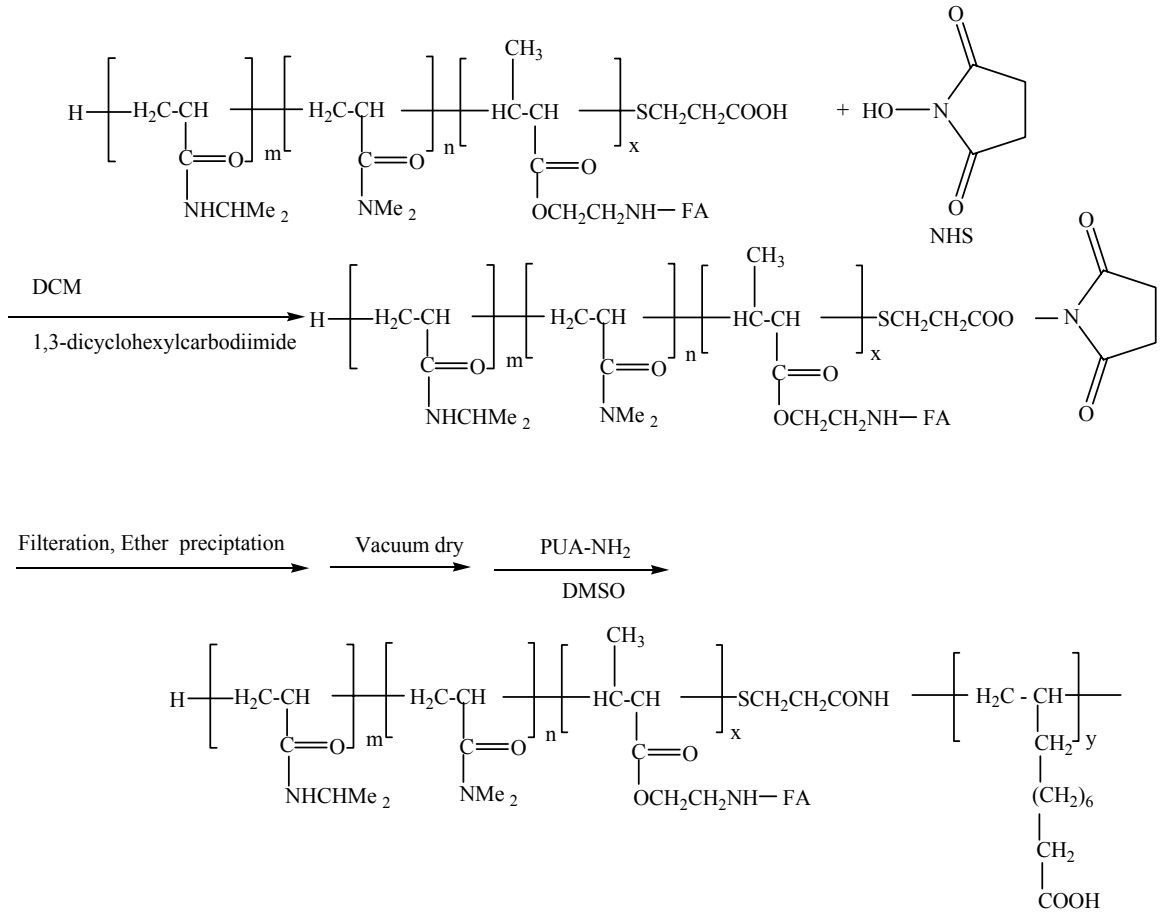

Figure 3.5 Conjugation of poly(10-undecenoic acid)-NH_2 to folate-conjugated Poly(NIPAAm-*co*-DMAAm-*co*-MAm)-COOH

3.3 Microspheres

3.3.1 Microspheres preparation

BSA-loaded micropsheres were fabricated using PNIPAAm-*b*-PLA and PLA polymers by a W/O/W double emulsion solvent evaporation method. Briefly, 600 mg polymer was dissolved in 12 mL DCM. 70 mg BSA was dissolved in 0.3 mL PBS containing 0.05% or 0.2% (w/v) PVA (the internal aqueous phase). The two solutions were mixed and sonicated for 20 seconds using a VC sonicator (Sonics & Materials Inc., CT, USA) to produce the first emulsion (water-in-oil, W/O). This emulsion was poured into 250 mL

PBS containing 0.2% (w/v) PVA to produce a double emulsion (water-in-oil-in-water, W/O/W). The solution was kept at 15°C, and stirred for 3.5 hours using a mixer (Cole-Parmer Instrument Co., IL, USA) with the stirring speed of 300 rpm. The resultant microspheres were filtered, washed and vacuum-dried overnight and stored at 4°C. The fabrication process was illustrated in Figure 3.6. The abbreviation, PNIPAAm-*b*-PLA (1:5, 0.2%), represents the microspheres fabricated with PNIPAAm-*b*-PLA having 1:5 molar ratio of PNIPAAm to PLA and 0.2% (w/v) PVA in the internal aqueous phase.

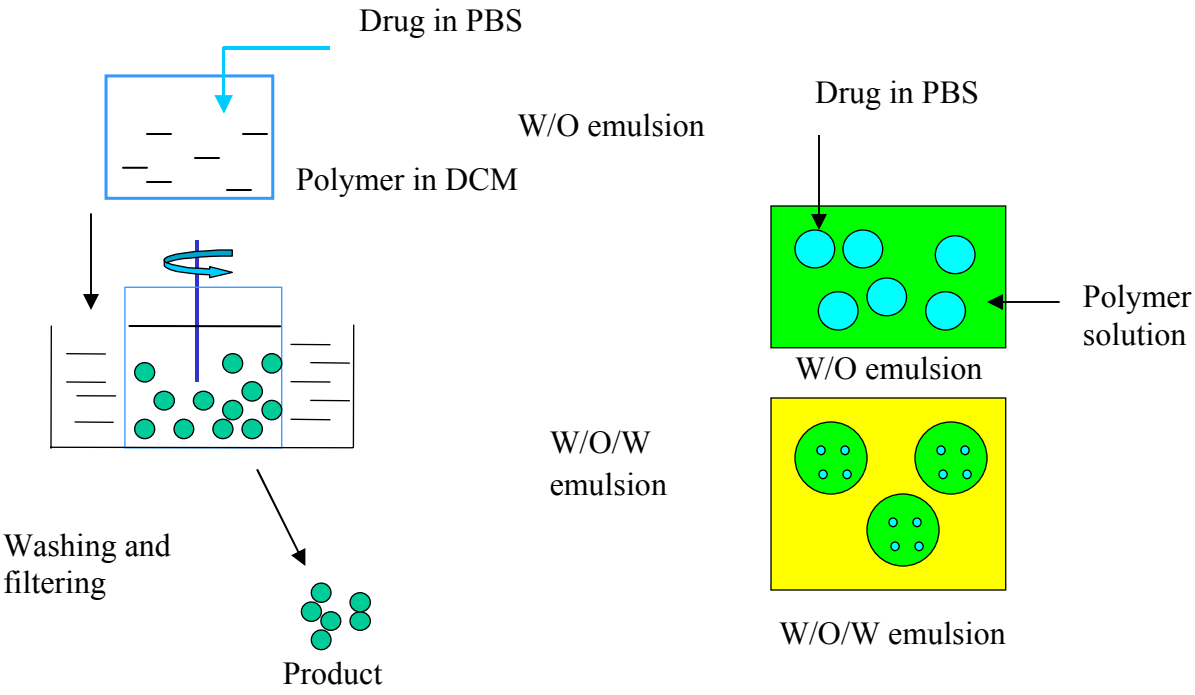

Figure 3.6 Microspheres fabrication using W/O/W emulsion technique

3.3.2 Characterization and analyses of microspheres

3.3.2.1 Evaluation of protein encapsulation efficiency

The BSA amount lost in the external aqueous phase during the fabrication process was analyzed by a high performance size exclusion chromatography (HPSEC). The HPSEC system consisted of a 1050 Quatern Pump, an 1100 autosampler injector and a Diode-Array UV detector. A Zorbax GF-250 column (4.6 mm × 25 cm, Dupont Company) was used as the separation column. The flow rate of the mobile phase (PBS, pH 7.0) was 1.0 mL/min, and the UV detection was at 210 nm. The encapsulation efficiency multiplied by 100% was calculated as the ratio of actual and theoretical BSA content. In this study, a confocal laser scanning microscope (Olympus FV500, Japan) was used to observe BSA distribution within the microspheres using BSA-FITC. An excitation wavelength of 488 nm was employed and an emission signal at 525 nm was detected. The laser power was 10%. All the observations were conducted using the same resolution.

3.3.2.2 Inherent viscosity (η_{inh}) measurement

The inherent viscosity of polymer in methylene chloride was determined according to ISO/DIS 3105 and ASTM D2515/D446 using the Schott Gerate AVS360, Viscometer: DIN Ubbelohde (Type: Capillary No. 52510/I Appt. No. 904473) at 25 °C. The inherent viscosity is calculated using the equation 3.1 as following:

$$\eta_{inh} = \ln (t/t_0)/C \qquad (3.1)$$

where t_0 is flow time of solvent, t is flow time of polymer solution and C is the concentration of the sample in g/dL. 600 mg of solid polymer was dissolved in 12 ml of solvent and filtered before being filled into the viscometer. Sample concentration was 0.5 g/dL.

3.3.2.3 Particle size analysis

The mean diameter and particle size distribution of the dried microspheres were measured using a laser light-scattering particle size analyzer (Coulter LS 230, a

microvolume module, Coulter Corporation, USA) after soaking the microspheres in an aqueous solution..

3.3.2.4 Morphological analysis

The surface and internal morphologies of the micropsheres were observed using a scanning electron microscope (SEM, Model JSM-5600, Tokyo, Japan). Microspheres and their sectioned samples were mounted on metal holders, and vacuum coated with a gold layer prior to SEM examination.

3.3.2.5 Chemical composition of the microspheres surface

The X-ray photoelectron spectroscope (XPS) was employed to investigate the chemical composition of the microspheres surface. The XPS measurements were performed using a VG ESCA LAB 220I-XL spectrometer with a magnesium anode source producing Mg K_α (1253.6 eV photons) X-ray with the pass energy of 20 eV for high-resolution narrow scans and 150 eV for low-resolution wide scans. The XPS data analysis was carried out using the software from VG ESCA LAB. To compensate for surface charges, all XPS binding energies were referred to the adventitious C 1s peak at the binding energy of 285.0 eV. Atomic concentration was determined from the peak areas under each peak component and correcting using the manufacturer's atomic sensitivity factors (ASF) with an estimated maximum error of ±5%. Spectral curve fitting was performed using the manufacturer-supplied software.

3.3.2.6 Elemental analysis

The composition of PLA, PNIPAAm, PNIPAAm-*b*-PLA and BSA was studied by elemental analysis using Perkin-Elmer Instruments Analyzer 2400.

3.3.2.7 FT-IR spectrum

A Fourier transform infrared spectrophotometer (FT-IR, Perkin-Elmer Spectrum 2000) was employed to explore the interactions between BSA and polymer. The samples were pressed into potassium bromide pellets prior to FTIR analysis.

3.3.2.8 Water uptake studies

A fixed amount of micropsheres was incubated in PBS (pH 7.4) at 37°C or 22°C (room temperature). The weight of the micropsheres was measured at predetermined time intervals. Water uptake was calculated from the following formula:

$$\text{Water update (\%)} = [(W_w - W_d)\times 100]/ W_d,$$

where W_w represents the weight of wet samples, W_d represents the weight of the dried samples.

3.3.2.9 *In vitro* protein release

In vitro BSA release analyses of microspheres were carried out in triplicate in PBS buffer (pH 7.4) at 37°C or 22°C. 40 mg of the dried microspheres were suspended in 1 mL PBS buffer. The medium for each sample was periodically removed, and replenished with fresh PBS buffer. The BSA content in the medium was analyzed using HPSEC as described in Section 3.3.2.1.

3.3.2.10 *In vitro* weight loss

170 mg of the dried microspheres were immersed in 5 mL PBS buffer at 37°C. The supernatant from each sample was removed, and replenished with fresh PBS periodically. At preset time intervals, samples were separated, and freeze-dried to constant weight. Mass loss was then examined gravimetrically.

3.3.2.11 Nuclear magnetic resonance (NMR)

The ^{1}H-NMR spectra of the degrading microspheres were studied using a Bruker Avance 400 spectrometer (400 MHz), and chloroform-d ($CDCl_3$) was used as the solvent.

3.3.2.12 Molecular weight determination

Molecular weights of the polymers and degrading microspheres were determined by a gel permeation chromatography (GPC) (Waters 2690, MA, USA) with a Differential Refractometer Detector (Waters 410, MA, USA). The mobile phase used was THF with a flow rate of 1 mL/min. Weight average molecular weights as well as polydispersity indices were calculated from a calibration curve using a series of polystyrene standards (Polymer Laboratories Inc., MA, USA, with molecular weight ranging from 1350 to 151,700).

3.3.2.13 Specific surface area and pore size analyses

The specific surface area and pore size analyses were carried out using a Nova 3000 analyzer (Quantachrome Instruments Corporate, FL, USA). Sorption measurements were performed using ultra-pure nitrogen gas as the adsorbate and liquid nitrogen as a coolant. Surface area was calculated by the Brunauer-Emmett-Teller (BET) method using 6 adsorption points in the p/p0 range of 0.05- 0.3. Average pore diameter was determined by the Barrett, Joyner and Halenda (BJH) method using 6 desorption points in the p/p0 range of 0.995-0.3 (Crotts and Sah et al., 1997). Data analysis was performed using Nova Enhanced Reduction Software Version 2.13.

3.4 Micelles

3.4.1 Micelles preparation and evaluation of encapsulation efficiency as well as drug loading capacity

3.4.1.1 DOX-Loaded micelles

Blank and DOX-loaded micelles were prepared by a membrane dialysis method. For blank micelles, the block copolymer (20 mg) was dissolved in 4 mL DMAc. The solution was then dialyzed against DI water at 20°C for 24 hours using a dialysis membrane with a molecular weight cut-off of 2,000 Da (Spectra/Por 7, Spectrum Laboratories Inc.). The water was replaced hourly for the first 3 hours. For DOX-loaded micelles, the block copolymer (20 mg) was dissolved in 2 mL of DMAc. DOX (10 mg) was neutralized with two moles excess triethylamine in 2 mL of DMAc. The DOX solution was added into the polymer solution and mixed by vortex for 5 minutes. The mixture was dialyzed against DI water at 20°C for 48 hours using a dialysis membrane with a molecular weight cut-off of 2,000 Da. After dialysis, the solution in the dialysis bag was collected and filtered with 0.45 μm syringe filter and freeze-dried for two days. To determine DOX loading level, a known amount of DOX-loaded nanoparticles was dissolved in 1 mL of DMAc. The DOX concentration was estimated by using the UV–VIS spectrophotometer at 485 nm. The drug loading was calculated based on the standard curve obtained from DOX in DMAc. The yield of micelles was calculated as the weight ratio of micelles recovered to initial polymer and drug.

3.4.1.2 Paclitaxel-loaded micelles

Paclitaxel-loaded micelles were prepared by dialysis method. 20 mg of polymer was dissolved in 4 ml of DMF, followed by addition of Paclitaxel. This solution was dialysis against de-ionized water for 24 h. The water was replaced hourly at the first 3 hours. After dialysis, the solution in the dialysis bag was collected and filtered with 0.45 μm syringe filter and freeze-dried for two days. 2 mg of drug-loaded micelles was first

dissolved in 1 mL of Chloroform, and 3 mL of ether was added to precipitate the polymer. The suspension was centrifuged at 10000rpm for 5 min. The supernatant was removed and dried. The sample was first dissolved in 2 mL mobile phase, which was composed of ammonium acetate aqueous solution (20 mM), methanol and acetonitrile (volume ratio 35: 20: 45). Then paclitaxel content was analyzed using high performance liquid chromatography (HPLC). The HPLC system consisted of a Waters 2690 separation module and Waters 996 PDA detector (Waters corporation, USA). A Waters Symmetyshield^{TM} C_8 4.6×15.0 cm column fitted with C_8 guard column was used. The temperature of column and samples were set at 28°C and 20°C, respectively. The detection wavelength was set at 229 nm. A calibration curve was constructed to determine paclitaxel concentration in the range of 5 to 50 ppm and the r^2 value was 0.999. Drug loading level and encapsulation efficiency were calculated as the following formula: Actual loading level (wt %) = mass of drug in micelles / mass of polymer and drug after dialysis × 100 %; Encapsulation efficiency (wt %) = mass of drug encapsulated / mass of drug loaded × 100 %

3.4.2 Characterization and analyses of the micelles

3.4.2.1 Nuclear magnetic resonance (NMR)

The ^{1}H-NMR spectra of the core-shell structure of the micelles were studied using a Bruker Avance 400 spectrometer (400 MHz). Chloroform-d ($CDCl_3$) and D_2O, was used as the solvent, respectively.

3.4.2.2 Fluorescence measurements

The critical association concentration (CAC) of the block polymer in DI water and PBS was estimated by fluorescence spectroscopy using pyrene as a probe. Fluorescence

spectra were recorded by a LS50B luminescence spectrometer (Perkin Elmer, USA) at room temperature. Aliquots of pyrene solutions in acetone (6.16×10^{-5} M, 100 μL) were added to 15 mL volumetric flasks, and the acetone was allowed to evaporate. Then, 10 mL of polymer solutions with different concentrations ranging from 0.01 ppm to 500 ppm were added to the vials. The final pyrene concentration is 6.16×10^{-7} M. The solutions were equilibrated for 24 hours at 20 °C. The excitation spectra were recorded from 300 to 360 nm with an emission wavelength of 395 nm. Both excitation and emission bandwidths were set at 2.5 nm. The intensity ratios of $I_{336.5}$ to $I_{334.5}$ were plotted as a function of logarithm of polymer concentration. The CAC value was taken from the intersection of the tangent to the curve at the inflection with the horizontal tangent through the points at low concentrations.

3.4.2.3 Particle size and zeta potential analyses

The particle size and zeta potential of the micelles in PBS were measured by Zetasizer 3000 HAS (Brookhaven Instrument Ltd., US) equipped with a He-Ne laser beam at 658 nm (scattering angle: 90°). Each sample was filtrated with 0.45 μm syringe filter prior to analysis. The concentration of micelles in PBS buffer is 1.5 mg/mL. Each measurement was repeated 5 times. An average value was obtained from the five measurements. The effect of proteins was studied by measuring the size of micelles in PBS buffer containing 10 (v/v) % FBS at 37ºC. The size measurements were performed by multimodel analysis.

3.4.2.4 Transmission electron microscopy (TEM) examinations

The morphologies of the blank and DOX-loaded micelles were analyzed by TEM (Philips CM300, Holland). Several drops of the freshly prepared micelles solution containing 0.01 (w/v) % phosphotungstic acid were placed on a copper grid coated with carbon film and

air-dried at room temperature. The TEM observations were carried out with an electron kinetic energy of 300 k eV.

3.4.2.5 Atomic force microscopy (AFM)

AFM (Nanoscope, USA) was performed by the tapping mode, micelles solution was put on the silicon wafer and dried at room temperature, and then the wafer was attached on a metallic sample stand using double-sided adhesive tapes and scanned by the AFM maintained in a constant temperature and vibration-free environment.

3.4.2.6 Differential Scanning Calorimetry (DSC)

The melting temperature of pacitaxel and the Tg of block copolymer as well as drug loaded micelles were measured with DSC (2920 Modulated, TA instruments, USA). The measurements were carried out using standard at temperatures ranging from 20°C to 300°C with a heating rate of 20°C/min.

3.4.2.7 Wide angle X-ray diffractometer (WAXRD) measurement

X-ray diffraction (XRD) patterns were recorded using Bruker GADDS diffractometer with area detector operating under voltage of 40kV and current of 40mA using CuKa radiation (l=1.5418 nm).

3.4.2.8 Polymer degradation studies

The polymer (100 mg) was immersed in 3 mL PBS buffer (pH 7.4) at 37°C. The supernatant from each sample was removed, and replenished with fresh PBS buffer periodically. At preset time intervals, the samples were separated, and freeze-dried to constant weight. Mass loss was then examined gravimetrically. The molecular weights of the degraded samples were determined by GPC as described in 3.3.2.12.

3.4.2.9 In vitro drug release

(a) DOX-loaded polymeric micelles

The DOX-loaded micelles solutions prepared were diluted to 1 mg/mL. The diluted solutions (5 mL) were transferred to dialysis membrane tubes with a molecular weight cut-off of 10,000 (Spectra/Por 7, Spectrum Laboratories Inc.). The tubes were then immersed in a beaker containing 30 mL PBS buffer, which was shaken with a speed of 100 rev/min. The release of DOX from the micelles was measured at 37.0°C (below the LCST) and 39.5°C (above the LCST), respectively. At specific time intervals, 1 mL solution was withdrawn from the release medium and replaced with fresh PBS buffer. The DOX content in the samples was analyzed using the UV–VIS spectrophotometer at 485 nm.

(b) Paclitaxel-loaded polymeric micelles

The paclitaxel-loaded polymeric micelles solution was diluted to 1mg/mL. The solutions were (5 mL) transferred in a dialysis membrane tube (Spectra/Por® 7, MWCO =10, 000), and then the membrane was immersed in a beaker containing 50 mL PBS. The release of paclitaxel from micelles was measured under mechanical shaking (100 rev/min) incubated at 37°C (below the LCST) and 39.5°C (above the LCST), respectively. At specific time intervals, the entire medium was removed and replaced with fresh buffer. The extraction of paclitaxel was carried out by adding 5 mL of dichloromethane (DCM) into the collected medium. The mixture was then vigorously vortexed for 3 minutes and left for phase separation. The extraction efficiency was determined to be 62%. The organic phase was drawn out carefully and left to evaporate overnight. The samples were

dissolved in 2 mL of mobile phase and analyzed with HPLC as described in Section 3.4.1.2.

3.4.3 Cellular distribution and cytotoxicity test

3.4.3.1 *Cellular distribution*

The cover glass was put in the 24-well plate before cells were seeded. Free DOX (10 mg/L) and DOX-loaded polymer micelles (DOX concentration: 10 mg/L) in RPMI 1640 medium were incubated with 4T1 cells for 4 h before examination. The cells on the cover glass were thoroughly washed three times with PBS and visualized by CLSM (Olympus FV300, Japan). DOX was excited at 532 nm with emission at 595 nm. The laser power was 10%. All the observations were conducted using the same resolution. The image of MDA-MB-435S (human breast carcinoma cell line) cells followed the same protocol as 4T1 cells. It should be noted that the culture medium for MDA-MB-435S cells was DMEM medium.

3.4.3.2 Cytotoxicity test

The 4T1 mouse breast cancer cells (ATCC) were cultured in RPMI1640 supplemented with 10% FBS, 5% penicillin, 2 mM L-glutamine (Sigma) and incubated at 37°C, 5 % CO_2. The cells were seeded onto 96-well plates at 10, 000 cells per well and incubated for one day. Free DOX, DOX-loaded polymer D micelles in RPMI1640 were filtered with 0.22 μm syringe filters and diluted with the growth medium to give final DOX concentrations of 0.1, 1.0, 5.0, 10.0, 20.0, 30.0, 50.0mg/L. The blank polymer D micelles in RPMI1640 was filtered and diluted to 1, 10, 50.0 and 100.0, 300.0, 600.0 mg/L. The media in the wells were replaced with 100 μL of the pre-prepared samples. The plates

were then returned to the incubator and maintained in 5% CO_2, at 37°C and 39.5°C, for 48 hours.

Fresh growth media and 10 μL aliquots of MTT solution were used to replace the mixture in each well after the designated period of exposure. The plates were then returned to the incubator and maintained in 5% CO_2, at 37°C, for a further 3 hours. The growth medium and excess MTT in each well were then removed. DMSO (150 μL) was then added to each well to dissolve the internalised purple formazan crystals. An aliquot of 100 μL was taken from each well and transferred to a fresh 96-well plate. Each sample was tested in eight replicates per plate. Three plates were used for each period of exposure, making a total of 24 replicates per sample. The plates were then assayed at 550 nm and 690 nm. The absorbance readings of the formazan crystals were taken to be that at 550 nm subtracted by that at 690 nm. The results were expressed as a percentage of the absorbance of the blank control.

Similarly, cell cytotoxicity of free drugs, drug-loaded micelles against MDA-MB-435S followed the same protocol as that of 4T1 cells. It should be noted that the culture medium for MDA-MB-435S cells was DMEM medium.

3.4.4 Animal experiment

Female balb/c (body weight 19-21 g) was subcutaneously implanted at mammal with an ATCC 4T1 mouse breast cancer epidermal carcinoma xenograft cell line, (10^7 cells per animal). Tumors were allowed to grow for 2 weeks. Tumor volume was calculated using the formula: $(4/3)\pi a^2 b$ (Yoo and Park, 2004), where a and b are the length of minor

and major axis of tumor, respectively. It was found that the tumor volume ranged from 612.5 mm^3 to 864.3 mm^3. Free DOX and micelles containing equivalent amount of DOX were administrated through the tail vein of animals at an equivalent dose of DOX = 5 mg/kg. At 10min, 30 min, 2h and 4h, the animals were sacrificed and then liver, lung, heart, spleen, kidney, blood and tumor were removed and kept at freezer (-80°C) for future analysis. The organs were weighted and homogenized. DOX distributed in different organs was extracted using chloroform and isopropanol and analyzed as described in literature (Yoo and Park, 2004). Briefly, homogenized tissue was added into an acidic hydrolysis buffer containing 2.0 M HCl solution at 80°C for 10 min. Supernatant was collected and then, 0.9 ml of chlorform: isopropanol (3:1, v/v) was added. After vigorous vortex-mixing, an organic layer was collected by centrifugation at 16000 rpm for 15 min at room temperature. The solution was dried and redissolved in mobile phase and analyzed by HPLC. The HPLC system consisted of a Waters 2690 separation module and Waters 2475 multi λ Fluorescence detector. The mobile phase was composed of 0.01% trifluoroacetic acid aqueous solution and acetonitrile; increasing the percentage of aceonitrile from 5% to 45% in 40 min. DOX peak was detected at an excitation wavelength of 480 nm and an emission wavelength of 580 nm.

CHAPTER FOUR

RESULTS AND DISCUSSION 1:

P(NIPAAm)-*b*-PLA Microspheres

4.1 Introduction

The rapid development of protein and peptide based drugs in the recent years has spurred a great demand for suitable delivery carriers, which are able to protect the proteins from hostile environment and to manipulate the protein release utilizing environmental stimuli such as temperature changes. Poly(*N*-isopropylacrylamide) (PNIPAAm) shows a well defined LCST at about 32^{o}C. PNIPAAm in an aqueous solution has reversible solubility and exhibits a remarkable hydration-dehydration change in response to temperature. Below the LCST, PNIPAAm is well soluble in water. However, as the temperature is increased above the LCST, it becomes hydrophobic and precipitates out from the aqueous solution. The LCST can be adjusted by introducing a hydrophobic or hydrophilic segment to PNIPAAm (Chen and Hoffman, 1995; Yoshida et al., 1994). Many researchers have examined the potential of PNIPAAm-based hydrogels for encapsulating and delivering proteins (Yeh et al., 1995; Bittner et al., 1999; Pistel et al., 2001).

Recently, there has been an increasing research interest on the development of protein delivery systems using poly(lactide) (PLA) and poly(lactide-co-glycolide) (PLGA) microspheres because of their superior biodegradability and biocompatibility as well as easy administration (Cohen et al., 1991; Lam et al., 2000; Kostanski et al., 2000; Cleand et al., 2001; Shive and Anderson, 1997). However, the release pattern of protein-loaded PLGA microspheres was characterized as an initial burst followed by a non-release. To circumvent this problem, several approaches have been explored in order to accelerate protein diffusion and polymer erosion by blending or copolymerization with

poly(ethylene glycol) (PEG) or poly(vinyl alcohol) (Yeh et al., 1995; Bittner et al., 1997; Pistel et al., 2001).

The aim of my study in protein delivery was to explore the possibility of using PNIPAAm-*b*-PLA microspheres. Specifically, PNIPAAm-*b*-PLA with different PNIPAAm contents were synthesized, and utilized to fabricate microspheres containing bovine serum albumin (BSA) by a water-in-oil-in-water (w/o/w) double emulsion solvent evaporation method. The surface and internal morphologies, *in vitro* degradation and BSA release of the microspheres were investigated. The effect of emulsifier concentration in the internal aqueous phase on microspheres erosion and protein release was studied. In addition, erosion and protein release of PLA microspheres were also studied as a comparison.

4.2 Results and discussion

4.2.1 Synthesis of PNIPAAm-*b*-PLA

Hydroxy-terminated PNIPAAm precursor polymer was prepared by the radical copolymerization, where hydroxy group was introduced to the end of the copolymer by telomerization using hydroxyethanethiol (chain transfer agent, CTA). PNIPAAm-*b*-PLA block copolymers were synthesized by ring opening esterification polymerization of D,L-lactide with the hydroxy-terminated precursor in toluene. Two PNIPAAm-*b*-PLA block copolymers with various lengths of PLA were obtained. The yield of the block copolymers was 52% and 60%, respectively. The ^{1}H-NMR spectra of block copolymer (the same as that of blank microspheres illustrated in Figure 4.7 B) showed that the peak

at δ 4.1 (signal b) was contributed to the protons of -NHC*H*Me_2 moieties. The broad peak at δ 5.1-5.3 (signal a) was from –C*H*MeO- groups in the lactide moieties. The molar ratio of the monomers was obtained from the integration values of Signals a and b. The increase in molecular weight after polymerization (Table 4.1) and the single peak appeared in the gel permeation chromatograms of the polymers proved that block copolymers were successfully synthesized. The properties of the block copolymers were summarized in Table 4.1.

Table 4.1 Properties of PNIPAAm-*b*-PLA diblock copolymers synthesized

Polymers	[NIPAAm]/[CTA]/[LA] [a]	M_w	M_n	M_w/M_n
1	1:0.01:4	12.9k	7.2k	1.8
2	1:0.01:5	16.7k	12.1k	1.4

a. Molar ratio of the monomers and the chain transfer agent (2-hydroethanethiol)
b. Lower critical solution temperature (LCST): Optical transmittance of aqueous precusor polymer solutions (5 mg/mL) at various temperatures was measured at 500 nm.
c. M_w and M_n of the precursor hydroxyl-terminated poly(*N*-isopropylacrylamide) polymers was 4.1k and 3.2k, respectively; LCST of this precusor polymer is 35°C.

4.2.2 Fabrication and characterization of BSA-loaded PNIPAAm-*b*-PLA micropsheres

4.2.2.1 Particle size analysis

As listed in Table 4.2, the mean diameter of microspheres fabricated under various conditions was quite similar, ranging from 29 to 35 μm. The size of microspheres very much depends on the viscosity of polymer solution and the concentration of emulsifier in the external aqueous phase (Yang and Chung et al., 2001; Yang and Wan et al., 2001). For all the formulations studied in this paper, the same concentration of PVA in the

external aqueous phase was utilized. In addition, the polymer solutions employed had a similar viscosity (Table 4.2). Therefore, the microspheres produced were of similar size.

Table 4.2 Mean size of microspheres fabricated under various conditions and inherent viscosity of polymer-DCM solutions

Formulations	Inherent Viscosity (dL/g)	Mean diameter (μm) after vacuum dry	
		Mean diameter (μm)	Standard deviation
PNIPAAm-*b*-PLA (1:4, 0.2%)	0.26	29	6
PNIPAAm-*b*-PLA (1:5, 0.05%)	0.35	30	3
PNIPAAm-*b*-PLA (1:5, 0.2%)	0.35	34	7
PLA (0.2%)	0.30	29	4

4.2.2.2 Surface and internal morphologies

Figure 4.1 shows the surface and internal morphologies of PLA and PNIPAAm-*b*-PLA microspheres fabricated under different conditions. PNIPAAm-*b*-PLA (1:4) and PNIPAAm-*b*-PLA (1:5) with a higher PVA concentration (0.2%) in the internal aqueous phase were porous. In contrast, PNIPAAm-*b*-PLA (1:5) at a lower PVA concentration (0.05%) yielded dense microspheres with a few big pores that were not inter-connected. At the lower concentration of PVA, the first emulsion was not stable, and the internal water droplets tended to coalesce, forming big pores within the microspheres after water was removed by vacuum drying (Chia and Yang et al., 2001). However, the first emulsion was more stable at the higher PVA concentration. Therefore, the pores were uniformly distributed. Similarly, hydrophobic PLA produced an unstable first emulsion as well, leading to a multi-vesicular internal structure with a dense skin layer (Figure

4.1). The average pore size and specific surface area of PLA and PNIPAAm-*b*-PLA (1:5, 0.2%) microspheres were listed in Table 4.3. It should be mentioned that measured pore size only ranges from 3.5 to 2000 Å. Thus, pores bigger than 0.2 μm were not detected. The average pore size of PLA microspheres was 593 Å, which was much greater than that of PNIPAAm-*b*-PLA (1:5, 0.2%) (224 Å). However, the specific surface area of PNIPAAm-*b*-PLA (1:5, 0.2%) was larger. These findings well agree with morphological observations of the microspheres.

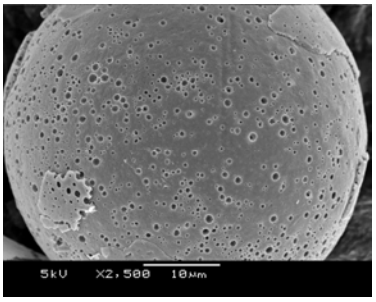

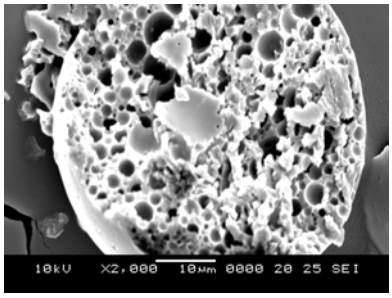

PNIPAAm-*b*-PLA (1:4, 0.2%)

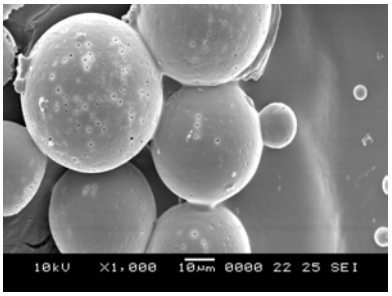

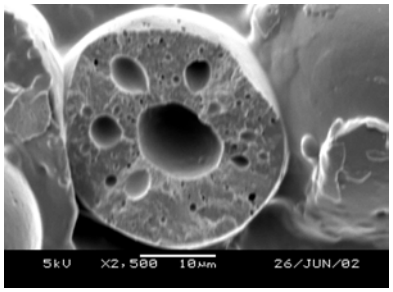

PNIPAAm-*b*-PLA (1:5, 0.05%)

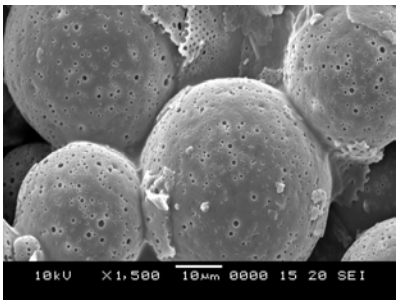

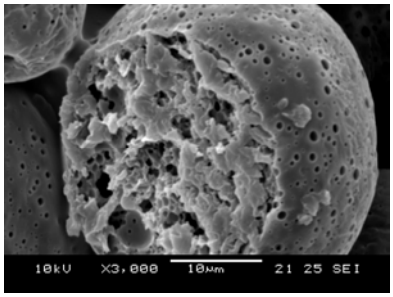

PNIPAAm-*b*-PLA (1:5, 0.2%)

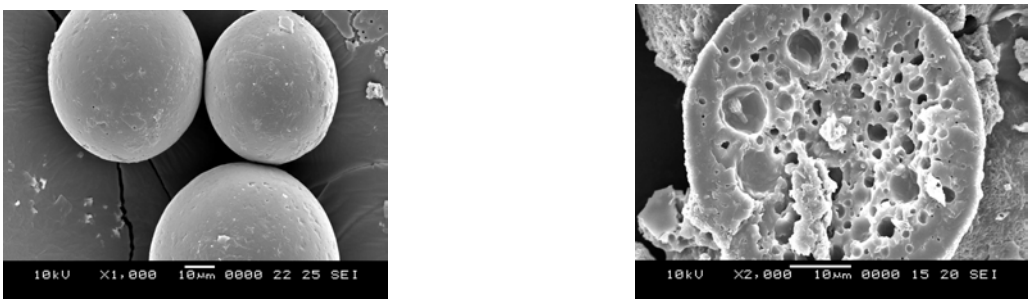

PLA (0.2%)

Figure 4.1 External and internal morphologies of microspheres fabricated by the double emulsion solvent evaporation method.

Table 4.3 Average pore size and specific surface area of the microspheres

Microspheres	PNIPAAm-*b*-PLA (1:5, 0.2%)	PLA (0.2%)
Average pore size (Å)	224	593
Specific surface area (m^2/g)	18.8	10.7

It was reported by Quellec and Peracchia et al. (Quellec et al., 1998; Peracchia et al., 1997) that PLA-PEG diblock copolymer yielded PEG chains in a "brush-like" arrangement on the surface and on the inner surface of aqueous domains of nanospheres due to the fact that PEG chains oriented to the external aqueous phase during the formation process, which drastically reduced protein adsorption on PEG-PLA nanospheres compared to PLA nanospheres. The atomic composition of the microspheres surface was analyzed using XPS. The real atomic composition of polymers was determined by elemental analysis. The N content of the surface of PNIPAAm-*b*-PLA (1:5, 0.2%) microspheres without BSA (5.92%) was similar to that of PNIPAAm-*b*-PLA (1:5, 0.2%) microspheres containing BSA (6.34%) (Table 4.4). This indicates that BSA was well entrapped within the microspheres. However, The N content of the surface of

PNIPAAm-*b*-PLA (1:5, 0.2%) microspheres without BSA was higher than that of PNIPAAm-*b*-PLA (1:5) polymer (3.91%), resulting from a higher concentration of the PNIPAAm block on the surface. Figure 4.2 shows the XPS high-resolution scans of the surface of PNIPAAm-*b*-PLA (1:5, 0.2%) microspheres, which can be curve-fitted with 3 peaks, with binding energy at 285.0 eV for *C*-H or *C*-*C*, 286.2 eV for O=C-*C*-H or *C*-N, as well as 288.6 eV for *C*=O. As listed in Table 4.5, the C=O content of the surface of PNIPAAm-*b*-PLA micropsheres (12.6%) was close to that of PNIPAAm polymer (10.0%). On the other hand, from Figure 4.1, much more pores were observed on the surface of PNIPAAm-*b*-PLA (1:5, 0.2%) microspheres compared to PLA microspheres. This might be contributed to the hydrophilic PNIPAAm blocks concentrated on the surface of the micropsheres. These findings suggest that the surface of PNIPAAm-*b*-PLA microspheres was rich in the hydrophilic PNIPAAm blocks. Since PNIPAAm is water soluble during fabrication process, it tended to migrate towards the external aqueous phase and inner aqueous phase during the fabrication process.

Table 4.4 Atomic composition of microsphere surface and polymers

Sample	C (%)	N (%)	O (%)	H (%)
PNIPAAm-*b*-PLA (1:5, 0.2%) microspheres[a] (without BSA)	68.11	5.92	25.97	
PNIPAAm-*b*-PLA (1:5, 0.2%) microspheres[a] (with BSA)	60.34	6.34	24.32	
PNIPAAm-*b*-PLA (1:5) polymer[b]	53.92	3.91		7.23
PLA polymer[b]	47.17		47.12[c]	5.31
PNIPAAm polymer[b]	61.31	11.66	--[d]	10.47
BSA[b]	45.97	14.28	--	7.02

a. Measured by XPS
b. Measured by elemental analysis
c. Calculated
d. Not determined

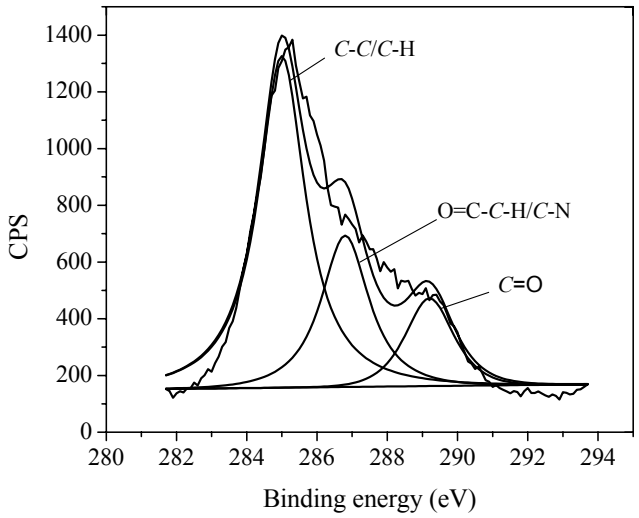

Figure 4.2 XPS C 1s high resolution scans of the PNIPAAm-*b*-PLA (1:5, 0.2%) micropsheres surface.

Table 4.5 Content of C=O in all the carbon bonds on the surface of samples

Sample	C-C/C-N, C-O/C=O	C=O (%)
PNIPAAm-*b*-PLA (1:5, 0.2%) micropsheres	3.97: 2.94: 1	12.6
PLA microspheres	1.16: 1.06: 1	31.0
PNIPAAm polymer	7: 2: 1	10.0

4.2.2.3 Entrapment of BSA

As listed in Table 4.6, the entrapment efficiency of BSA was higher than 90% except for PNIPAAm-*b*-PLA microspheres fabricated with a PVA concentration of 0.05% in the

internal aqueous phase. This was probably due to the fact that the unstable first emulsion led to more BSA lost into the external aqueous phase during the fabrication process. The CLSM images indicated that PNIPAAm-*b*-PLA (1:5, 0.2%) (Figure 4.3 b, c, d) yielded uniform BSA distribution as well as high BSA encapsulation efficiency. In contrast, PNIPAAm-*b*-PLA (1:5, 0.05%) showed aggregated BSA distribution (Figure 4.3 a). The CLSM results are agreeable with SEM pictures. Figure 4.4 shows FT-IR spectra of PNIPAAm-*b*-PLA (1:5) copolymer, BSA and BSA-loaded micropsheres respectively. The spectrum of PNIPAAm-*b*-PLA copolymer shows an ester carbonyl band in the lactide unit at 1756.7 cm^{-1} (a) and an amide carbonyl band in both polymer and BSA at 1649.8 cm^{-1} (b). From the spectrum of BSA-loaded PNIPAAm-*b*-PLA microspheres, it can be observed that there were no significant shifts in these two bands. It is suggested that there were no strong chemical interactions between BSA and the polymer, and the physicochemical integrity of BSA was retained within the micropsheres.

Table 4.6 Encapsulation efficiencies of BSA (Initial loading: 10% in weight)

PNIPAAm-*b*-PLA (1:5, 0.2%)	PNIPAAm-*b*-PLA (1:5, 0.05%)	PLA (0.2%)
91.0 %	80.0 %	98.0 %

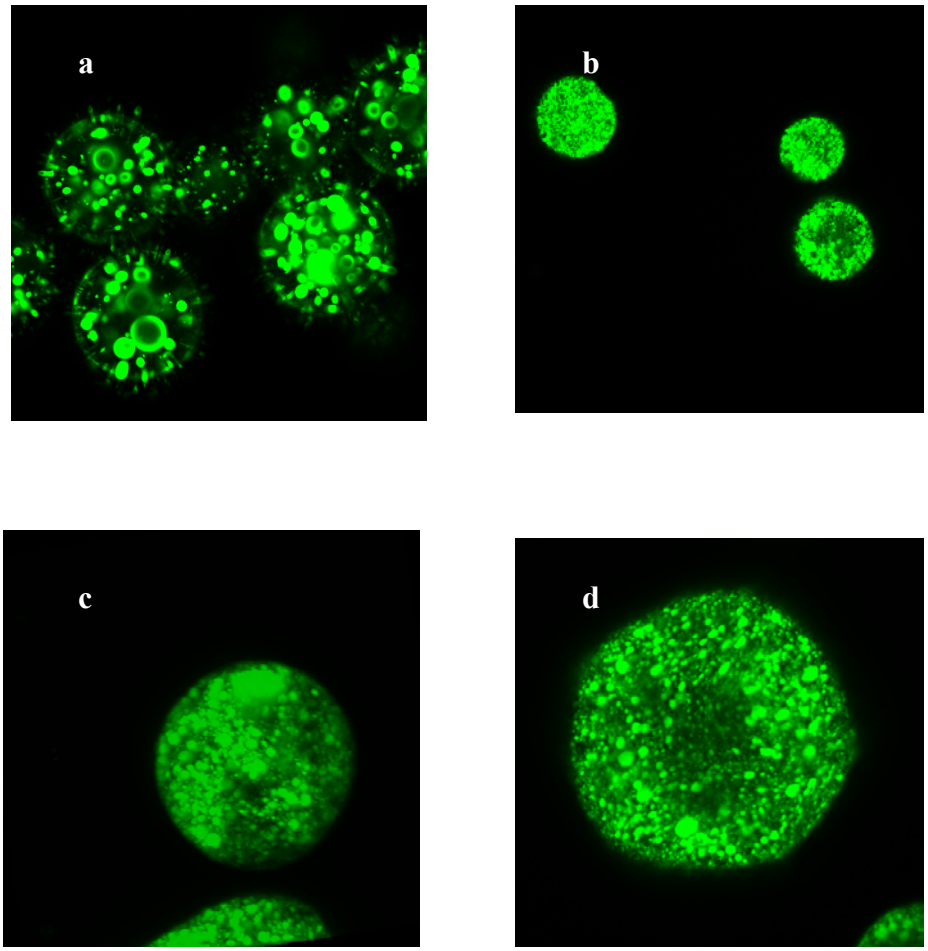

Figure 4.3 Confocal images of the FITC-BSA loaded microspheres (a) PNIPAAm-*b*-PLA (1:5, 0.05%), 20 times; (b) PNIPAAm-*b*-PLA (1:5, 0.2%), 20 times; (c) PNIPAAm-*b*-PLA (1:5, 0.2%), 3D, 20 times; (d) PNIPAAm-*b*-PLA (1:5, 0.2%), 40 times.

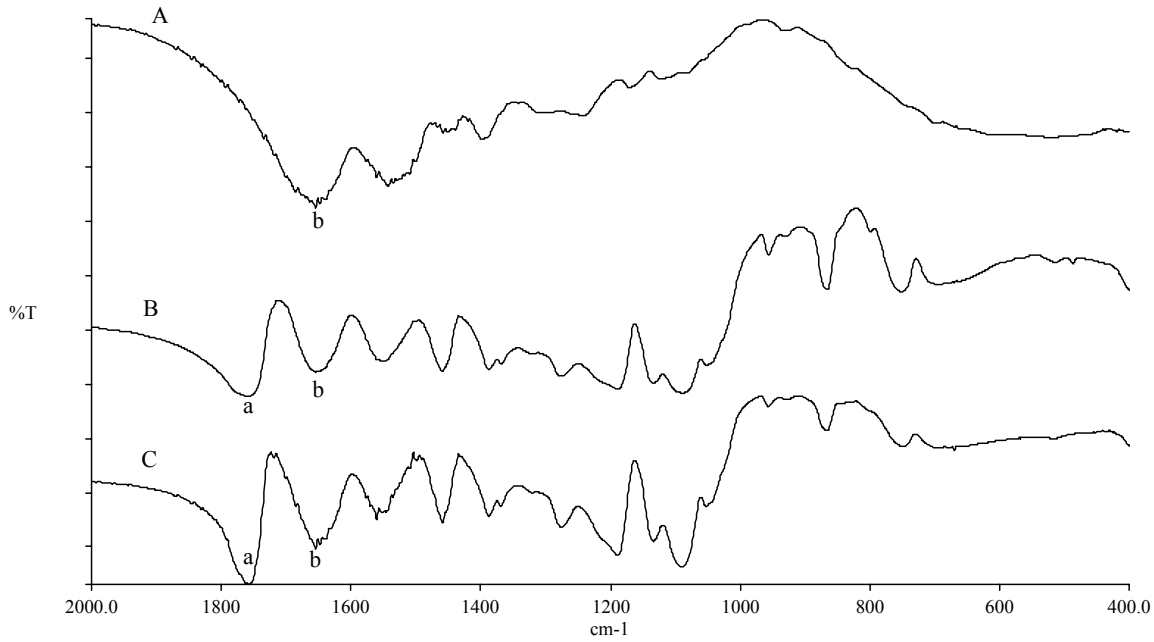

Figure 4.4 FT-IR spectra of BSA (A), PNIPAAm-*b*-PLA (1:5) copolymer (B), and BSA-loaded micropsheres (C).

4.2.3 Microspheres erosion and polymer degradation

4.2.3.1 Morphologies of the degrading micropsheres

The SEM pictures of the degrading PLA microspheres over 3 months *in vitro* are illustrated in Figure 4.5. After one month *in vitro*, the particles still remained spherical. However, after two months, it showed an evidently shrunken shape due to extensive bulk erosion. After three months, the particles degraded into pieces. Figure 4.6 shows the morphologies of the degrading PNIPAAm-*b*-PLA (1:5, 0.2%) microspheres. With the progression of polymer degradation, the micropsheres were broken and lost their spherical shape, indicating a decrease in the mechanical strength. In particular, they were broken into pieces after three months *in vitro*. However, PNIPAAm-*b*-PLA (1:5, 0.05%) microspheres kept their spherical shape even after two months *in vitro* but lost their

spherical shape after three months (*pictures not shown*). These observations indicate that both PLA and PNIPAAm-*b*-PLA (1:5) microspheres experienced bulk erosion.

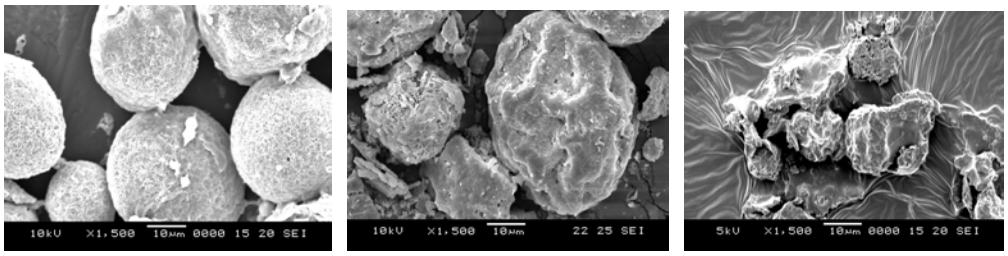

1 month 2 months 3 months

Figure 4.5 SEM scans of the degrading PLA microspheres.

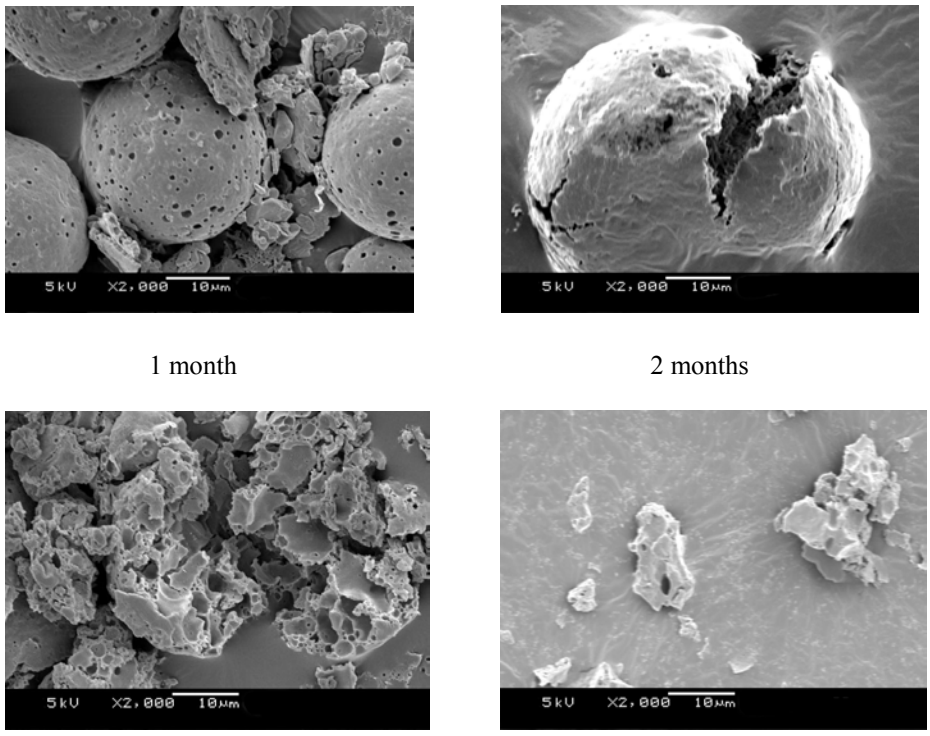

1 month 2 months

3 months 4 months

Figure 4.6 SEM scans of the degrading PNIPAAm-*b*-PLA (1:5, 0.2%) microspheres.

4.2.3.2 NMR analysis

The NMR experiments were performed to study the degradation mechanism of PNIPAAm-*b*-PLA microspheres. The ^{1}H-NMR spectra of PLA, PNIPAAm-*b*-PLA and the degrading microspheres are illustrated in Figure 4.7. The proton signal at δ 5.2 ppm (a, -OC*H*MeCOO-) was from PLA. However, the proton signal at δ 4.0 ppm (b, -C*H*Me$_2$) was from PNIPAAm. The molar ratio of PLA to PNIPAAm in the degrading micropheres was obtained from the integration values of Signals a and b. The mole ratio of PLA to PNIPAAm was decreased from 5:1 to 3.5:1 and 0.45:1 after 1 and 4 months *in vitro*, respectively. In particular, Signal a from the PLA block disappeared after 5 months *in vitro*. However, the characteristic peak of PNIPAAm block existed over the entire period of *in vitro* test. This finding proves that PNIPAAm-*b*-PLA was degradable, and the cleavage occurred in the PLA block.

4.2.3.3 FT-IR study

Figure 4.8 shows the FTIR spectra of the degrading PNIPAAm-*b*-PLA (1:5, 0.2%) micropsheres. The IR spectrum of PNIPAAm-*b*-PLA (1:5, 0.2%) micropsheres exhibited two strong absorptions at 1757.8 cm^{-1} ($\nu_{O\text{-}C=O}$, a) and 1089.4 cm^{-1}($\nu_{C\text{-}O}$, b) from the PLA block. Another two strong absorptions at 1654.6 cm^{-1} ($\nu_{HN\text{-}C=O}$, c) and 1550.8 cm^{-1} ($\nu_{C\text{-}N}$, d) came from the PNIPAAm block. These peaks were evident and strong within the first 4 weeks. However, the intensity of peaks at 1757.8 cm^{-1} ($\nu_{O\text{-}C=O}$) and 1089.4 cm^{-1}($\nu_{C\text{-}O}$) from the PLA block became weaker and weaker with the progression of polymer degradation and disappeared after 5 months. However, the peaks from PNIPAAm existed through the entire period of *in vitro* test. The FTIR study supported the results from NMR.

The disappearance of ester carbonyl group found in the lactide unit suggests the complete degradation of PLA after 5 months.

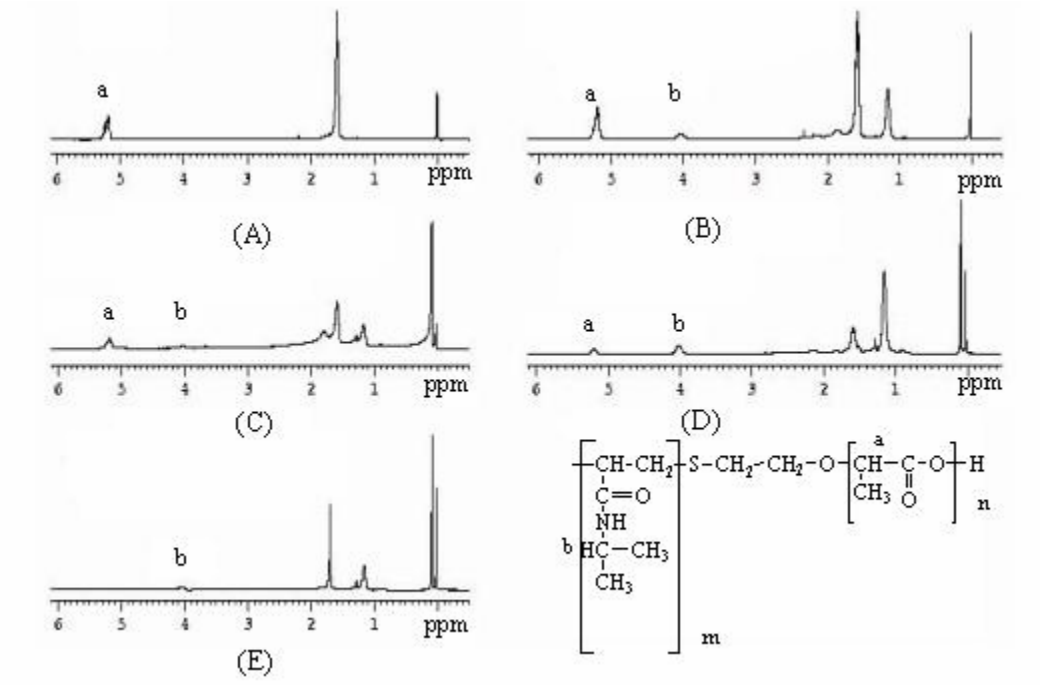

Figure 4.7 ^{1}H-NMR spectra of PLA and degrading PNIPAAm-*b*-PLA (1:5, 0.2%) microspheres. (A) PLA microspheres before degradation; (B) PNIPAAm-*b*-PLA (1:5, 0.2%) microspheres before degradation; (C) PNIPAAm-*b*-PLA (1:5, 0.2%) microspheres after one month *in vitro*; (D) PNIPAAm-*b*-PLA (1:5, 0.2%) microspheres after four months *in vitro*; (E) PNIPAAm-*b*-PLA (1:5, 0.2%) microspheres after five months *in vitro*.

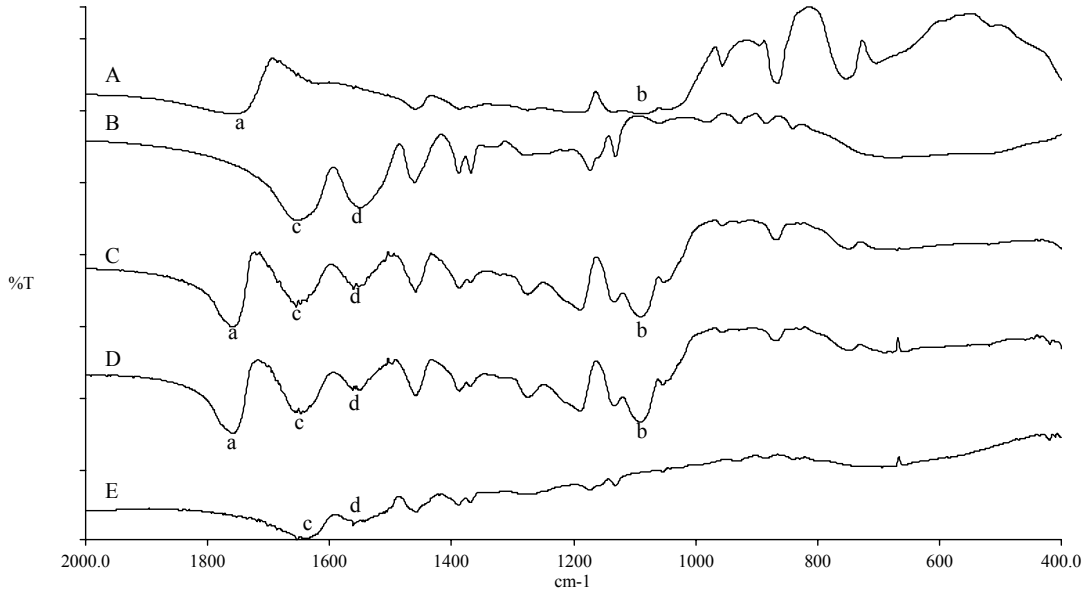

Figure 4.8 FT-IR spectra of PLA, PNIPAAm and degrading PNIPAAm-*b*-PLA (1:5, 0.2%) microspheres. A: PLA; B: hydroxyl-terminated PNIPAAm; C: PNIPAAm-*b*-PLA (1:5, 0.2%) microspheres before degradation; D: PNIPAAm-*b*-PLA (1:5, 0.2%) microspheres after one month *in vitro*; E: PNIPAAm-*b*-PLA (1:5, 0.2%) microspheres after five months *in vitro*.

4.2.3.4 Molecular weight and mass loss study

Based on the NMR, FT-IR and GPC studies, the copolymer degradation occurred in the PLA block. Belbella et al. (1996) reported that PLA degradation in aqueous media followed two main mechanisms: surface erosion and bulk erosion. In the surface erosion process, the total mass of PLA decreased but its molecular weight remained constant. However, in the bulk erosion process, the chain cleavage was random, and both mass and molecular weight decreased as a function of time. From Figures 4.9 and 4.10, it is observed that both molecular weigh and mass of PLA, PNIPAAm-*b*-PLA (1:5, 0.2%) and PNIPAAm-*b*-PLA (1:5, 0.05%) microspheres decreased as a function of incubation time, indicating they experienced the bulk erosion mechanism. Interestingly, the molecular

weight of all the formulations did not change very much during the first month. However, as degradation proceeded, the matrices experienced faster molecular weight loss probably because of self-catalysis by the degradation products of PLA. The degradation of PNIPAAm-*b*-PLA (1:5, 0.2%) microspheres was faster than that of PNIPAAm-*b*-PLA (1:5, 0.05%) microspheres. For instance, after four months *in vitro*, the mass loss of PNIPAAm-*b*-PLA (1:5, 0.2%) and PNIPAAm-*b*-PLA (1:5, 0.05%) microspheres was 86 and 54%, respectively. This is due to the more porous structure of PNIPAAm-*b*-PLA (1:5, 0.2%) microspheres. Compared to PNIPAAm-*b*-PLA (1:5, 0.2%) microspheres, the mass loss of PLA microspheres was slower during the first month because of the existence of the thick wall (Figure 4.10). However, after one month, the mass loss of PLA increased significantly. Initially, degradation products of PLA were difficult to diffuse out of the PLA microspheres because of the diffusion barrier presented by the thick wall. Thus, the acidic degradation products were accumulated, and thus catalysed the hydrolysis of the matrix. These results suggest that the internal structure of micropsheres had a significant impact on erosion rate. The more porous the microspheres, the faster they eroded.

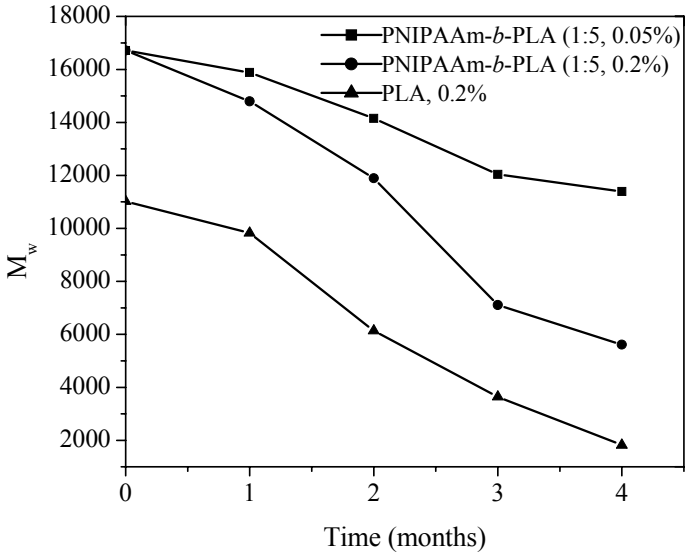

Figure 4.9 Weight molecular weight changes of the degrading micropsheres as a function of incubation time.

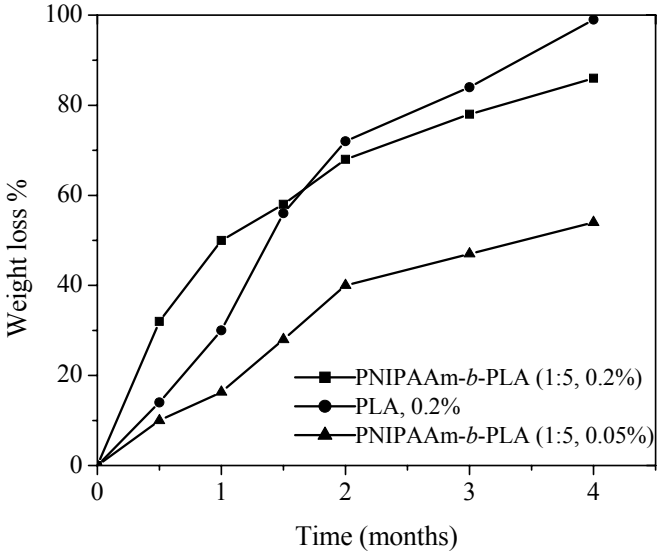

Figure 4.10 Weight loss of the degrading micropsheres as a function of incubation time.

4.2.4 Water uptake and swelling

Figure 4.11 shows the water uptake of microspheres after immersed for two days in PBS (pH 7.4) at 22 or 37^{o}C. Water uptake is affected by matrix porosity and polymer

chemistry. Compared to PLA and PNIPAAm-*b*-PLA (1:5, 0.05%) micropsheres, PNIPAAm-*b*-PLA (1:5, 0.2%) microspheres yielded much higher water uptake because of their more porous structure. However, the difference in water uptake between PLA and PNIPAAm-*b*-PLA (1:5, 0.05%) micropsheres was not significant. From Figure 4.11, it can also be seen that the water uptake of both PNIPAA-*b*-PLA formulations was higher at 22ºC (below the LCST) than at 37ºC (above the LCST). This is because PNIPAAm is water-soluble and exists in an extended chain form at temperatures below its LCST. This allows the microspheres matrix to bind more water molecules, resulting in greater water uptake.

Significant swelling was observed for PNIPAAm-*b*-PLA (1:5, 0.2%) microspheres incubated at 22^{o}C (Table 4.7). The mean diameter of the microspheres increased from 34 to 45 μm after two days incubation. It decreased to 37 μm on the seventh day due to polymer degradation. However, the other formulations did not swell. In addition, the swelling of PNIPAAm-*b*-PLA (1:5, 0.2%) microspheres was not obvious at 37^{o}C because of its hydrophobicity at temperatures above the LCST. These phenomena are consistent with water uptake data.

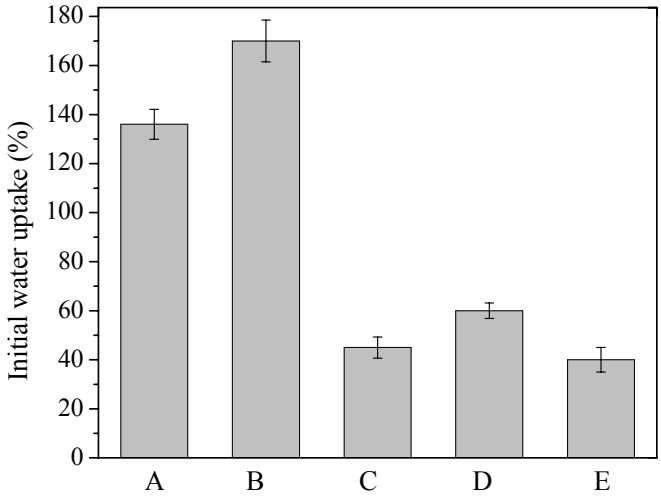

Figure 4.11 Water uptake of the microspheres after 2 days incubation in PBS (pH 7.4) at 22ºC and 37 ºC. A: PNIPAAm-*b*-PLA (1:5, 0.2%), 37°C; B: PNIPAAm-*b*-PLA (1:5, 0.2%), 22°C; C: PNIPAAm-*b*-PLA (1:5, 0.05%), 37°C; D: PNIPAAm-*b*-PLA (1:5, 0.05%), 22°C; E: PLA (0.2%), 37°C.

Table 4.7 Mean diameters (μm) of the degrading microspheres

Microspheres	Before release		Day 2				Day 7			
			37°C		22°C		37°C		22°C	
	D[a]	S.D.[b]	D	S.D.	D	S.D.	D	S.D.	D	S.D.
PNIPAAm-*b*-PLA (1:5, 0.2%)	34	7	34	5	45	8	38	7	37	5
PNIPAAm-*b*-PLA (1:5, 0.05%)	30	3	28	6	32	5	28	5	31	9
PLA (0.2%)	29	4	30	3	-		31	6	-	

a. Mean diameter
b. Standard deviation

4.2.5 In vitro release kinetics of BSA

As shown in Figure 4.12, BSA release from PLA microspheres was characterized with an initial burst followed by a non-release phase. This finding is consistent with the results reported previously (Crotts and Park, 1997; Puri and Jones et al., 2000). The initial release of BSA from PLA microspheres was due to the release of BSA molecules loaded near the surfaces of the microspheres. As described earlier, PLA microspheres were wrapped with a dense skin layer, which prevented water penetration and BSA diffusion, and thus led to slow initial release. The non-release phase of proteins was often found in PLA and PLGA microspheres. This was caused by protein aggregation or non-specific adsorption (Boury et al., 1997). The acidic microclimate resulting from the degradation products of PLA within the microspheres led to the instability and aggregation of BSA. The residual BSA remaining in micropsheres after release had become water-insoluble non-covalent aggregates in the residue (Jiang and Schwendeman, 2001). The adsorption of proteins onto hydrophobic polymer surface might also cause the instability and aggregation of BSA. XPS analysis shows that the N content of BSA-loaded PLA microspheres increased from 0% to 2.2% and 2.8% after one and two months *in vitro* respectively, indicating the aggregation or adsorption of proteins. The total amount of BSA released over one month *in vitro* was only about 20%.

Like PLA, the PNIPAAm-*b*-PLA (1:5, 0.05%) microspheres shared a similar release pattern (Figure 4.12). The presence of dense wall and disconnected porous structure limited water penetration and BSA diffusion prior to a significant degradation of the polymer. Consequently, BSA release was mainly controlled by erosion of the matrix.

However, it can be seen from Figure 4.12 that only 17% mass loss was detected during the first one month *in vitro*. The initial release of BSA was slightly higher at 22°C than at 37°C. This is because of the more hydrophilic nature of the PNIPAAm block at 22°C (below the LCST). For PNIPAAm-*b*-PLA (1:5, 0.05%) microspheres, the non-release phase of BSA might be caused by slow polymer degradation, protein aggregation or non-specific adsorption.

In contrast, BSA release from PNIPAAm-*b*-PLA (1:5, 0.2%) microspheres was more sustained, which lasted more than three weeks (Figure 4.12). More BSA molecules were released out from the microspheres. As reported in the previous paragraphs, the PNIPAAm-*b*-PLA (1:5, 0.2%) microspheres had an inter-connected porous structure and greater surface area, which would allow the degradation products of polymer to easily diffuse into the *in vitro* release medium, providing a mild environment for BSA release. In addition, the diffusion of BSA molecules was easier through the more porous matrix. On the other hand, the PNIPAAm block was the dominant component of the surface of PNIPAAm-*b*-PLA microspheres, which prevented non-specific adsorption of BSA molecules, leading to more BSA release. From Figure 4.12, it can also be seen that BSA release was faster at 22^{o}C than at 37^{o}C at the initial stage of *in vitro* test. However, after about 10 days, BSA release rate became higher at 37^{o}C. Since the microspheres were more hydrophilic at 22^{o}C and underwent significant swelling, water molecules were easier to penetrate into the matrix, leading to faster BSA release. After a certain period of time when the whole matrix was wetted, the diffusion of BSA molecules was the dominant factor. Faster BSA diffusion at 37^{o}C yielded higher BSA release rate. BSA

release from PNIPAAm-*b*-PLA (1:5, 0.2%) microspheres was mainly based on diffusion, swelling as well as polymer degradation.

BSA release from PNIPAAm-*b*-PLA (1:4, 0.2%) microspheres was characterized with a very high initial burst followed by a slow release over about two weeks (Figure 4.13). This is because of their highly porous structure. It was also observed that the initial burst of BSA was higher at 22ºC than at 37ºC. In addition, compared to PNIPAAm-*b*-PLA (1:5, 0.2%) microspheres, PNIPAAm-*b*-PLA (1:4, 0.2%) microspheres provided much faster initial release because of their more porous structure and greater portion of hydrophilic PNIPAAm block.

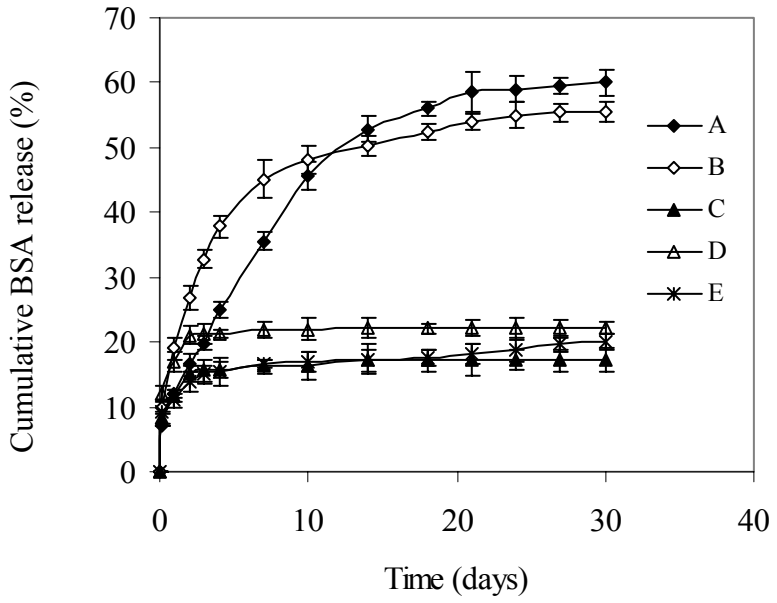

Figure 4.12 Release profiles of BSA from PLA, PNIPAAm-*b*-PLA (1:5, 0.2%) and PNIPAAm-*b*-PLA (1:5, 0.05%) microspheres incubated at different temperatures. (A): PNIPAAm-*b*-PLA (1:5, 0.2%), 37°C; (B) PNIPAAm-*b*-PLA (1:5, 0.2%), 22°C;(C): PNIPAAm-*b*-PLA (1:5, 0.05%), 37°C; (D): PNIPAAm-*b*-PLA (1:5, 0.05%), 22°C; (E): PLA, 37°C.

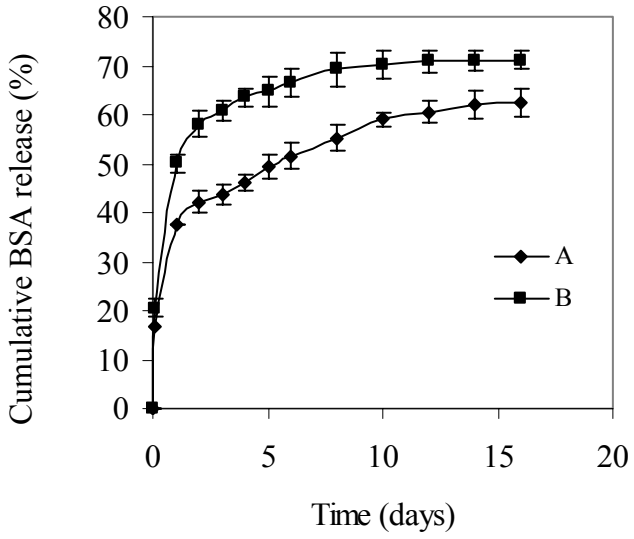

Figure 4.13 Release profiles of BSA from PNIPAAm-*b*-PLA (1:4, 0.2%) microspheres incubated at different temperatures. (A): PNIPAAm-*b*-PLA (1:4, 0.2%), 37°C; (B) PNIPAAm-*b*-PLA (1:4, 0.2%), 22°C.

4.3 Conclusions

Temperature-sensitive microspheres were synthesized using PNIPAAm-*b*-PLA diblock copolymers. PNIPAAm was a dominant component of the microspheres surface. The microspheres were erodible in the *in vitro* medium, and polymer degradation occurred in the PLA block. The erosion of microspheres was dependent upon their morphology. The more porous the microspheres, the faster erosion they experienced. Under the optimized fabrication conditions, more than 90% encapsulation efficiency of BSA was achieved. BSA release from the microspheres was sensitive to the external temperature. BSA release was faster at the temperature below the LCST. The microspheres fabricated with PNIPAAm-*b*-PLA having 1:5 molar ratio of PNIPAAm to PLA and a PVA concentration of 0.2% (w/v) in the internal aqueous phase were able to provide a sustained release of BSA over three weeks in PBS (pH 7.4) at 37ºC.

CHAPTER FIVE

RESULTS AND DISCUSSION 2A:

Temperature sensitive Core-Shell micelles Made from P(NIPAAm-*co*-DMAAm)-*b*- PLGA

5.1 Introduction

As discussed in Chapter 2 and Chapter 4, thermo-responsive microspheres may be a good carrier for protein delivery. For anticancer drug delivery, polymeric micelles are a promising approach (Torchilin, 2001). Polymeric micelles structured from amphiphilic copolymers are regarded as one of the most promising carriers for drug delivery (Kwon and Kataoka, 1995). Polymeric micelles have a small size (<200 nm) and can solubilize hydrophobic drugs in their inner cores, while exposing their hydrophilic shells to the external environment. This enables them to exhibit prolonged activity in the systemic circulation by avoiding the scavenging of the reticuloendothelial systems (RES). Poly(lactide) (PLA) and poly(lactide-*co*-glycolide) (PLGA) are often used as hydrophobic core-forming segments for fabrication of micelles because of their superior biocompatibility and biodegradability (Yasugi et al., 1998; Jeong and Park, 2001). On the other hand, by changing the composition of PLGA, the hydrophobicity of core-forming segment can be easily modulated to design micelles with desirable properties. Poly(*N*-isopropylacrylamide) (PNIPAAm) is a well-known thermosensitive polymer and exhibits a lower critical solution temperature (LCST) of about 32ºC. It has been utilized as a hydrophilic shell-forming segment together with various kinds of hydrophobic moieties to make thermosensitive micelles (Chung et al., 1997; Chung et al., 2000; Chaw et al., 2004). With micelles having PNIPAAm or its copolymer as the shell, both passive and active targeting to tumors can be achieved through an enhanced permeability and retention effect (EPR effect) (Kohori et al., 1999) and external temperature changes. It is expected that selective anticancer drug release from the micelles accumulated in tumors through the EPR effect may be triggered by local heating at a temperature slightly higher

than the LCST. However, Most of the hydrophobic moieties reported in the literature such as polystyrene, poly(butyl methacrylate) and alkyl are not degradable (Chung et al., 1997; Chung et al., 2000). In this study, we synthesized temperature-sensitive block copolymers, P(NIPAAm-*co*-DMAAm)-*b*-PLGA with different compositions and lengths of PLGA to modulate the hydrophobicity of the core-forming block. The micelles self-assembled from the polymers would be more readily degraded compared to the micelles fabricated from P(NIPAAm-*co*-DMAAm)-*b*-PLA (Burersroda et al., 2002). The important parameters of micelles, such as LCST, critical association concentration (CAC), particle size, zeta potential and morphology in the phosphate buffered-saline (PBS, pH7.4) or PBS buffer containing serum, were investigated. DOX (amphiphilic) and paclitaxel (hydrophobic), as model anticancer drugs, were encapsulated into the micelles by a membrane dialysis method and presented in 5.2 and 5.3, respectively. The dialysis parameters were optimized to achieve higher encapsulation efficiency (EE) and drug loading level. The micelles were characterized by DLS, TEM, AFM, NMR, DSC, WAXRD. The effect of the composition and length of PLGA on drug loading and *in vitro* drug release were examined. Cellular uptake and cytotoxicity of the polymers, free drugs, and drug-loaded micelles were also studied and compared.

5.2 DOX-loaded polymer micelles

5.2.1 Synthesis of P(NIPAAm-*co*-DMAAm)-*b*-PLGA

Hydroxy-terminated P(NIPAAm-*co*-DMAAm) precursor polymer was prepared by the radical copolymerization, where hydroxy group was introduced to the end of the copolymer by telomerization using hydroxyethanethiol (chain transfer agent, CTA). As

listed in Table 5.1, the weight average molecular weight (M_w) and polydispersity index of polymer decreased when the content of CTA increased from 0.75 to 1.5% of the monomers (NIPAAm and DMAAm). In addition, the LCST of polymer increased with increasing CTA content. This is because the portion of hydroxy groups in each polymer chain increased as the molecular weight of the polymer decreased. An ideal LCST would be slightly higher than the normal human body temperature so that a small temperature increase by local heating could induce the deformation of the micelles to trigger the release of enclosed drug molecules. Therefore, hydroxy-terminated P(NIPAAm-*co*-DMAAm) polymer synthesized with a CTA content of 1.0% was chosen as the precursor for the block copolymer in the following studies. P(NIPAAm-*co*-DMAAm)-*b*-PLGA block copolymers were synthesized by ring opening esterification polymerization of D,L-lactide and glycolide with the hydroxy-terminated precursor in toluene. Five P(NIPAAm-*co*-DMAAm)-*b*-PLGA block copolymers with various compositions and lengths of PLGA were obtained. The yield ranged from 65 to 76%. The ^{1}H NMR spectra of all the five polymers shared a similar pattern. Figure 5.1 shows a typical ^{1}H-NMR spectrum of Polymer E. The peak at δ 4.1 (Signal a) was contributed to the protons of -NHC*H*Me_2 moieties. The broad peak at δ 2.9-3.1 (Signal b) was from -N*Me*$_2$ groups in the DMAAm moieties. The broad peak at δ 5.1-5.3 (Signal c) was from –C*H*MeO- groups in the lactide moieties. Signal d at δ 4.6-4.9 was from -CH_2O- groups in the glycolide moieties. The molar ratio of the monomers was obtained from the integration values of Signals a, b, c and d. The increase in molecular weight after polymerization and the single peak appeared in the gel permeation chromatograms of the polymers further proved that block

copolymers were successfully synthesized. The properties of the block copolymers were summarized in Table 5.2.

Table 5.1 Properties of the precursor copolymers.

Samples	[a] CTA/Monomer (% in mole)	M_w (kDa)	M_n (kDa)	[b] Polydispersity	LCST in PBS buffer (°C)
P(NIPAAm-*co*-DMAAm)-OH 1	0.75	18.6	7.9	2.3	39.4
P(NIPAAm-*co*-DMAAm)-OH 2	1.0	10.6	5.1	2.1	42.0
P(NIPAAm-*co*-DMAAm)-OH 3	1.5	6.8	6.0	1.1	47.6

[a] CTA: chain transfer agent
[b] Polydispersity: M_w/M_n
The feed molar ratio of NIPAAm to DMAAm was 4:1, the final molar ratio estimated by NMR was 3:1.

Table 5.2 Properties of the block copolymers.

Polymer samples	Molar ratio of PLGA to P(NIPAAm-*co*-DMAAm)[a]	LA:GA[b]	M_w (kDa)	M_n (kDa)	Polydispersity	LCST of micelles in PBS solution (°C)
A	0.25	1:0	13.0	8.9	1.5	39.1
B	0.28	10:1	13.3	9.6	1.4	39.1
C	0.30	85:15	13.9	9.5	1.5	39.0
D	0.60	85:15	16.1	11.2	1.4	39.0
E	0.72	70:30	17.9	12.0	1.5	38.9

[a,b] Estimated from ^{1}H-NMR spectra

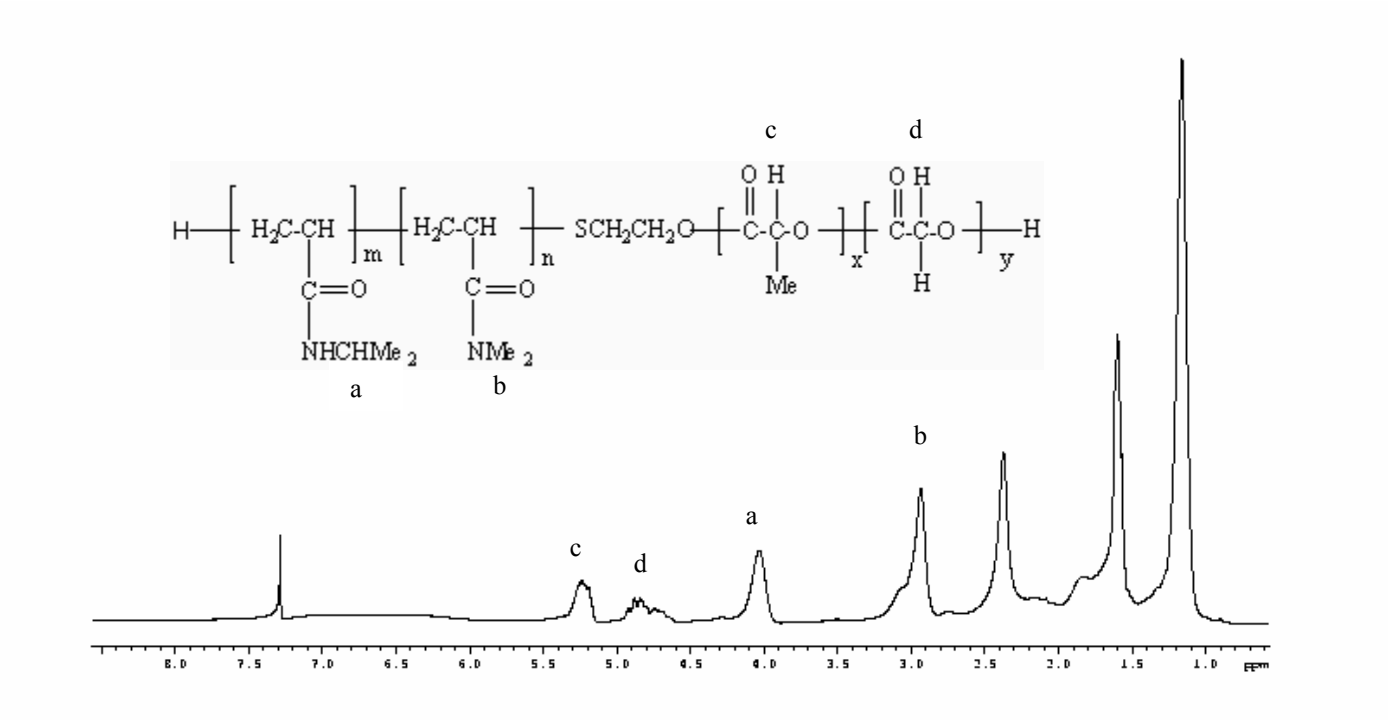

Figure 5.1 A typical ^{1}H-NMR spectrum of Polymer E in $CDCl_3$.

5.2.2 Critical association concentration (CAC) determination

The amphiphilic polymers consisting of hydrophilic segment and hydrophobic segment can self-associate to form micellar structure in aqueous solutions. The formation of micelles with P(NIPAAm-*co*-DMAAm)-*b*-PLGA was examined by the detection of CAC using a fluorescence technique, where pyrene was chosen as a fluorescent probe. The gradual shift of the third peak in the excitation spectra of pyrene from 334.5 nm to 336.5 nm was observed (Figure 5.2), indicating the change in vibration structure of pyrene emission (Kim and Lee, 2000). The peak intensity increased markedly when the polymer concentration was above 1 mg/L. At low concentrations, the intensity ratio of $I_{336.5}$ to $I_{334.5}$ changed slightly. However, as polymer concentration increased, the intensity ratio increased sharply, indicating the partitioning of pyrene into the hydrophobic core of the

micelles. Table 5.3 lists the CAC values of the polymers in DI water, ranging from 4.0 to 25.0 mg/L. The low CAC values indicate that the micelles can be formed at low concentrations, allowing their use in very dilute medium such as body fluids. An increased length of PLGA block yielded lower CAC. This finding is consistent with the results obtained from poly(propylene oxide)-*b*-poly(ethylene oxide)-*b*-poly(propylene oxide) polymers reported by Gadelle et al. (1995). The CAC value of Polymer D in PBS buffer was also obtained, similar to that in DI water (6.5 and 5.0 mg/L respectively). This is due to the non-ionic nature of the block copolymer, and the presence of salts did not affect its CAC significantly.

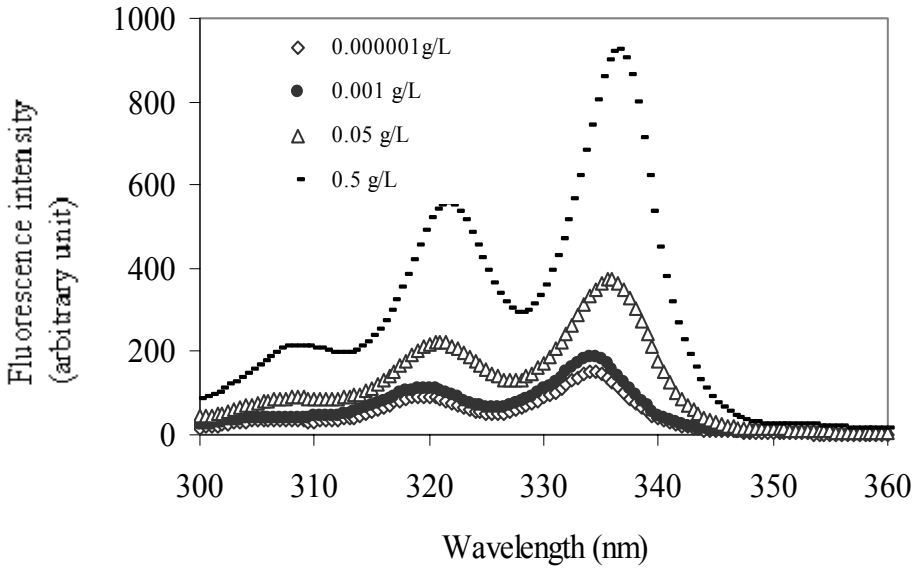

Figure 5.2 Excitation spectra of pyrene as a function of Polymer D concentration in PBS buffer.

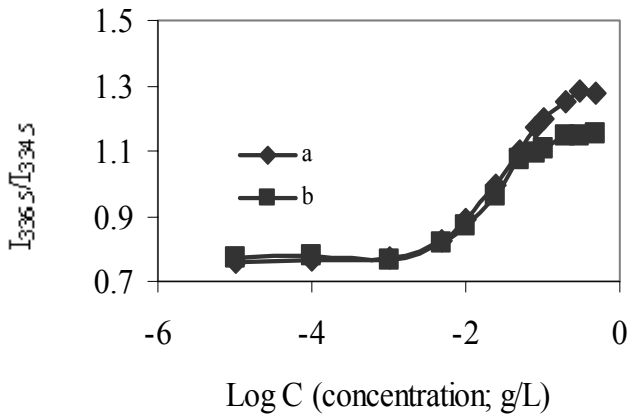

Figure 5.3 Plot of intensity ratio of $I_{336.5}/I_{334.5}$ as a function of log C for Polymer D in DI water (a) and PBS buffer (b).

5.2.3 Inner core deformation

Pyrene was used as a fluorescence probe to study the changes in the polarity of the core of the micelles at different temperatures. The $I_{336.5}/I_{334.5}$ ratio obtained from pyrene excitation spectra was monitored as a function of temperature at a polymer concentration above the CAC (Figure 5.4). At temperatures below the LCST, the ratio was high and relatively constant, indicating a low polar microenvironment (Kim and Lee, 2000). This is because pyrene was in the hydrophobic core of the micelles. However, as the temperature increased above the LCST, the intensity ratio decreased rapidly, indicating pyrene molecules were exposed to a more polar environment. At the temperatures above the LCST, the hydrophilic shell of the micelles became hydrophobic, inducing deformation of the core-shell structure of the micelles. This deformation allowed pyrene to be exposed to the external aqueous phase, increasing the polarity of its microenvironment. The reversibility of the change of pyrene microenvironment in response to temperature was examined through cooling the micelles solution. It was

found that the pyrene polarity reduced to its initial level when the solution was cooled to the temperatures below the LCST, suggesting that the shell of the micelles became hydrated and the core-shell structure of the micelles reformed. These data were in agreement with dynamic light scattering measurements. The size of the micelles was temperature-dependent, as shown later.

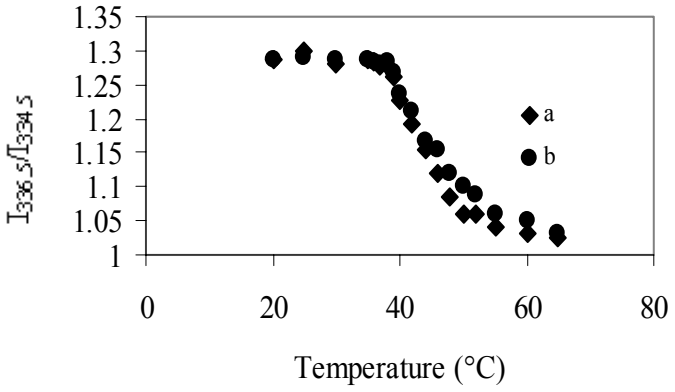

Figure 5.4 Plots of the $I_{336.5}/I_{334.5}$ ratio from the excitation spectra of pyrene in Polymer D/PBS solution as a function of temperature. (a) heating; (b) cooling (λ_{em} = 395 nm; heating rate: 1°C/min; pyrene concentration: 6.17×10^{-7} M; polymer concentration: 1.0 g/l).

5.2.4 Characterization of blank and DOX-loaded micelles

5.2.4.1 Particle size and zeta potential analyses

The particle size and size distribution of the micelles in PBS buffer are shown in Table 5.3. The average diameters of the blank and drug-loaded micelles except for the drug-loaded micelles made from Polymer E were less than 200 nm, making them less susceptible to clearance by the reticuloendothelial systems (RES) (Nagarajan and Ganesh, 1989). The polydispersity indices of blank and drug-loaded micelles were below 0.30, indicating that the micelles had a relatively narrow size distribution. Compared to Micelles B and C, Micelles A were bigger probably because the structure of Micelles A

was loosely packed due to smaller ratio of its hydrophobic chain to hydrophilic chain (Lee and Jung, 2004). However, further increasing PLGA chain length led to an increased particle size (e.g. Micelles D and Micelles E). This may be because the micelles made from the polymers with longer hydrophobic chain had greater aggregation number per micelle (Shuai and Ai et al., 2004; Allen and Maysinger et al., 1999). In addition, compared to the blank micelles, the corresponding drug-loaded micelles were bigger, contributed by the encapsulated drug molecules. Figure 5.5 shows TEM pictures of blank and DOX-loaded micelles made from different polymers. All the micelles were spherical, and drug loading as well as the presence of salts in PBS did not change the morphology of the micelles (Figure 5.5 f). The particle size estimated from the TEM pictures was in agreement with that obtained from dynamic light scattering analyses (Table 5.3). The size of the micelles was temperature-dependent. At 37°C in PBS, the micelles were stable, having a size in the range of 60 to 130 nm. However, when heated to 39.5°C, the size of the micelles increased to 250 nm and 600 nm respectively because the shell of the micelles became hydrophobic at the temperature above the LCST, leading to intermicellar hydrophobic association. Interestingly, this size change was reversible. This finding was consistent with that reported by Kohori et al. (1998). The surface charges of both the blank and DOX-loaded micelles in PBS buffer are also listed in Table 5.3. All the micelle formulations had negative surface charges at room temperature. The negative surface charge of micelles can be explained as follows. Firstly, hydrogen bonds were formed between amide group of P(NIPAAm-*co*-DMAAm) and water molecules. Oxygen atom from water molecules was exposed externally and hence micelles were surrounded by electron cloud, making the surface of micelles negatively charged. The more negative

the zeta potential, the more stable the micelles. This was due to the electrostatic repulsive interactions among the charged micelles. The micelles did not aggregate in the presence of FBS (data not shown), which was attributed to the hydrophilic nature and negative surface charge of the micelles. These properties can reduce the adsorption of various proteins to the surface of micelles.

Table 5. 3 Properties of blank and DOX-loaded micelles.

Samples	CAC (mg/L)	Blank micelles			DOX-loaded micelles		
		E.D. (nm)	P.D.	Zeta Potential (mV)	E.D. (nm)	P.D.	Zeta Potential (mV)
A	25.0	77.2 ± 0.9	0.29 ± 0.01	-16.2± 6.1	113.6± 1.6	0.29± 0.01	-14.6±1.5
B	20.0	52.6± 0.5	0.18± 0.01	-16.9± 3.1	76.0±0.2	0.23± 0.01	-14.9±1.1
C	7.9	52.5± 0.5	0.23± 0.00	-18.2± 2.2	74.9±0.4	0.23± 0.00	-15.8±0.5
D	5.0	104.5±0.9	0.15± 0.02	-25.4± 2.2	122.7± 1.7	0.12± 0.01	-25.3±2.4
E	4.0	133.5±1.5	0.09±0.01	-28.2±1.3	242.9±9.5	0.19±0.01	-20.6±1.7

E.D.: Effective diameter
P.D.: Polydispersity

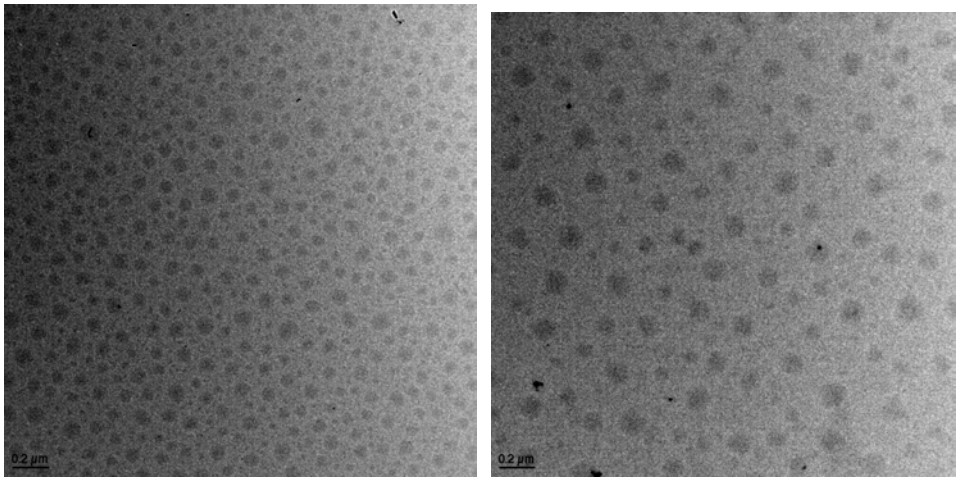

a b

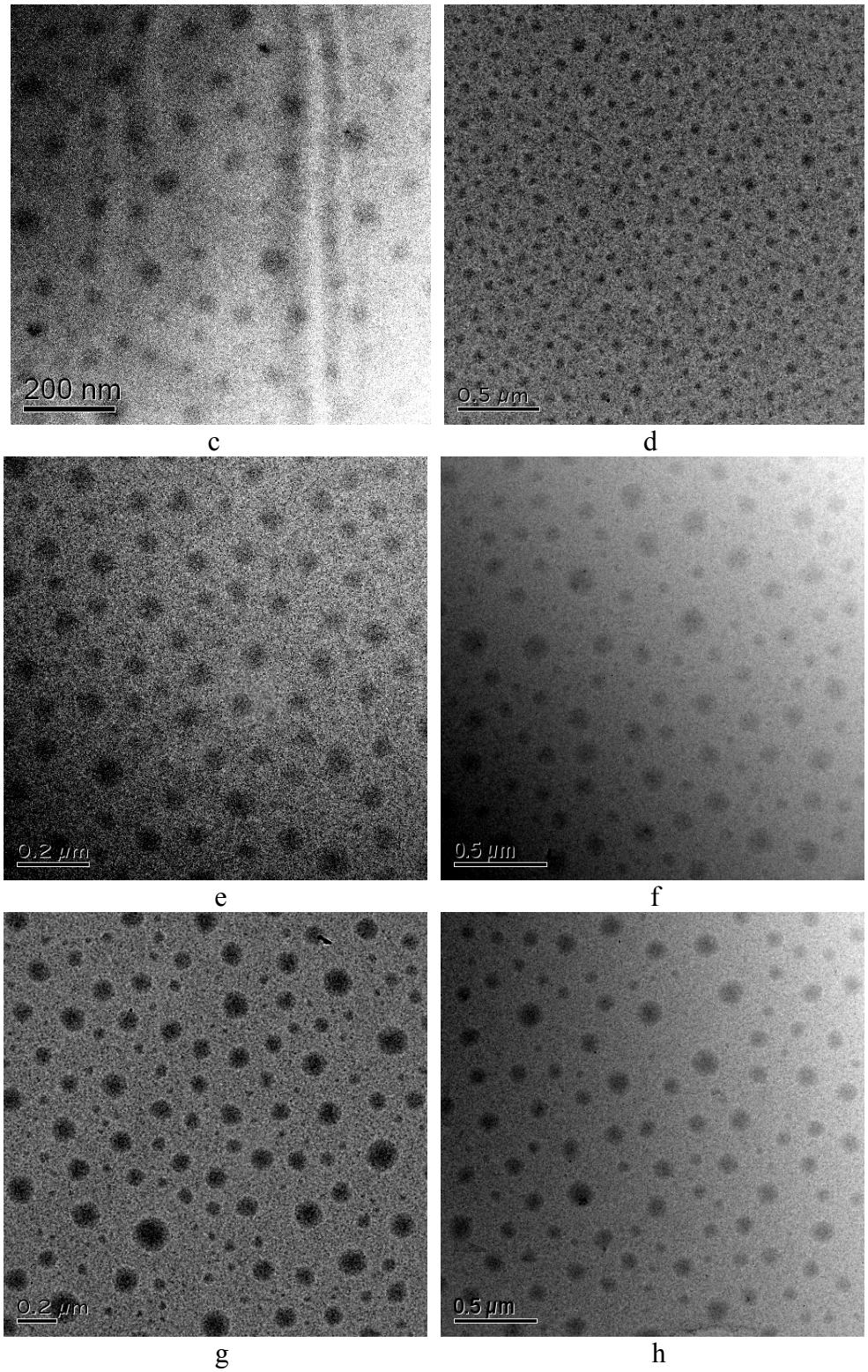

Figure 5.5 TEM pictures, blank micelles made from Polymer A in DI water (a) and DOX-loaded micelles in DI water (b); DOX-loaded micelles made from Polymer B in DI water (c); blank micelles made from Polymer C in DI water (d, e); blank micelles made

from Polymer C in PBS (f); Polymer D micelles in DI water (g) and DOX-loaded micelles in DI water (h).

5.2.4.2 Core-shell structure

The core-shell structure of the micelles was studied by NMR analyses (Kim and Lee, 2000). Figure 5.6 shows ^{1}H-NMR spectra of the micelles in D_2O and $CDCl_3$. In the spectrum of the micelles in D_2O, the peak at δ 3.8 (Signal a) was contributed by the protons of -NHC*H*Me_2 groups in the NIPAAm moieties. The broad peak at δ 2.8-3.0 (Signal b) was from -N*Me*$_2$ groups in the DMAAm moieties. The characteristic peaks of PLGA blocks were not found in the spectrum. This result indicated the formation of the well-defined core-shell structure of the block polymer in aqueous solution, which exhibited a shell of P(NIPAAm-*co*-DMAAm) and a core of PLGA. On the other hand, the micelles had a spectrum similar to that of the block copolymers (Figure 5.6) after dissolved in $CDCl_3$, in which the characteristic peaks of NIPAAm, DMAAm and PLGA were observed. This is due to the fact that the core-shell structure disappeared in the organic solvent.

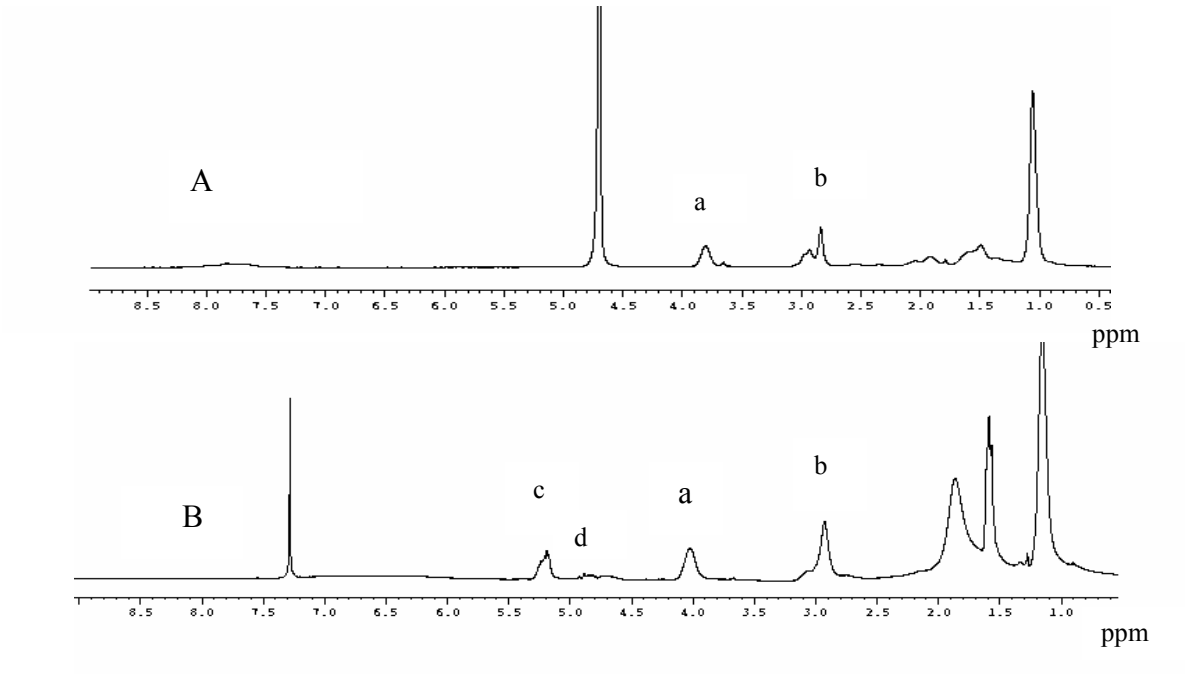

Figure 5.6 ^{1}H-NMR spectra of the micelles made of Polymer D dissolved in (A) D_2O and (B) $CDCl_3$.

5.2.4.3 LCST of precursor polymers and micelles in PBS buffer

PNIPAAm exhibits a LCST of 32°C in water. The LCST can be modulated *via* introducing hydrophobic or hydrophilic monomers (Chen and Hoffman, 1995). In this study, a hydrophilic comonomer *N, N*-dimethylacrylamide (DMAAm) was employed to adjust the LCST of the precursor copolymer. As shown in Table 5.1, the LCST increased by the incorporation of DMAAm. As discussed earlier, hydroxy-terminated P(NIPAAm-*co*-DMAAm) polymer synthesized with a CTA content of 1.0% was chosen as the precursor for the synthesis of the block copolymer, which had a LCST of 42.0°C in PBS buffer. The micelles made from all the P(NIPAAm-*co*-DMAAm)-*b*-PLGA block copolymers had a LCST ranging from 38.9 to 39.1ºC (Table 5.2), which is lower than that of the precursor polymer due to the disappearance of the hydroxy group after the

formation of the block copolymers. The block copolymers formed core-shell micellar structures with completely isolated hydrophobic inner cores from an aqueous phase. Therefore, the composition of the shell determined the LCST of the micelles regardless of the length of PLGA used, leading to the similarity in the LCST among all types of micelles. More importantly, the LCST of the micelles did not change significantly after dispersed in a simulated physiological condition (PBS containing 10% serum in volume) (38.6ºC *vs.* 39.0ºC, Figure 5.7).

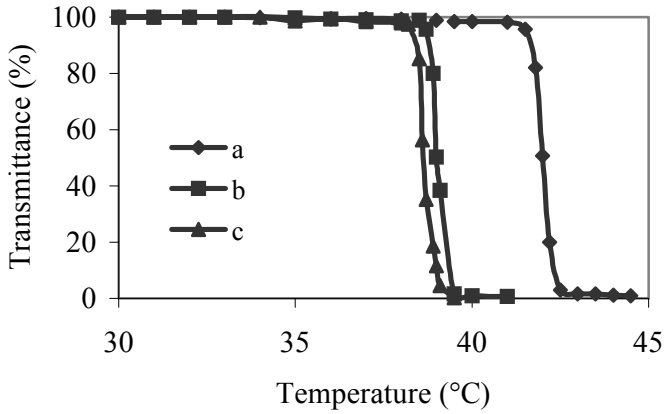

Figure 5.7 Transmittance changes as a function of temperature. (a) Selected precursor polymer in PBS buffer; (b) Polymer C micelles in PBS buffer; (c) Polymer C micelles in PBS buffer containing 10% FBS. (Polymer concentration: 5 mg/mL, at 500 nm).

5.2.4.4 Yield of micelles and drug loading level

Hydrophobic drugs can be incorporated in micelles by physical entrapment through a membrane dialysis method. The formation of micelles and drug loading during the dialysis process were affected by various parameters including the nature of solvents, polymers and drugs, dialysis temperature and medium used, solvent exchange rate, and

initial drug loading (Lee and Na *et al.*, 2003). The fabrication parameters described in Chapter 3 were the optimized ones, under which the DOX-loaded micelles solution obtained was transparent and exhibited the original color of DOX in aqueous solution. As shown in Table 5.4, the yield of the micelles ranged from 15.2 to 41.3%, and the drug loading level was from 2.1 to 8.0%. The yield of micelles fabricated from Polymers A, B, C and D was similar. In addition, from Polymer A to Polymer D, an increased length of the core-forming block PLGA yielded a higher drug loading level. Physical entrapment of drugs in polymeric micelles is driven by the hydrophobic interactions between the drug and hydrophobic block of polymers. Strong polymer-drug interactions enhance drug loading (Allen and Maysinger et al., 1999). An increased length of PLGA chain may enhance the polymer-drug interactions, resulting in higher drug loading level. However, comparing Polymer B with Polymer C, it seems that the composition change of PLGA block did not affect drug loading level significantly. In addition, Polymer E, with the longest PLGA block, produced the smallest amount of micelles and the lowest drug loading level because of the precipitation of drug and polymer during the fabrication process. This indicates that there is an optimized length of PLGA block for achieving high drug loading level and great yield of micelles.

Table 5.4 Yield of micelles and drug loading level.

Samples	A	B	C	D	E
Yield (%)	37.5	38.3	41.3	40.5	15.2
Loading level (% in weight)	5.6	6.0	6.2	8.0	2.1

5.2.5 Polymer degradation

The degradation of P(NIPAAm-*co*-DMAAm)-*b*-PLA (Polymer A) and P(NIPAAm-*co*-DMAAm)-*b*-PLGA block copolymers (Polymer C) in PBS was examined and compared by mass loss and M_w change as a function of time (Figures 5.8). Both M_w and mass of the degrading polymers decreased as a function of incubation time. Compared to Polymer A, Polymer C underwent faster weight loss and molecular weight decrease. For instance, the weight loss of Polymer A and Polymer C after six weeks was 65% and 98%, respectively. The molecular weight of Polymer C residues was not detectable after 6 weeks, while the residues of Polymer A still had a molecular weight of 4.8 kDa. It is well known that PLA and PLGA degraded in a random scission of ester linkage in the polymer chain, resulting in water-soluble oligomers with carboxylic acid at the chain end. According to Jiang *et al.* (2001), few acidic species were produced during early incubation for Polymer A due to slow degradation of PLA. In contrast, the amount of oligomers produced by PLGA was much higher than that produced by PLA (Giunchedi and Conti, 1998). Therefore, the degradation of Polymer C was accelerated in the acidic environment created by the degradation products. It should be noted that although the hydrophilic block of the polymer is non-degradable, it is water-soluble after the disappearance or extensive degradation of PLA or PLGA block because the *in vitro* temperature is lower than the LCST.

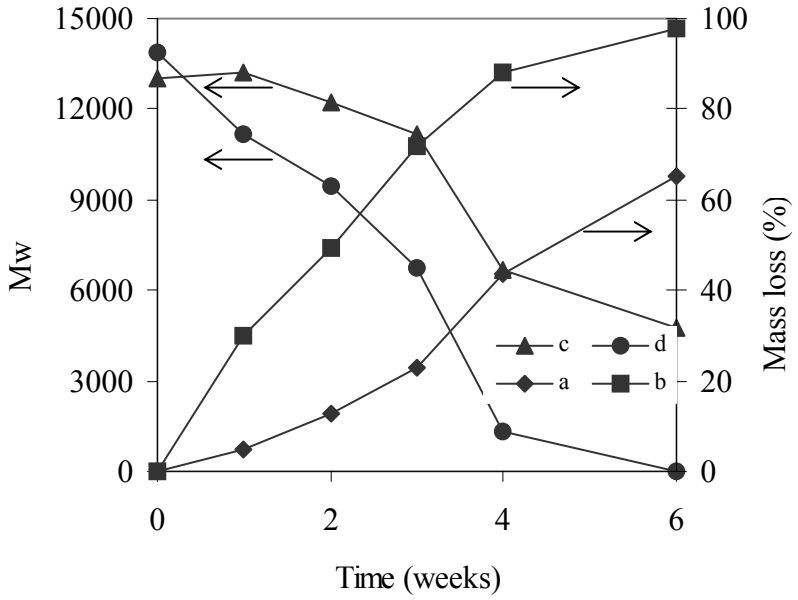

Figure 5.8 Mass loss (a, b) and molecular weight changes (c, d) of the degrading polymer as a function of incubation time. (a) and (c), Polymer A; (b) and (d), Polymer C.

5.2.6 In vitro drug release

In vitro DOX release from the micelles was studied in PBS buffer at 37ºC (below the LCST) and 39.5ºC (above the LCST). As shown in Figure 5.9, DOX release from the micelles at 37ºC was characterized with an initial burst followed by a non-release phase. The initial burst release of DOX was attributed to DOX molecules located within the corona or at the interface between the micelle core and corona (Allen and Maysinger, 1999). Polymer A micelles yielded the fastest initial burst release of DOX, reaching 45.0% within the first eight hours. However, the initial burst release of DOX from Polymer D micelles was the slowest. In contrast, at 39.5ºC, DOX release from the micelles was much faster. Within the first eight hours, more than 80% DOX was released. The results show that drug release well responded to the environmental

temperature change. When the temperature was below the LCST, the core-shell structure was stable, and DOX diffusion was slow. However, when the temperature increased to a value above the LCST, the outer shell collapsed. The collapsed shell might induce the deformation of the core-shell structure (Chung and Yokoyama, 2000), exposing DOX molecules to the external *in vitro* release medium and thus accelerating drug release. An increased length of PLGA block (i.e. the core-forming block) yielded slower drug release. The increased length of PLGA block caused greater polymer aggregation number per micelle, resulting in stronger PLGA-DOX interactions and thus hampering drug release. These findings indicate that drug release from the micelles could be tailored by varying the length of core-forming block PLGA.

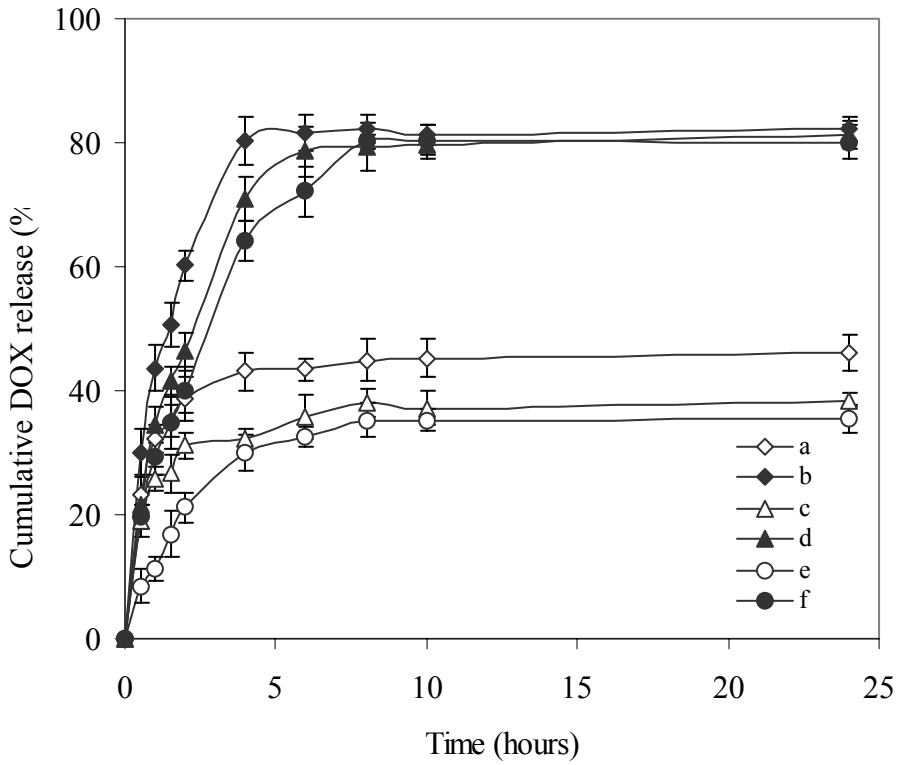

Figure 5.9 Release profiles of DOX from DOX-loaded micelles incubated at different temperatures. (a) Polymer A micelles incubated at 37°C; (b) Polymer A micelles incubated at 39.5°C; (c) Polymer C micelles incubated at 37°C; (d) Polymer C micelles incubated at 39.5°C; (e) Polymer D micelles incubated at 37°C; (f) Polymer D micelles incubated at 39.5°C.

5.2.7 Cellular uptake and cytotoxicity study

In order to examine the cellular uptake and in vitro cytotoxicity of DOX-loaded micelles against different cells, 4T1 cells and MDA-MB-435S cells were employed in this study. As shown in Figure 5.10, after 4 h of 4T1 cell incubation with free DOX, strong fluorescence was observed in cell nuclei with no signal in cytoplasm. In contrast, DOX fluorescence was observed only in the cytoplasm instead of the cell nuclei for DOX-loaded Polymer D micelles incubated at 37ºC (below the LCST), suggesting that DOX-loaded micelles may be internalized through an endocytosis pathway. This finding is

consistent with the results reported Savic et al. (2003). In contrast, the cells incubated at 39.5°C (above the LCST) gave strong fluorescence in cytoplasm and fluorescence was also seen in the nuclei. This may be attributed to the fact that drug release from micelles was much faster at a temperature above the LCST (Figure 5.9).

Figure 5.11 compared cytotoxic effects of free DOX, DOX-loaded Polymer D micelles against 4T1 cells incubated at different temperatures. There was no significant cytotoxicity observed up to 600 mg/L of blank Polymer D micelles for 48 h regardless of the environmental temperature (data not shown). Although the monomer and oligomers of PNIPAAm and PDMAAm are toxic, but the polymers used in this study would not degrade to low molecular weight oligomers. Additionally, cytotoxicity assay for blank polymer A-D were performed against 4T1 and L929 cell line. There was no significant cytotoxicity observed up to 600 mg/L of blank Polymer A-D micelles for 48 h regardless of the environmental temperature (data not shown), indicating that polymers used in this study were biocompatible. However, DOX-loaded micelles presented cytotoxicity in a temperature dependent manner. The DOX-loaded micelles exhibited great superior cytotoxic activities at a temperature above the LCST (IC_{50} = 3.1 mg/L) as compared to those below the LCST (IC_{50} = 7.9 mg/L). On the other hand, IC_{50} value of free DOX at 37°C (3.2 mg/L) was similar to that of at 39.5°C (2.4 mg/L). Therefore, the temperature-dependent cytotoxicity was caused by the difference in the release rate of DOX at different temperatures.

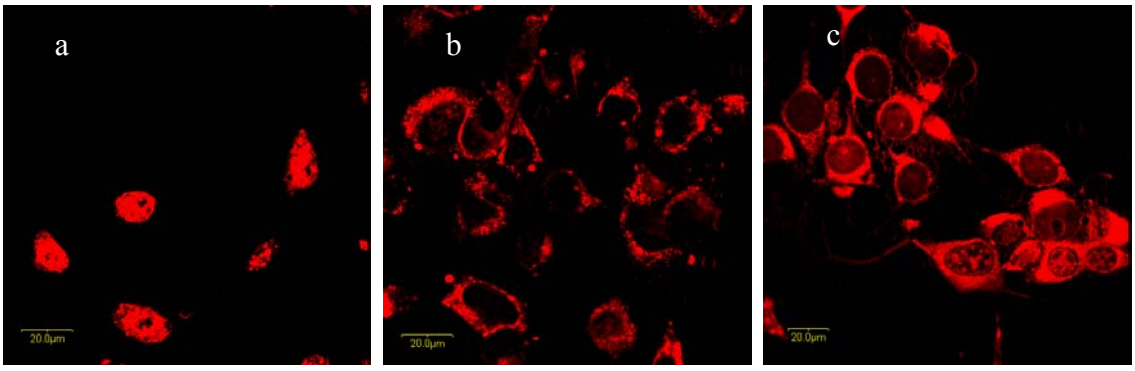

Figure 5.10 Confocal microscopic images of 4T1 cells incubated with (a) free DOX, (b) DOX-loaded Polymer D micelles at 37°C and (c) DOX-loaded Polymer D micelles at 39.5°C. (DOX concentration = 10 mg/L)

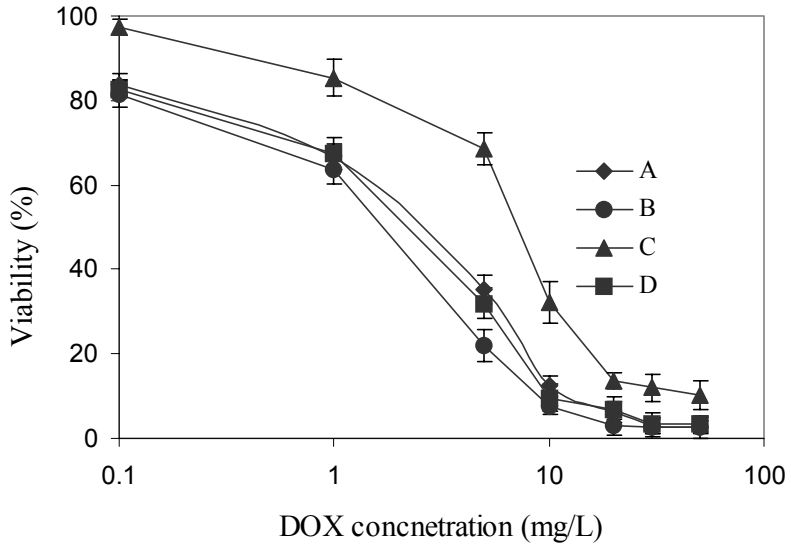

Figure 5.11 Viability of 4T1 cells incubated with free DOX and DOX-loaded polymer D micelles for 48 h at 37°C and 39.5°C respectively. (A) free DOX at 37°C; (b) free DOX at 39.5°C; (C) DOX-loaded Polymer D micelles at 37°C and (D) DOX-loaded Polymer D micelles at 39.5°C

Similarly, MDA-MB-435S cells were incubated with free doxorubicin or doxorubicin-loaded Polymer D micelles for 4 hours. In the case of free DOX molecules, they were

mainly present within the nucleus, but the signal was weak (Figure 5.12 a). This is because free doxorubicin molecules were transported into the cell *via* a passive diffusion pathway, and some doxorubicin molecules might be pumped out of the cells due to a multi-drug resistance effect (Yoo and Park, 2004). In contrast, the fluorescence was found in both the nucleus and the cytoplasm for the doxorubicin-loaded micelles incubated at 37ºC (Figure 5.12 b), indicating that the doxorubicin-loaded micelles were internalized by the cells through non-specific endocytosis. A similar phenomenon was also observed by Luo and Tam (2002) for poly(ethylene oxide)-*b*-poly(ε-caprolactone) micelles. The fluorescence intensity in the nucleus was attributed to free doxorubicin released from the micelles. On the other hand, greater fluorescence intensity was observed in the nucleus when the cells were incubated with doxorubicin-loaded micelles at 39.5ºC (Figure 5.12 c). This is due to the fact that at the temperature above the LCST, the core-shell structure of doxorubicin-loaded micelles deformed, accelerating doxorubicin release. For example, 64% of doxorubicin was released from the micelles within the first 4 hours at 39.5ºC whereas only 30% of doxorubicin was released during the same period of time at 37ºC (Figure 5.9).

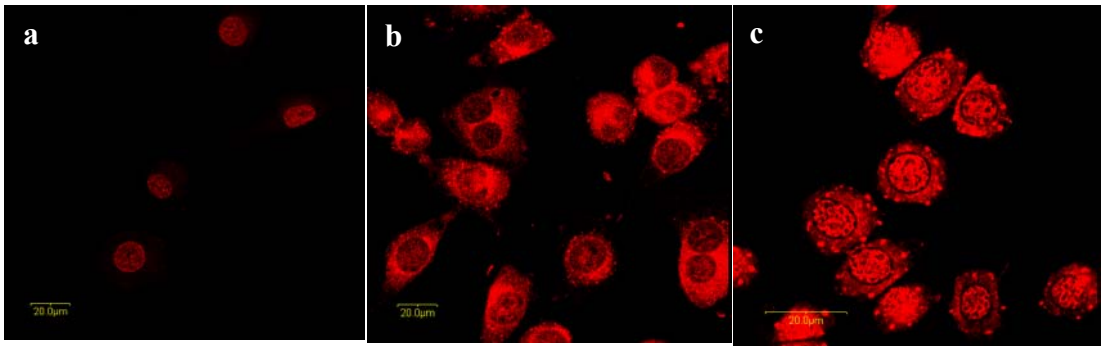

Figure 5.12 Confocal images of MDA-MB-435S cells incubated with (a) free doxorubicin, (b) doxorubicin-loaded Polymer D micelles at 37°C and (c) doxorubicin-

loaded Polymer D micelles at 39.5°C. (doxorubicin concentration = 10 mg/L; incubation time: 4 hours)

The *in vitro* cytotoxicity of free drugs (DOX *versus* paclitaxel) and drug-loaded micelles to MDA-MB-435S cells was analyzed and compared. As seen in Figure 5.13, there was no significant difference in the cytotoxicity of DOX at different incubation temperatures (IC_{50} = 1.0 mg/L at 39.5°C *vs* IC_{50} = 1.1 mg/L at 37°C). However, DOX-loaded micelles incubated at 39.5°C (IC_{50} = 0.30 mg/L) showed noticeable enhanced cytotoxicity than those incubated at 37.0°C (IC_{50} = 0.75mg/L). Cytotoxicity of blank micelles was also tested. The results showed that blank micelles had no cytotoxicity at both incubation temperatures. As stated before, the pronounced cytotoxicity of DOX-loaded micelles at 39.5°C was attributed to the enhanced release of DOX (Figure 5.9).

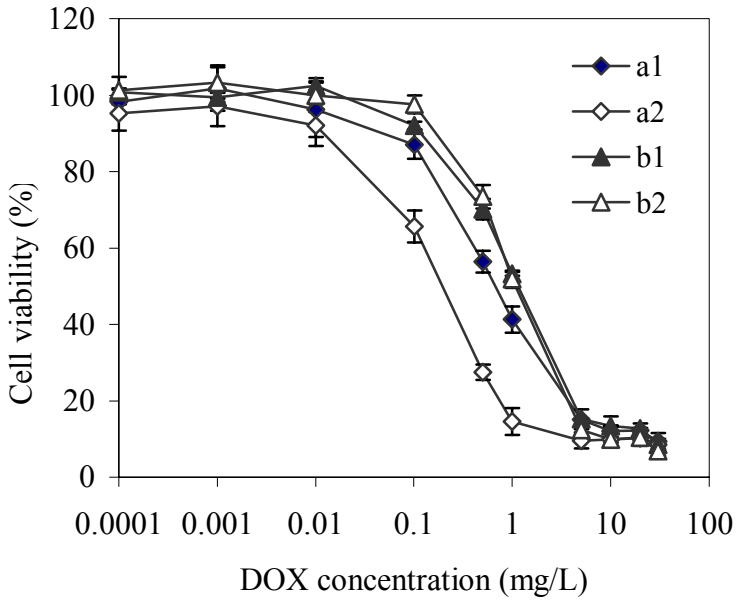

Figure 5.13 Viability of MDA-MB-435S cells incubated with (a1) DOX-loaded polymer D micelles at 37°C and (a2) DOX-loaded Polymer D micelles at 39.5°C. (b1) free DOX 37°C; (b2) free DOX 39.5°C.

5.3 Paclitaxel-loaded micelles

5.3.1 Size and morphology of blank and paclitaxel-loaded micelles

P(NIPAAm-*co*-DMAAm)-*b*-PLGA block copolymers with two different PLGA contents (Polymer C and Polymer D) were synthesized. The CAC values of polymers were 7.9 and 5.0 mg/L respectively (Table 5.3). The size and size distribution of blank and paclitaxel-loaded micelles in DI water are listed in Table 5.5. The average effective diameters of the blank and drug-loaded micelles were in the range of 60 to 120 nm with a relatively narrow size distribution (polydispersity < 0.3), making them less susceptible to clearance by the reticuloendothelial system. The micelles made from Polymer D were bigger than those fabricated from Polymer C because of its longer core-forming block (Shuai and Ai et al., 2004). After loading of paclitaxel, the size of the micelles increased. TEM and AFM images show that the blank and paclitaxel-loaded micelles made from the two polymers were spherical in shape (Figure 5.14 and Figure 5.15). The size of the micelles measured by dynamic light scattering (Table 5.5) is consistent with that visualized by TEM and AFM images. Furthermore, it was observed that the size and morphology of the micelles remained unchanged after freeze-drying. This is an important property for storage and transportation of the end products. It was frequently reported that freeze-dried polymeric micelles did not re-dissolve in aqueous media (Huh and Lee, 2005). The surface charges of both the blank and paclitaxel-loaded micelles are also listed in Table 5.5. All the micelles formulations had negative surface charges at room temperature in DI water. The micelles did not aggregate in the presence of FBS (fetal bovine serum), which was attributed to the hydrophilic nature and negative surface charge of the micelles. The LCST of both Polymer C and Polymer D micelles was 39.0°C (Table 5.2).

Table 5.5 Properties of blank and paclitaxel-loaded micelles.

Samples	CAC[a] (mg/L)	Blank micelles			Paclitaxel-loaded micelles		
		E. D.[b] (nm)	P. D.[c]	Zeta potential (mV)	E.D. (nm)	P.D.	Zeta potential (mV)
C	7.9	66.3± 1.0	0.23± 0.00	-14.4± 3.2	85.7±3.8	0.23±0.01	-11.8±1.0
D	5.0	104.5±0.9	0.15± 0.02	-19.0±5.5	119.5±0.7	0.20±0.01	-17.2±3.0

[a]CAC: Critical aggregation concentration determined from $I_{336.5}/I_{334.5}$ ratios as a function of polymer concentration
[b]E. D.: Effective diameter
[c]P. D.: Polydispersity

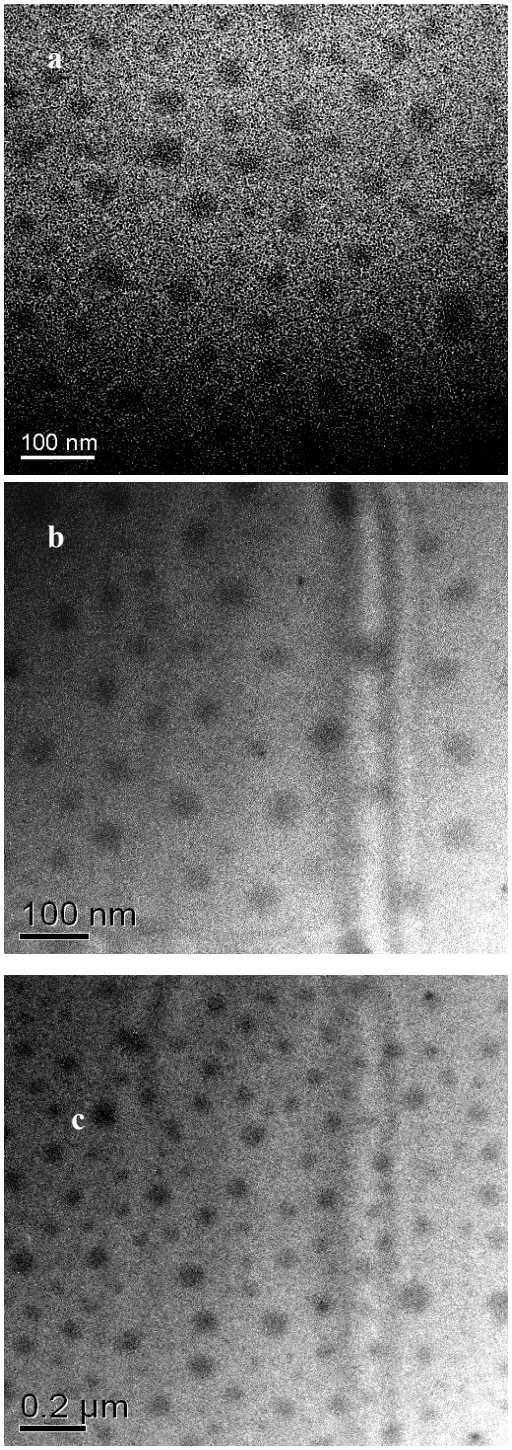

Figure 5.14 TEM images. (a) blank Polymer C micelles; (b) paclitaxel-loaded Polymer C micelles; (c) paclitaxel-loaded Polymer D micelles.

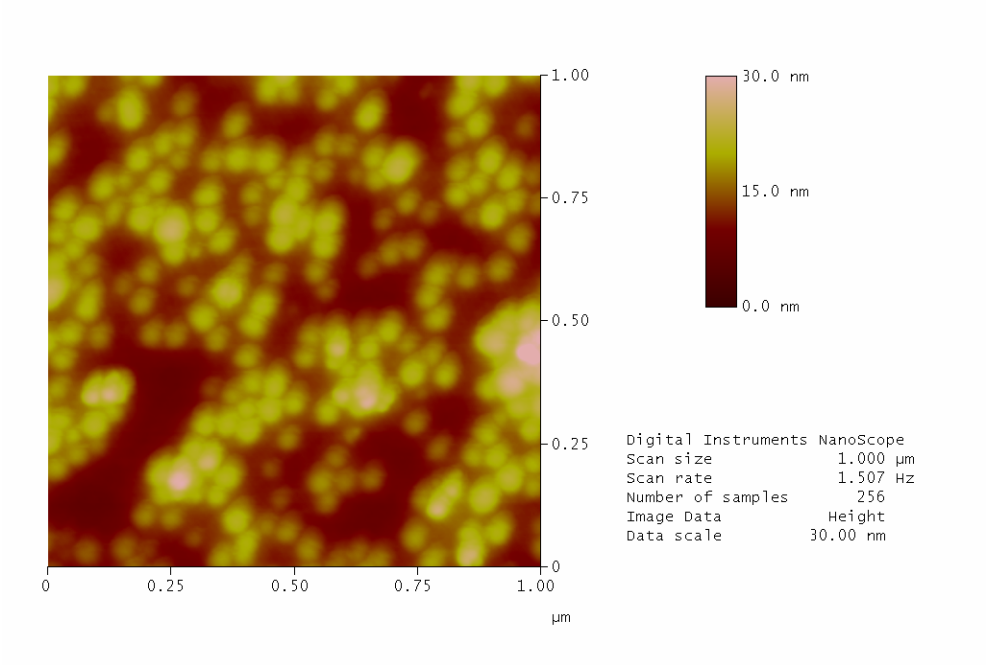

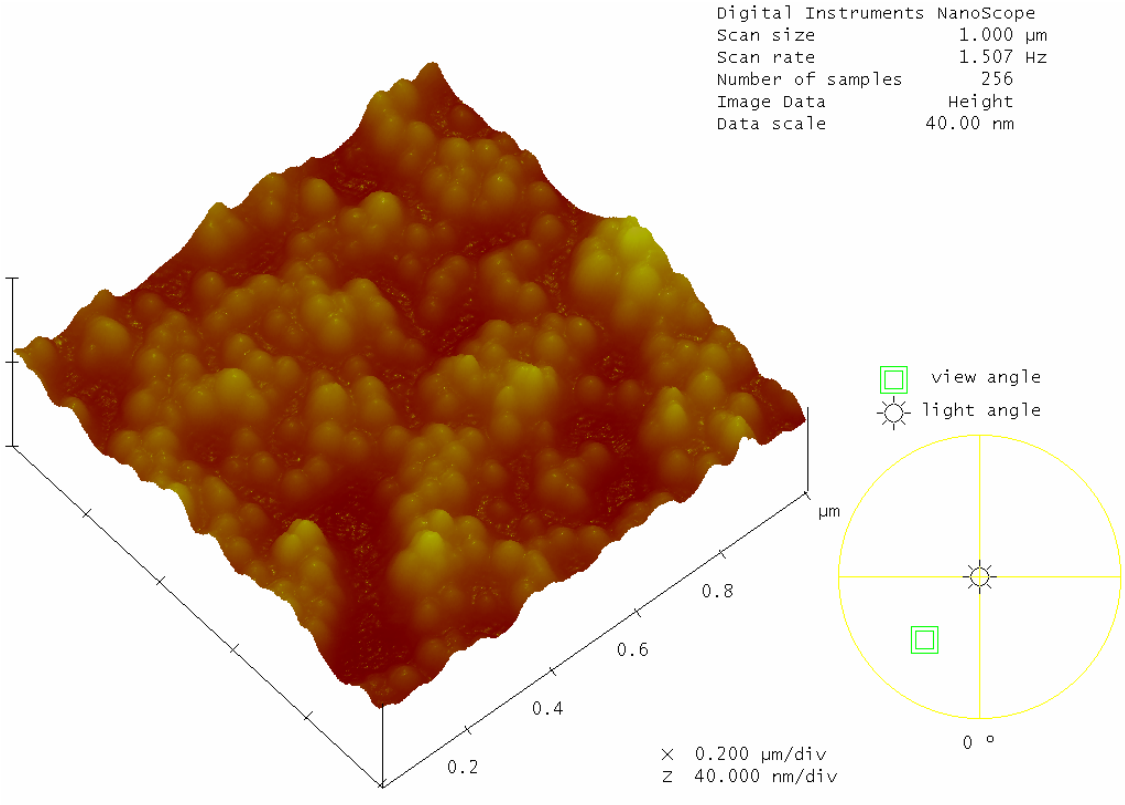

Figure 5.15 AFM images of blank Polymer C micelles.

5.3.2 Drug encapsulation

The loading level and encapsulation efficiency of drug-loaded polymeric micelles are affected by various parameters including fabrication temperature, polymer concentration and initial drug loading (Jones and Leroux, 1999). As reported in our previous study (Chaw et al., 2004), higher polymer concentrations yielded greater higher encapsulation efficiency and drug loading level. However, the particle size also increased. In this study, polymer concentration was fixed at 0.50 (w/v) % to maintain a small size. As shown in Figure 5.16, when the initial paclitaxel loading increased from 9.1% to 20.0%, the encapsulation efficiency of paclitaxel decreased from 50% to 27%, while the actual paclitaxel loading level increased and reached the maximum of 8.2% at the initial loading of 16.7%. Further increasing the initial drug loading level to 20.0% did not lead to greater actual drug loading level and paclitaxel precipitates were found inside the dialysis membrane tube possibly because the initial paclitaxel loading reached the maximum loading capacity of the micelles.

As shown in Figure 5.17, fabrication temperature was another factor influencing the loading level and encapsulation efficiency of paclitaxel. An increased temperature from 4 to 20°C yielded higher encapsulation efficiency and loading level of paclitaxel. However, further increasing the temperature did not lead to any improvement of encapsulation efficiency and loading level. It was observed that at low temperatures such as 4, 10 and 15°C, precipitates were observed inside the dialysis membrane tube probably because of limited water solubility of paclitaxel at these temperatures, leading to lower encapsulation efficiency and drug loading level. However, at a higher temperature such as 25°C, solvent

removal rate increased, leading to faster solidification of the PLGA core before the incorporation of paclitaxel. Therefore, there is an optimized fabrication temperature to achieve high encapsulation efficiency and loading level of paclitaxel. In the following in vitro release, cellular uptake and cytotoxicty studies, the paclitaxel-loaded micelles were fabricated at 20°C.

Figure 5.17 also shows that Polymer D with the longer hydrophobic segment of PLGA yielded greater encapsulation efficiency and loading level of paclitaxel. For instance, the encapsulation efficiency and loading level of paclitaxel was 34.6% and 8.2% respectively for Polymer C micelles, and 46.8% as well as 11.5% respectively for Polymer D micelles. This may be because longer hydrophobic block resulted in a big core and thus offered greater capacity for drug loading (Allen and Maysinger, 1999). It is also possible to assume that the hydrophobic interaction between the drug and the core increased with a longer core-forming length, resulting in higher loading capacity.

5.3.3 Core-shell structure of micelles and drug distribution

The core-shell structure of paclitaxel-loaded micelles and distribution of paclitaxel in the micelles were studied by comparing ^{1}H-NMR spectrum of paclitaxel-loaded micelles in D_2O with that in $CDCl_3$. Figure 5.18 shows the typical spectra of paclitaxel-loaded Polymer C micelles in D_2O with that in $CDCl_3$. In D_2O, only the peaks of the precursor copolymer P(NIPAAm-*co*-DMAAm) existed (i.e. -C*H*$_3$ at δ 1.0; -C*H*-C=O-NH at δ 1.5; -C*H*$_2$-CH at δ 2.0; -NHC*H*Me$_2$ at δ 3.8; -N*Me*$_2$ at δ 2.8-3.0) but the characteristic peaks of PLGA block and drug were not found. However, in $CDCl_3$, the characteristic peaks

of paclitaxel were observed at δ 4.2-5.0, δ 5.6-6.3 and δ 7.4-8.2 in addition to those of PLGA (i.e. –C*H*MeO- at δ 5.1-5.3 and -CH_2O- at δ 4.6-4.9) and P(NIPAAm-*co*-DMAAm). These results suggested that the paclitaxel-loaded micelles had a well-defined core-shell structure having a core of PLGA and a shell of P(NIPAAm-*co*-DMAAm), and paclitaxel molecules were located in the core.

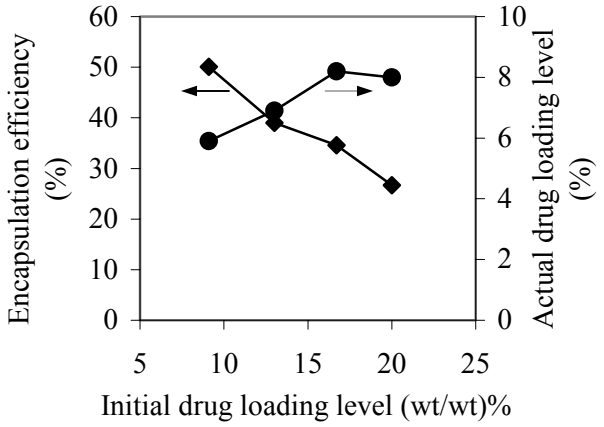

Figure 5.16 Effect of initial paclitaxel loading level on encapsulation efficiency and actual loading level of paclitaxel. (Polymer C micelles; fabrication temperature: 20ºC)

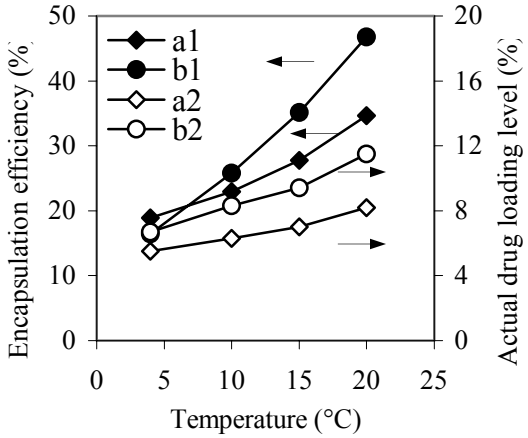

Figure 5.17 Effect of fabrication temperature on encapsulation efficiency and actual loading level of paclitaxel. (a1, a2: Polymer C micelles; b1, b2: Polymer D micelles; initial paclitaxel loading: 16.7% in weight)

The physical status of paclitaxel inside the micelles was further studied by thermal analysis. From Table 5.6, pure paclitaxel exhibited a melting point of 224°C. However, it was not observed in the paclitaxel-loaded micelles, indicating that paclitaxel molecules were in an amorphous phase. In addition, Polymer D micelles had two glass transition temperatures, which were 131°C from P(NIPAAm-*co*-DMAAm) block and 46°C from PLGA block. After loading of paclitaxel, T_g of PLGA block increased to 51°C but T_g of P(NIPAAm-*co*-DMAAm) block remained unchanged. This finding further confirmed that paclitaxel molecules were located in the core of the micelles. The increase in Tg of PLGA block was possibly because the rigid paclitaxel molecules block the movement of the PLGA block. Figure 5.19 shows WAXRD spectra of pure paclitaxel and paclitaxel-loaded micelles. The X-ray diffraction spectrum of paclitaxel exhibited a number of sharp peaks, indicating a highly crystallized structure of paclitaxel. After encapsulated into the micelles, the crystalline structure disappeared. Thus the T_m of paclitaxel was not

observed in the DSC curves. This finding further confirmed that paclitaxel molecules were molecularly distributed in the micelles.

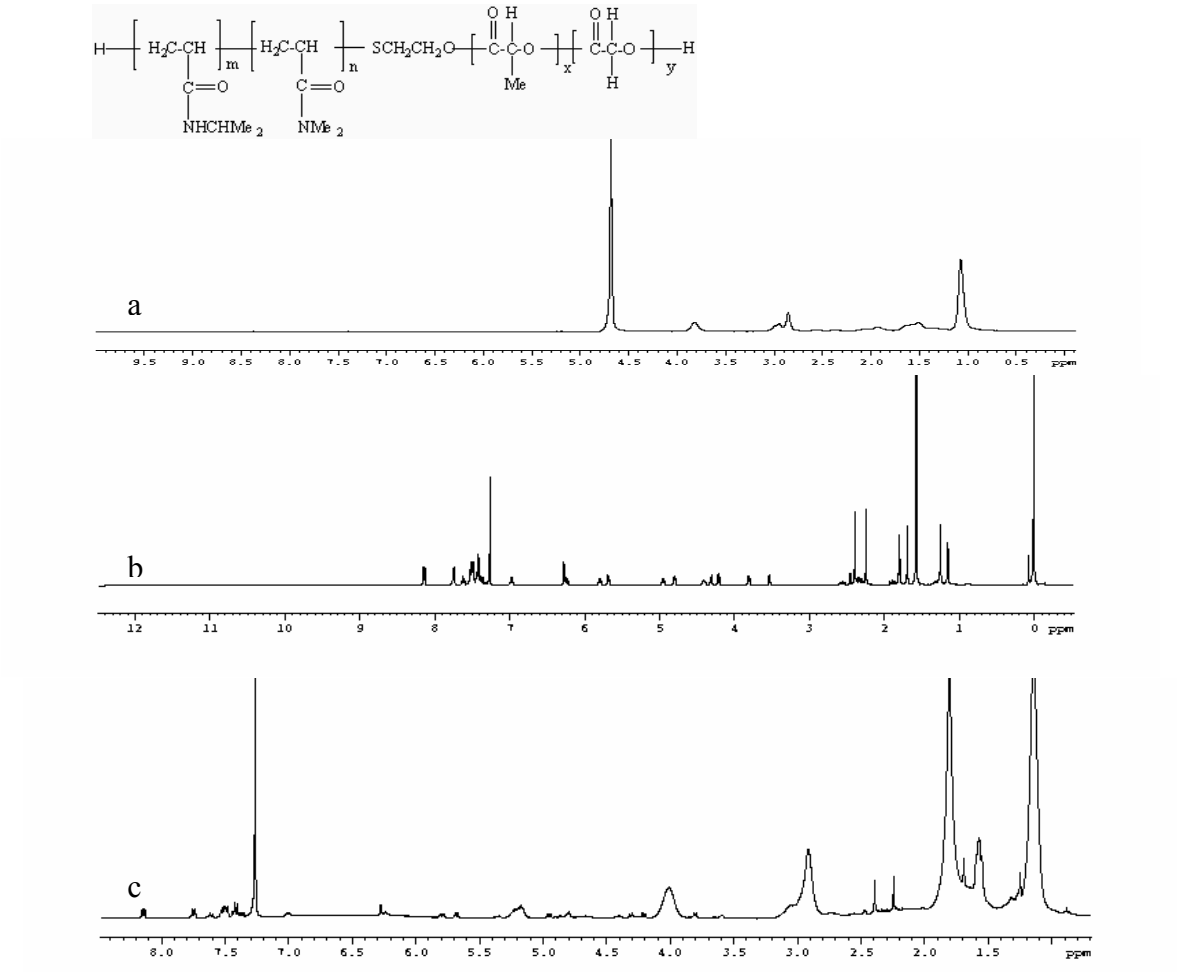

Figure 5.18 ^{1}H-NMR spectra of the paclitaxel-loaded Polymer D micelles dissolved in D_2O (a); paclitaxel in $CDCl_3$ (b); paclitaxel-loaded Polymer D micelles in $CDCl_3$ (c).

Table 5.6 Glass transition temperatures (T_g) and melting points (T_m) of paclitaxel, blank micelles and paclitaxel-loaded micelles.

	T_g (°C) of P(NIPAAm-*co*-DMAAm) block	T_g (°C) of PLGA block	T_m (°C)
Paclitaxel	-	-	224
Polymer D micelles	131	46	-
Paclitaxel-loaded Polymer D micelles	131	51	-

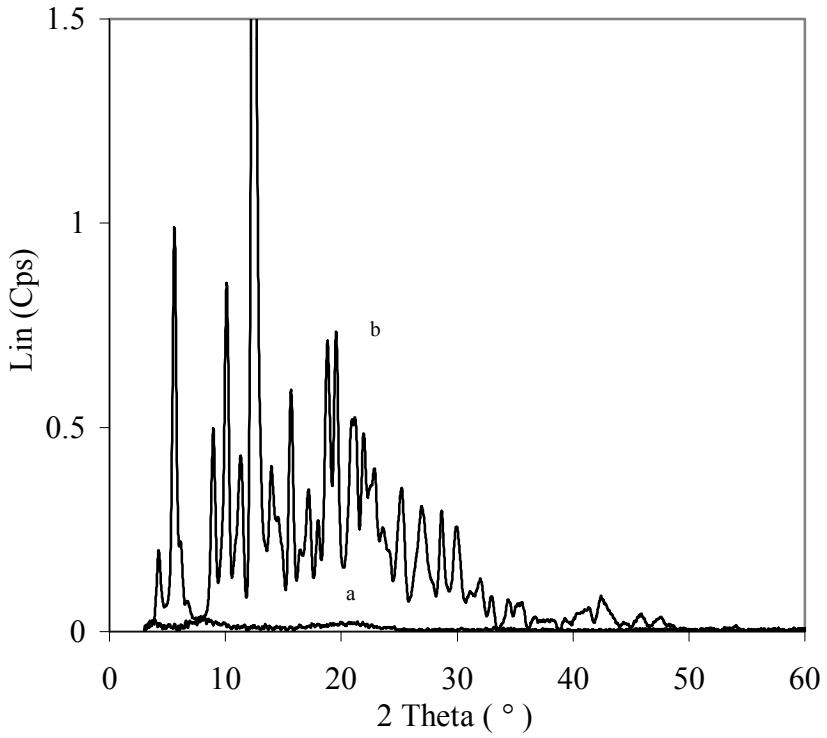

Figure 5.19 WAXRD spectra of paclitaxel-loaded Polymer D micelles (a) and free paclitaxel (b).

5.3.4 In vitro release of paclitaxel

Figure 5.20 shows the cumulative release of paclitaxel from the micelles incubated in PBS buffer at 37ºC (below the LCST) and 39.5ºC (above the LCST). A sustained release of paclitaxel was achieved from all the formulations. The paclitaxel release was accelerated at the temperature above the LCST. For instance, more than 80% of paclitaxel was released within three days from Polymer C micelles at 39.5ºC whereas less than 30% of paclitaxel was released within the same period of time at 37ºC. The results show that paclitaxel release was in response to the external temperature change. When the temperature was below the LCST, the core-shell structure was stable, and paclitaxel release depended on its slow diffusion. However, when the temperature increased to a value above the LCST, the outer shell collapsed. The collapsed shell induced the deformation of the core-shell structure, exposing paclitaxel molecules to the external *in vitro* release medium and thus accelerating paclitaxel release.

Comparing Polymer C micelles with Polymer D micelles, paclitaxel release from Polymer C micelles was faster. The increased length of PLGA block caused greater polymer aggregation number per micelle, resulting in stronger PLGA-paclitaxel hydrophobic interactions and thus hampering paclitaxel release. On the other hand, the increased length of PLGA block led to larger core of the micelles, providing a longer distance for paclitaxel molecules to diffuse into the external *in vitro* release medium and thus decreasing paclitaxel release rate.

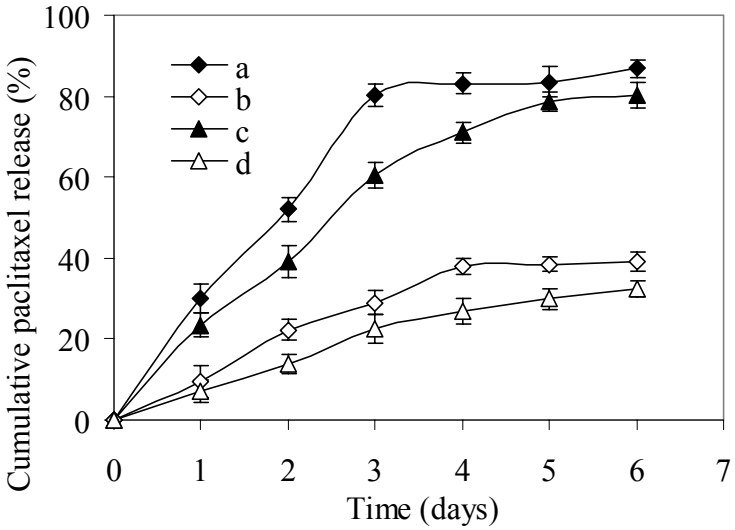

Figure 5.20 Release profiles of paclitaxel from Polymer C micelles incubated at 39.5°C (a) and 37°C (b); Polymer D micelles incubated at 39.5°C (c) and 37°C (d).

5.3.5 Cytotoxicity study

The *in vitro* cytotoxicity tests of blank micelles, free paclitaxel and paclitaxel-loaded Polymer D micelles were performed against MDA-MB-435S cells at different temperatures. As shown in Figure 5.21, there was no significant effect of incubation temperature on the cytotoxicity of free paclitaxel (IC_{50} = 0.063 mg/L at 39.5°C *vs* IC_{50} = 0.082 mg/L at 37°C). However, paclitaxel-loaded micelles showed much greater cytotoxicity at 39.5°C than at 37ºC (IC_{50} = 0.0061 mg/L at 39.5°C *vs* IC_{50} = 0.048 mg/L at 37°C). It should be mentioned that no obvious cytotoxcicity (over 90% cell viability) of blank micelles (up to 500 ppm) at 37ºC or 39.5°C (data not shown). The pronounced cytotoxicity of paclitaxel-loaded micelles at 39.5°C was attributed to the enhanced release of paclitaxel (Figure 5.20). Free paclitaxel showed less cytotoxicity as compared to paclitaxel-loaded micelles, possibly due to multi-drug resistance effect.

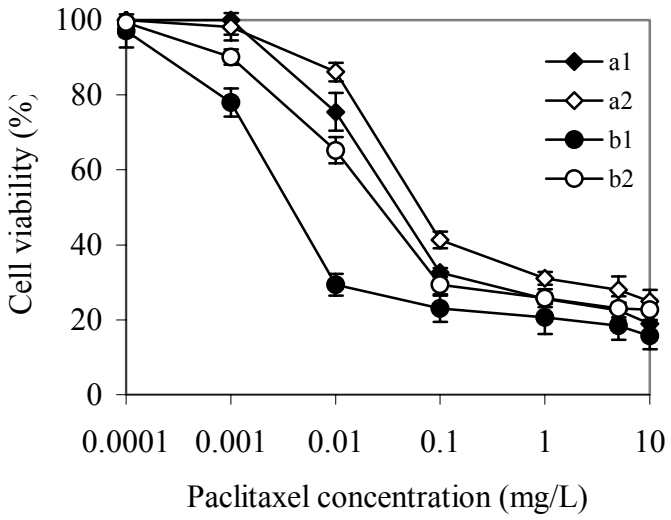

Figure 5.21 Viability of MDA-MB-435S cells incubated with (a1) free paclitaxel at 39.5°C; (a2) free paclitaxel at 37°C; (b1) paclitaxel-loaded Polymer D micelles at 39.5°C and (b2) paclitaxel-loaded Polymer D micelles at 37°C.

5.4 A comparison between DOX-loaded polymer micelles and paclitaxel-loaded polymer micelles

DOX and paclitaxel were employed as model anticancer drugs and loaded into polymer micelles. As discussed earlier, micelles properties are affected by various parameters such as polymer composition and fabrication process. Furthermore, drug physicochemical properties, biological properties and disease properties are critical to designing micelles.

5.4.1 Effect of physicochemical properties on encapsulation efficiency

In addition to other factors presented in the previous paragraphs, drug physicochemical properties greatly affected drug incorporation into polymer micelles. As shown in Table 5.7, under the optimized fabrication condition, encapsulation efficiencies of paclitaxel-

loaded micelles were much higher than those of DOX-loaded micelles. For example, encapsulation efficiency yielded by Polymer D micelles was 9.7% and 46.8% for DOX-loaded micelles and paclitaxel-loaded micelles, respectively. The physicochemical properties of drugs such as polarity, hydrophobicity, charge and degree of ionization have been found to greatly influence the incorporation. Among these factors, hydrophobicity plays a key role in drug loading for physical entrapment of drugs. Unlike paclitaxel, deprotonated DOX (after treatment with TEA) is less hydrophobic because of its polar hydroxyl and amino groups (Shuai and Ai et al., 2004). However, loading level was similar. This may be because the core space is limited for a specific core-forming block.

Table 5.7 Comparison of drug loading between DOX-loaded and paclitaxel-loaded micelles.

Samples	DOX		Paclitaxel	
	Loading level	Encapsulation efficiency	Loading level	Encapsulation efficiency
Polymer C	6.2	7.6	8.2	34.6
Polymer D	8.0	9.7	11.5	46.8

5.4.2 Effect of physicochemical properties on drug release

As shown in Figure 5.9 and Figure 5.20, similar to DOX release, paclitaxel release from pacltaxel-loaded micelles was accelerated when the environmental temperature was raised slightly above the LCST. However, a more sustained release of paclitaxel was achieved from the paclitaxel-laoded micelles compared to DOX release. For instance, complete doxorubicin release from the micelles was achieved within the first 10 hours at 39.5ºC (Figure 5.9) whereas complete paclitaxel release was achieved after 3 days

incubation at 39.5ºC (Figure 5.20). It is known that drug release is a complicated process. Several mechanisms of drug release from biodegradable polymeric micelles have been proposed: drug release by polymer erosion, diffusion, drug dissolution and micelles stability (Allen and Maysinger, 1999). It is difficult to predict a drug release profile because it is governed by two or more mechanisms listed. A lot of studies have reported that polymer erosion had a great effect on drug release (Potineni and Lynn, 2003). However, in this study, the time required for complete degradation was more than one month (Section 5.2.5). Therefore, it seems that drug release from micelles was affected mainly by diffusion, drug dissolution and micelles stability. Furthermore, diffusion is affected by various factors such as the strength of the interactions between the drug and the core-forming block. Paclitaxel is more hydrophobic than DOX, the interaction between paclitaxel and core-forming block is thus stronger than that between DOX and, resulting in slow drug release. Besides, the water solubility of DOX is much higher than that of paclitaxel, leading faster release.

5.4.3 Effects of biological properties on cytotoxicity

The *in vitro* cytotoxicity of free drugs (DOX *versus* paclitaxel) and drug-loaded micelles against various cells was analyzed and compared (Table 5.8). Similar to paclitaxel loaded micelles, IC_{50} values of DOX-loaded micelles for MDA-MB-435S cells were lower than those of free DOX. This may be because of increased cellular uptake of DOX-loaded micelles. However, IC_{50} values of both free DOX and DOX-loaded micelles for MDA-MB-435S cells were higher than those of paclitaxel, indicating DOX was less toxic than paclitaxel. On the other hand, it was found paclitaxel ($IC_{50} > 50$ ppm) was not as efficient

as DOX (IC_{50} = 3.2 ppm) for *in vitro* cytotoxicity against 4T1 cells and MCF-7 cells. As described in Chapter 2, DOX exerts its effects on cancer cells *via* inhibiting the synthesis of DNA as well as DNA transcription. However, paclitaxel is a unique antimicrotubule agent which binds and stabilizes microtubululin during the later G2 mitotic phase of the cell cycle. It is possibly to assume that the different effect of drugs on *in vitro* cytotoxicity was attributed to the different extent of damage caused by drugs involved in different cells. Therefore, formulation should be well designed in order to achieve a desired effect of chemotherapy.

Table 5.8 Comparison of IC_{50} of free drug and drug-loaded micelles against various cells.

IC_{50} (mg/L) (drug concentration)	4T1 cells		MDA-MB-435S		MCF-7	
	37°C	39.5°C	37°C	39.5°C	37°C	39.5°C
Free DOX	3.2	2.4	1.1	1.0	0.055	0.047
DOX loaded polymer D micelles	7.9	3.1	0.75	0.3	0.16	0.062
Free paclitaxel	59.2	57.3	0.082	0.063	26.1	24.8
Paclitaxel loaded polymer D micelles	48.9	35.4	0.048	0.0061	28.5	15.2

5.5 Conclusions

Thermally sensitive block copolymers, P(NIPAAm-*co*-DMAAm)-*b*-PLGA with various compositions and lengths of PLGA block were successfully synthesized to incorporate doxorubicin and paclitaxel into micelles. The block copolymers were degradable, and the degradation of PLGA-based block copolymer was faster than that of PLA-based block copolymer. The block copolymers had a low CAC value in both DI water and PBS buffer. The micelles made from the block copolymers were spherical. The LCST of the micelles in PBS buffer was slightly higher than the normal body temperature, desirable

for *in vivo* applications. The micelles were stable in PBS buffer at 37ºC. An increased length of PLGA block led to a slight increase in drug loading capacity. Polymer D provided a favorable balance of hydrophilicity and hydrophobicity for drug loading. Fast drug release was achieved at a temperature higher than the LCST. Drug-loaded micelles were internalized through an endocytosis pathway. Drug-loaded micelles showed higher cytotoxicity against cells at a temperature above the LCST. In addition, drug encapsulation efficiency, *in vitro* drug release and *in vitro* cytotoxicity of micelles were affected by drug properties. *In vitro* cytotoxicity of drug loaded micelles were also affected by cell biological properties. The micelles made from P(NIPAAm-*co*-DMAAm)-*b*-PLGA with an optimized PLGA block may be employed for anticancer drug delivery.

CHAPTER SIX

RESULTS AND DISCUSSION 2B:

pH-Triggered thermally sensitive micelles for targeted delivery of DOX

6.1 Introduction

Micelles self-assembled from poly (*N*-isopropylacrylamide-*co*-*N, N*-dimethylacrylamide)-based amphiphilic copolymers have also been studied for delivery of other therapeutics (Chaw and Chooi *et al.*, 2004). However, a major disadvantage of such systems is that their application is limited to surface organ or tumors (Soppimath *et al.*, 2005). An alternative approach to targeting drugs to tumor tissues is to use pH-sensitive polymeric micelles. The pH value of disease site such as tumor tissue is significantly lower than that under normal physiological conditions (pH 7.0 *versus* pH 7.4) (Haag, 2004). The pH-sensitive drug carriers remained intact until they have reached tumor tissue or subsequently been taken up by a cell but deformed and drug release was triggered under low pH conditions (Bae and Fukushima *et al.*, 2003). In addition, active targeting could be further improved by introducing recognition signals such as folic acid onto the surface of the nanoparticles. The choice of folic acid is because its corresponding receptor is abundantly distributed on the surface of most cancer cell types. Based on these concepts, we have developed temperature and pH-sensitive folate-conjugated poly(*N*-isopropylacrylamide-*co*- *N, N*-dimethylacrylamid-co-methacrylate)-*b*-PUA (FA conjugated Poly(NIPAAm-*co*-DMAAm-*co*-MAm)-*b*-PUA) micelles for DOX delivery. The novelty of this system is the ability to target drugs to deep tissues or organs without external heating. In this study, DOX-load micelles were fabricated by a membrane dialysis method. DOX release was responsive to environmental pH changes. *In vitro* cytotoxicity of blank micelles, free DOX and DOX-loaded micelles against 4T1 cells were investigated and compared. Mouse breast cancer

model induced by 4T1 cells was employed to study biodistribution of DOX and its blood concentration as a function of time.

6.2 Results and discussion

6.2.1 Synthesis of folate- conjugated Poly(NIPAAm-*co*-DMAAm-*co*-MAm)-*b*-PUA

The folate(FA)-conjugated copolymer was synthesized by multiple steps. Firstly, carboxylic acid-terminated poly(NIPAAm-*co*-DMAAm-*co*-MAm) was prepared by the radical copolymerization using benzoyl peroxide (BPO) as an initiator and 3-mercaptopropionic acid as a chain transfer agent (Figure 3.2). MAm monomer was introduced due to the presence of amine group for further conjugation of folic acid. The precursor polymer was obtained after purification by a liquid-liquid diffusion method (THF/Et_2O), followed by dialysis against DI water. The molecular weight of this polymer is 6.8 kDa, having a polydispersity of 1.7 (Table 6.1). Subsequently, activated folic acid was conjugated to the amine group of carboxylic acid-terminated poly(NIPAAm-*co*-DMAAm-*co*-MAm). Although folic acid has α- and γ--carboxylic acid, γ--carboxylic acid was primarily activated in the DCC/NHS reaction (Figure 3.3 (a). Therefore, γ--carboxylic acid was conjugated to precursor polymer due to its higher reactivity (Figure 3.3(b)). The resulting solution was centrifuged to discard the pellets, followed by dialysis against DI water. Pale-yellow polymer was obtained after freeze-dry. The molecular weight of this polymer was 7.1 kDa, having a polydispersity of 1.8. Thirdly, amine group-terminated PUA polymer was prepared by the radical copolymerization using the redox agent ammonium persulfate (APS) as an initiator and 2-aminoethanethiol as a chain transfer agent (Figure 3.4). The success of the polymerization of UA monomer in

the presence of chain transfer agent was evidenced by the absence of vinylic proton signals at δ 4.8-5.0 (CH_2 = $CHCH_2$) and δ 5.7-5.9 (CH_2 = $CHCH_2$) (Figure 6.1 A). The peaks at δ 1.3, 1.5 and 2.2 were assigned to CH_2CH_2 (Signal a), $HOOCCH_2CH_2$ (Signal b) and $HOOCCH_2$ (Signal c), respectively (Figure 6.1 B). The lack of absorption at 3084 cm^{-1} and 911 cm^{-1} in the FT-IR spectrum of PUA further proved the successful polymerization of UA monomer (Figure 6.2, A). The spectrum of PUA-NH_2 showed an carbonyl band (($\nu_{O\text{-}C=O,}$ a) in the COOH at 1712.3 cm^{-1} (Figure 6.2, A). Finally, the carboxylic acid group of folate-conjugated poly(NIPAAm-*co*-DMAAm-*co*-MAm)-COOH was activated using DCC/NHS in DCM, followed by precipitation two times using ether and vacuum drying. The activated folate-conjugated poly(NIPAAm-*co*-DMAAm-*co*-MAm)-COOH was dissolved in DMSO, and reacted with an excess amount of poly(10-undecenoic acid)-NH_2 (Figure 3.5). The resulting solution was purified by dialysis. The final pale-yellowish product was obtained by freeze-drying, and characterized by GPC, NMR, FTIR and titration. The NMR spectra of the final product shared a similar pattern to that of folate-conjugated poly(NIPAAm-*co*-DMAAm-*co*-MAm)-COOH. As shown in Figure 6.3, the peak at δ 3.8 (Signal a) was contributed to the protons of -NHC*H*Me_2 moieties, the broad peak at δ 2.7-3.0 (Signal b) was from -N*Me*$_2$ groups in the DMAAm moieties, the weak peaks at δ 6.6 (Signal c), δ 7.7 (Signal d) and δ 8.7 (Signal e) were from folic acid moieties. The FTIR spectrum showed two strong absorptions at 1647.1 cm^{-1} ($\nu_{HN\text{-}C=O}$) and 1547.8 cm^{-1} ($\nu_{C\text{-}N}$) caming from the poly(NIPAAm-*co*-DMAAm-*co*-MAm) block. Another weak absorption at 1720 cm^{-1} ($\nu_{O\text{-}C=O}$, b) was from the PUA-NH_2 block and folate moieties (Figure 6.2 B). Mw of the final product was 7.7 kDa with a polydispersity of 1.5. The increase of Mw indicated

that PUA-NH_2 was successfully conjugated to folate-conjugated poly(NIPAAm-*co*-DMAAm-*co*-MAm)-COOH (Table 6.1). The COOH content was estimated to be 18.4 mg per gram of polymer.

Table 6.1 Properties of the copolymers.

Samples	M_w (kDa)	M_n (kDa)	Polydispersity
Carboxylic-terminated Poly(NIPAAm-*co*-DMAAm-*co*-MAm)	6.8	4.1	1.7
Folate-conjugated Poly(NIPAAm-*co*-DMAAm-*co*-MAm)-COOH	7.1	3.9	1.8
Folate-conjugated Poly(NIPAAm-*co*-DMAAm-*co*-MAm)-*b*-PUA	7.7	5.0	1.5

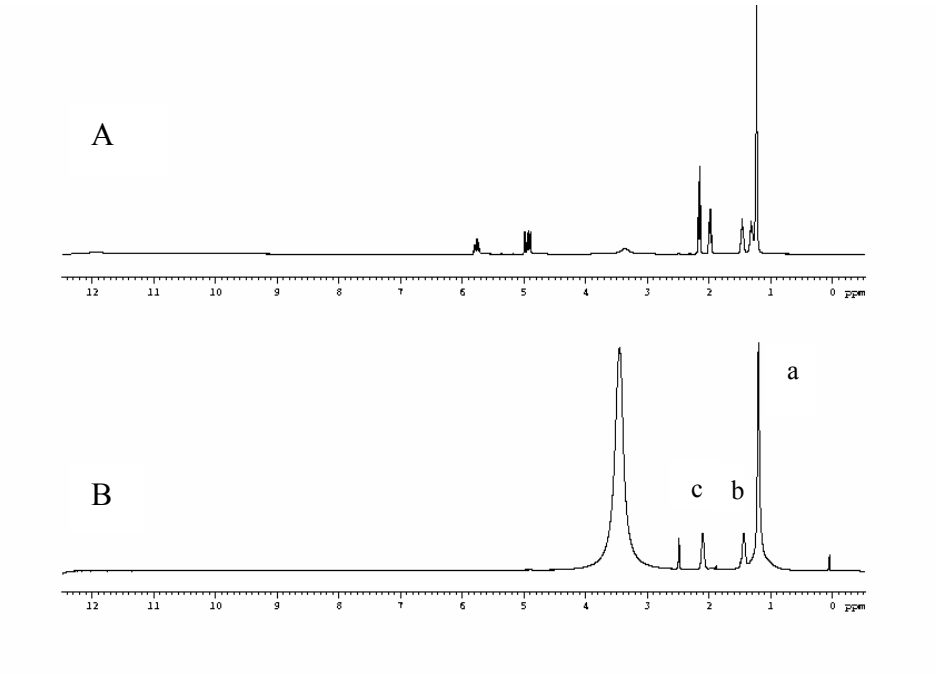

Figure 6.1 Typical ^{1}H-NMR spectra of UA (A) and PUA (B) (*d*-DMSO as solvent).

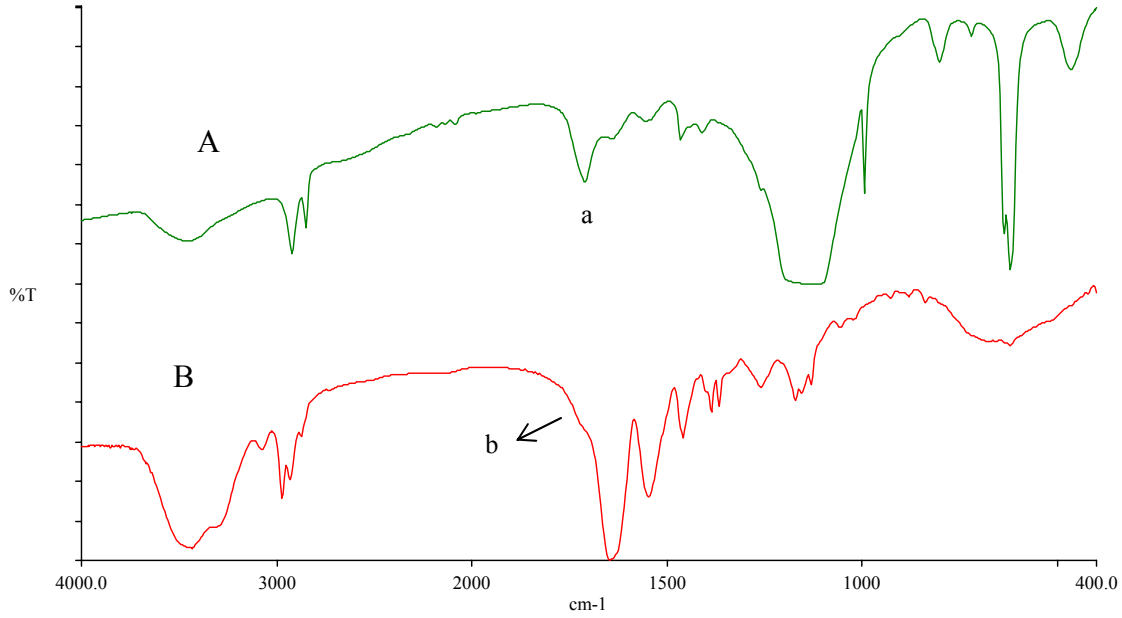

Figure 6.2 FT-IR spectra of PUA-NH_2 (A) and folate-conjugated poly(NIPAAm-*co*-DMAAm-*co*-MAm)-*b*-PUA (B).

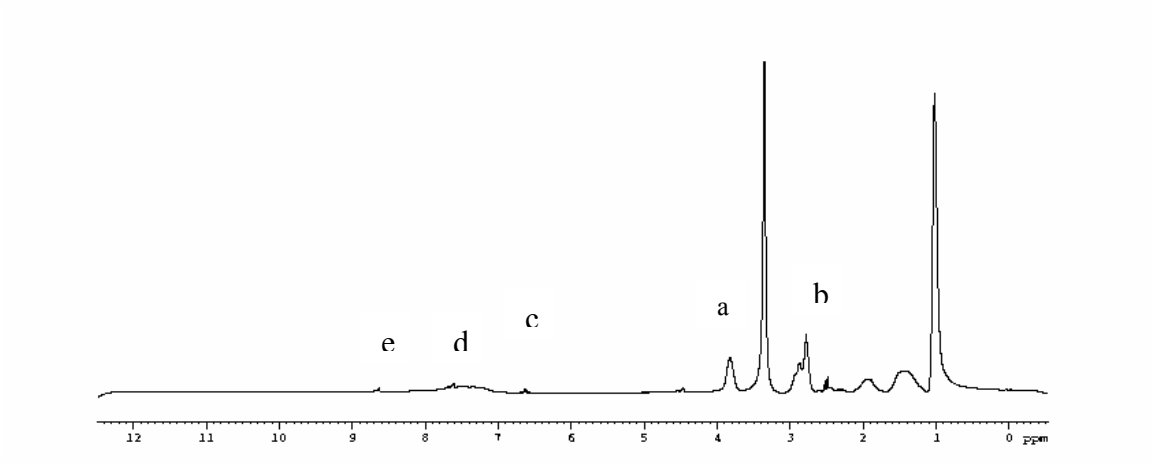

Figure 6.3 ^{1}H-NMR spectrum of folate-conjugated poly(NIPAAm-*co*-DMAAm-*co*-MAm)-*b*-PUA.

6.2.2 LCST of micelles and effect of pH

PNIPAAm exhibits an LCST of 32ºC in water. The LCST can be modulated *via* introducing hydrophobic or hydrophilic monomers. In this study, poly(10-undecenoic acid) was used as the hydrophobic block. The carboxylic group in the hydrophobic block could influence the hydrophobicity of the polymer. Figure 6.4 shows the LCST of precursor polymer and final micelles measured in buffer solutions of different pH. The LCST of the precursor polymer was found to be 39.5°C and 38.4°C at pH 7.4 and pH 6.6, respectively. This may be due to the protonation effect of the carboxylic acid group of folic acid and that of carboxylic acid-containing chain transfer agent. With the incorporation of a terminal hydrophobic group of PUA, the LCST of micelles at pH 7.4 decreased to 38.0°C. The LCST of micelles at pH 6.6 was 36.2°C. The results indicated that the LCST values of micelles are pH dependent. This is because with the decrease of pH, the carboxylic acid groups in the 10-undecenoic acid segment (pKa of 10-undecenoic acid = 6.8) protonated. The hydrophobicity of polymer thus increased. Since the LCST of the micelles is higher than the normal body temperature in the physiological environment (pH 7.4) but lower than the normal body temperature in acidic environments (e.g. pH 6.6), these micelles can be used for intracellular drug delivery. In the endosomes or lysosomes (pH 5.0-7.0 in endosomes and pH 4-5 in lysosomes), the micelles can adsorb protons and the shell of the micelles becomes hydrophobic due to the decrease in the LCST. These may help to break down the endosome or lysosome membrane, releasing the enclosed drug molecules into cytoplasm.

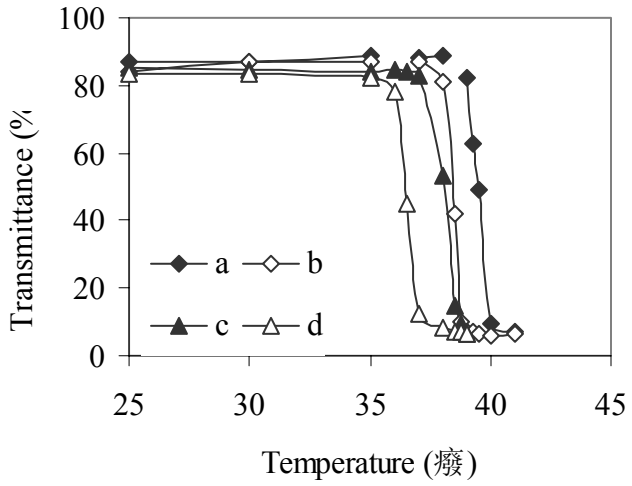

Figure 6.4 Plot of transmittance of polymer solutions as a function of temperature at varying pH at 500 nm. (a) precursor polymer in PBS (pH 7.4); (b) precursor polymer at pH 6.6; (c) micelles in PBS (pH 7.4); (d) micelles at pH 6.6.

6.2.3 CAC determination

The formation of micelles from the polymer was investigated by the detection of CAC using a fluorescence technique. The excitation spectra of pyrene are illustrated in Figure 6.5. As polymer concentration increased, the fluorescence intensity increased and the third peak shifted from 334.0 nm to 335.5 nm. The red shift of the third peak indicated that pyrene molecules transferred to less polar domains of the core of micelles. Figure 6.6 shows the change of ratio of I334.0 to I335.5 against polymer concentrations at DI water. The CAC value was determined from the intersection of the tangent curve to the curve at the inflection with the horizontal tangent through the points at low polymer concentrations. The CAC of polymer at DI water was 17.8 mg/L. The low CAC value indicates that such micelles would remain stable under conditions of extreme dilution, as would be the case in the physiological environment, after administration.

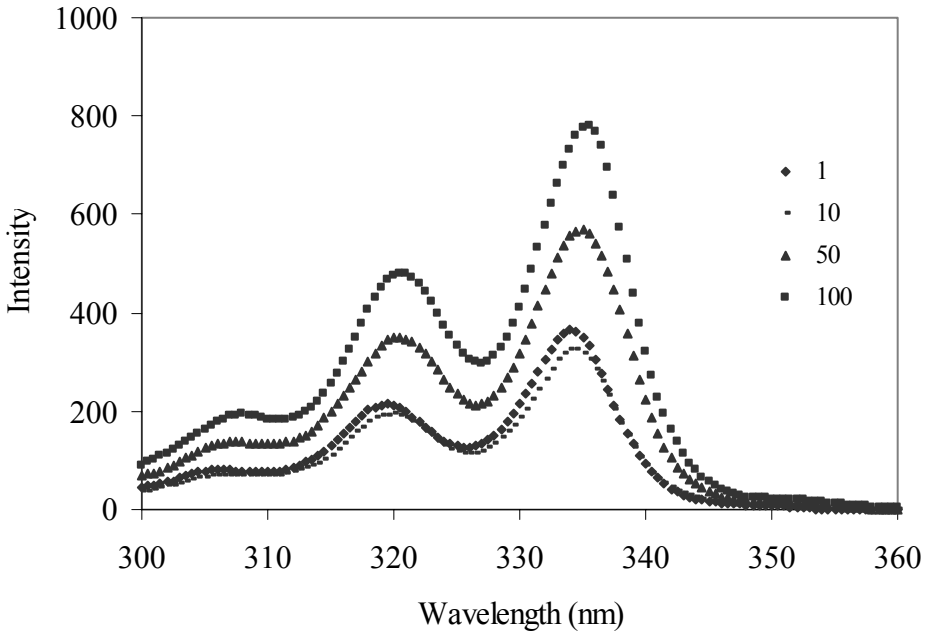

Figure 6.5 Excitation spectra of pyrene as a function of polymer concentration in DI water.

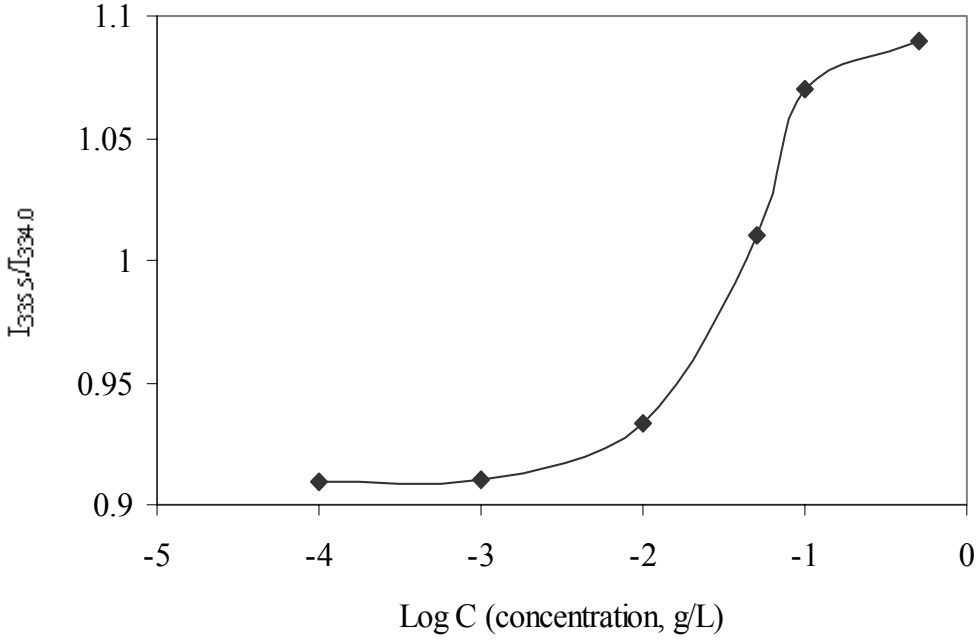

Figure 6.6 Plot of intensity ratio of $I_{335.5}/I_{334.0}$ as a function of log C for polymer in DI water.

6.2.4 pH effect on structural changes of micelles

To study the effect of pH on the structural change of micelles, the change of the intensity ratio ($I_{335.5}/I_{334.0}$) of pyrene at 37°C in the presence of micelles prepared in buffers of different pH was investigated (ionic strength = 154 mM). As shown in Figure 6.7, for micelles at pH 7.4 and pH 7.2, the ratio of I 335.5 nm to I 334.0 nm was high and relatively constant, indicating that pyrene molecules were in a low polar microenvironment. However, the intensity ratio sharply decreased as the pH decreased from pH 7.0, indicating pyrene molecules were exposed to a more polar environment (aqueous medium) as the pH decreased. As stated earlier, carboxylic acid group in the micelles deionized below pH 6.8, leading to a lower LCST. Internal structure of micelles was thus perturbed due to the dehydration of micelles at 37°C.

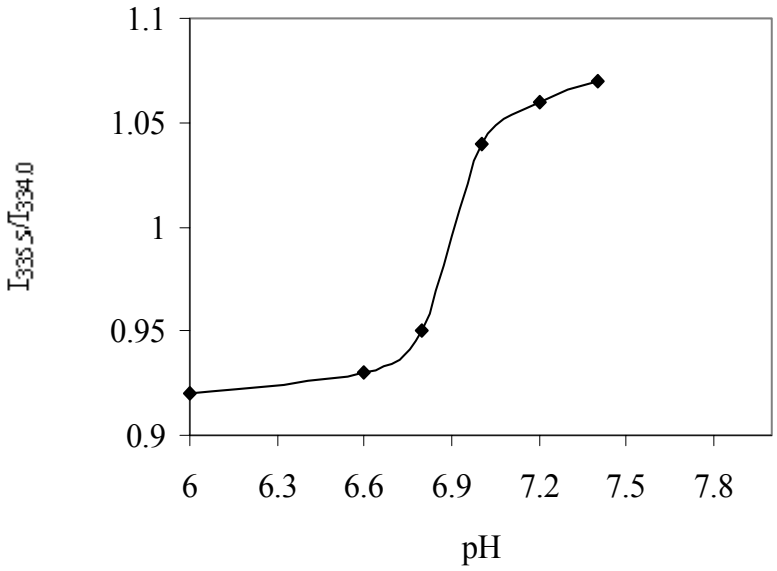

Figure 6.7 Plot of intensity ratio of $I_{335.5}/I_{334.0}$ as a function of pH for polymer in buffers.

6.2.5 Size and morphology of the micelles

Table 6.2 lists the size and size distribution of the micelles fabricated in DI water. It was found that micelles have a relatively narrow size distribution and the average effective diameter of blank micelles was 92.8 nm. The effective diameter of the DOX-loaded micelles was 98.5 nm, indicating that micelles size was slightly affected by drug loading. The morphologies of the micelles are spherical (Figure 6.8). The particle size observed from the TEM picture is in good agreement with that measured by dynamic light scattering. Physical stability of the micelles is another important aspect to be considered for clinical applications because the aggregation of micelles may cause blood vessel occlusion and make them more susceptible to clearance by the RES. It is found that the diameter remained little difference in PBS medium over 1 week at room temperature (87nm-97nm), suggesting that particles are stable in the PBS. On the other hand, the particle size does not change for diluted micelles (87.0nm *vs.* 92.1nm) (5 times dilution). This is crucial since dissociation of micelles after administration will lead to rapid release of the drug, resulting in side effects *in vivo*. Furthermore, the particle size of the blank micelles did not change significantly in PBS buffer containing 10% BSA, indicating that the interactions between particles and protein are weak. This can be attributed to the negative surface charge (Table 6.2). It is expected that the micelles would have good physical stability *in vivo*. The size of micelles in buffer solutions of different pH was studied. It was observed that the effective diameter of micelles was pH dependent (117.2 nm in pH7.4 *vs.* 612.6 nm in pH 6.6 at 37°C). The increase of particle size was due to the aggregation of micelles in pH 6.6. Furthermore, the particle size was also temperature dependent. For instance, the particle size was about 117.2 nm at 37°C in

PBS, the size increased to 740.0 nm at 40°C due to the aggregation of micelles above the LCST. These results indicate that the micelles were both temperature and pH sensitive. In particular, the change in particle size was reversible.

Table 6.2 Properties of empty micelles and DOX-loaded micelles

Samples	Effective diameter (nm)	Polydispersity	Zeta potential (mV)
Blank micelles	92.8±0.1	0.27±0.01	-14.6±3.0
DOX-loaded micelles	98.5±2.1	0.28±0.01	-11.2±1.0

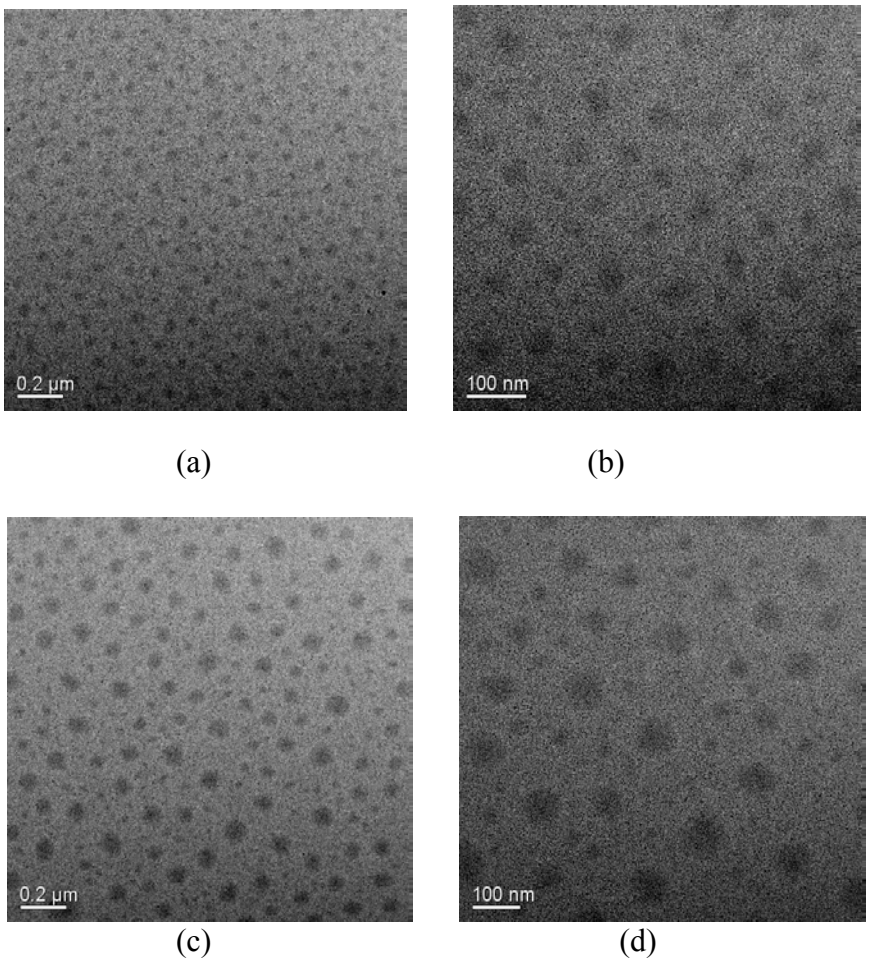

Figure 6.8 TEM images. (a, b) blank micelles; (c, d) DOX-loaded micelles.

6.2.6 Drug encapsulation and in vitro drug release

The incorporation of DOX into micelles was carried out under the conditions stated in Section 3.3. The actual loading level of DOX in the micelles was about 2.5 % in weight. Unlike the polymer D micelles stated in Section 5.2, in which the actual loading level was about 8.0%, this relatively low loading level in this pH sensitive micelles was because of the less hydrophobic core. Figure 6.9 shows *in vitro* DOX release from the micelles under a physiological condition (PBS, pH 7.4) and in an acidic environment (pH 6.6). DOX release was accelerated for micelles incubated at pH 6.6 and 37°C, with approximately 85% of the drug released within 24 h. However, DOX release from the micelles in pH 7.4 at 37ºC was much slower, with 40% released over 24 h. As discussed in Section 6.2.2, at pH 6.6, the LCST of the micelles decreased to 36.2ºC, leading to hydrophobic shells of the micelles. The loss of hydrophilicity/hydrophobicity balance of the micelles led to the deformation of the core-shell structure, releasing the enclosed drug molecules.

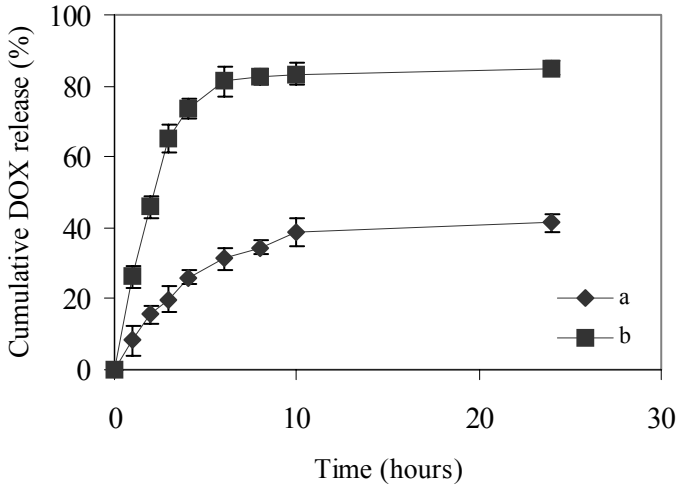

Figure 6.9 Release profiles of DOX from the micelles incubated at 37°C (a) pH 7.4; (b) pH 6.6.

6.2.7 Cellular uptake and *in vitro* cytotoxicity

Cellular uptake of free DOX, DOX-loaded micelles by 4T1 cells was examined and results are shown in Figure 6.10. When free DOX was incubated with 4T1 cells, free doxorubicin molecules are transported into the cell *via* a passive diffusion pathway, doxorubicin molecules are only accumulated in the nucleus. However, strong fluorescence was observed in the cytoplasm as well as nucleus for the cells incubated with DOX-loaded micelles. It is known that endosomes are acidic (Haag, 2004). Due to their acidity, endosomes can alter the LCST of micelles (from a value higher than the normal body temperature to a value lower than the normal body temperature), breaking down the endosome membrane. Therefore, intracellular drug delivery into the cells can be achieved. This indicates that the DOX-loaded micelles were internalized by the cells through endocytosis, and then escaped from the endosome and lysosome to enter the cytoplasm. In addition, it was also found that cellular uptake of DOX-loaded micelles was higher than that of DOX-loaded Polymer D micelles (Figure 5.10). This may be because DOX-loaded micelles were taken up by folate-receptor-mediated endocytosis. The strong signals appeared in the nucleus of the cells were attributed to the doxorubicin molecules released from the micelles.

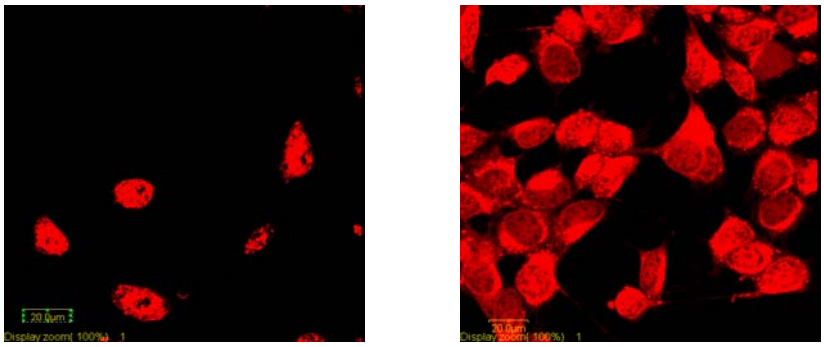

Figure 6.10 Confocal microscopic images of 4T1 cells incubated at 37°C with (a) free DOX, (b) DOX-loaded micelles. (DOX concentration = 10 mg/L)

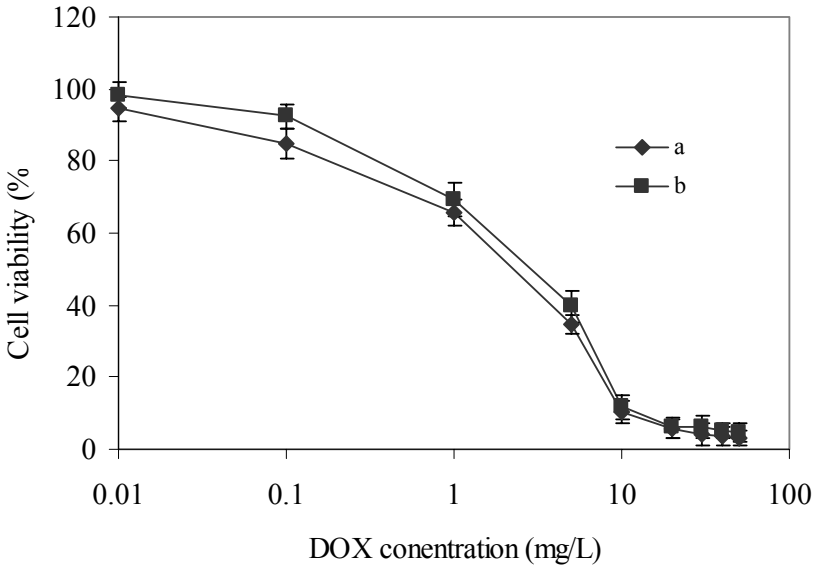

Figure 6.11 Viability of 4T1 cells incubated at 37°C with (a) free DOX; (b) DOX-loaded micelles.

Cell cytotoxicity of free DOX and DOX-loaded micelles against 4T1 cells was investigated. DOX-loaded micelles showed a comparable cytotoxicity when compared to

free DOX (IC_{50}: 3.8 mg/L *versus* 3.0 mg/L), suggesting that DOX released from the micelles remained bioactive. DOX-loaded folate-conjugated micelles were found to be more cytotoxic than DOX-loaded Polymer D micelles discussed in Section 5.2 (IC_{50}: 3.8 mg/L *versus* 7.9 mg/L). This is because of the increased cellular uptake of DOX-loaded micelles due to folate-mediated endocytosis as well as enhanced drug release in endosomes and lysosomes (Figure 6.10). It should be mentioned that no cytotoxcicity was observed for blank micelles at a concentration of up to 500 mg/L.

6.2.8 Biodistribution

The biodistribution of free DOX and DOX-loaded micelles (DOX micelles) was evaluated and compared in mice bearing 4T1 cells-induced breast cancer. As shown in Figure 6.12, the levels of free DOX in the blood were 10.8 μg/g at 10 min, 5.2 μg/g at 30 min, and decreased to 1.2 μg/g at 240 min. Although the biodistribution of free DOX and the DOX micelles in blood showed similar pattern, DOX administrated in the micelles formulation exhibited a longer circulation time, which is consistent with previous studies (Crowns and Creaven *et al.*, 1993). For example, the levels of DOX administrated in the micelles in the blood were 11.8 μg/g at 10 min, 9.1 μg/g at 30 min and 3.5 μg/g at 240 min (Figure 6.13). The $t_{1/2}$ of DOX micelles in the blood was found to be about 140 min, while the $t_{1/2}$ of free DOX was approximately 30 min. This enhanced circulation may be due to slower release in the blood and thus slower elimination of DOX.

The DOX levels in tissues including spleen, kidney, heart, liver and lung after administration of free DOX or DOX micelles are shown in Figure 6.12 and Figure 6.13,

respectively. It was found that free DOX had a wide tissue distribution, accumulating uniformly in heart, lung and liver. However, when administrated in the micelles, a significant reduce in DOX level was found in heart, indicating that the micelles might reduce the cardiotoxicity of DOX considerably. This reduced accumulation in the heart might be due to the selective localization of DOX in the tumor. It was also found that DOX administrated in micelles preferentially accumulated in organs containing the macrophages of the RES, such as liver and spleen. This higher accumulation amount in the liver was possibly attributed to the non-specific uptake of the micelles by the RES. This could be minimized by further modifying the surface and/or particle size of the micelles.

The amount of DOX in tumor tissue was also examined (Figure 6.14). It was observed that the DOX level of free drug reached a peak level of 2.9μg/g at 30 min, and decreased to 1.4μg/g at 120 min, further dropped to 1.0 μg/g at 240 min. However, the level of DOX administrated in the micelles reached 5.0 μg/g at 30 min, increased to 5.8 μg/g at 120 min, and then decreased to 3.8 μg/g at 240 min. These results indicate that higher accumulation of DOX micelles in tumor tissues may be due to EPR effect (Shiah and Dvorak et al., 2001; Shiah and Sun et al., 2000) as well as the folate receptor mediated endocytosis (Yoo and Park, 2004).

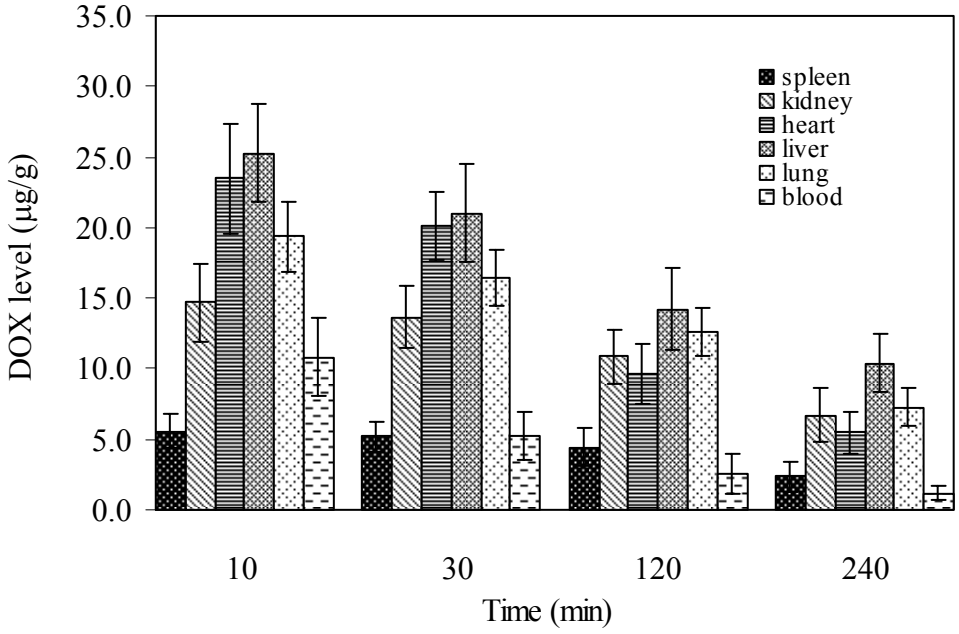

Figure 6.12 Biodistribution of free DOX.

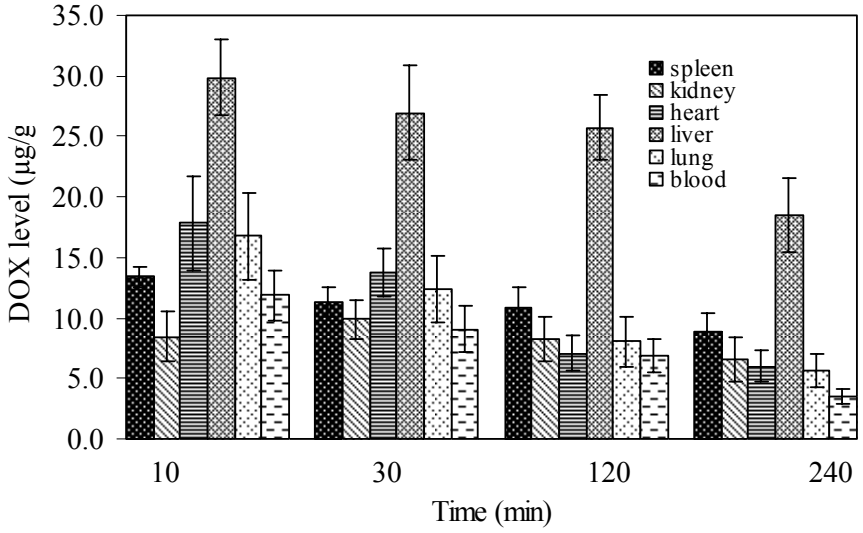

Figure 6.13 Biodistribution of DOX-loaded micelles

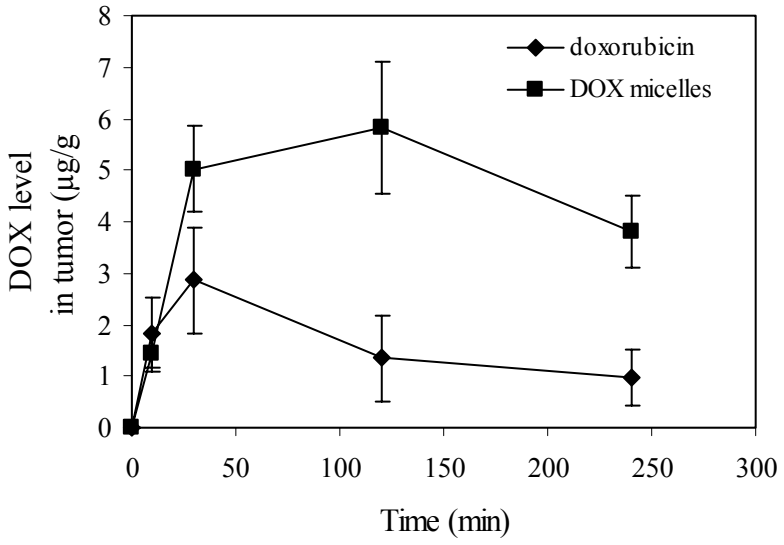

Figure 6.14 DOX concentrations in the tumor for free DOX and DOX-loaded micelles.

6.3 Conclusions

Folate-conjugated poly(*N*-isopropylacrylamide-*co*- *N,* *N*-dimethylacrylamid-*co*-methacrylate**)**-*b*-polyfatty acid was successfully synthesized and utilized to fabricate micelles for targeted delivery of DOX. The morphologies of the nanoparticles were spherical and the mean diameters of the micelles were less than 100 nm. The lower critical solution temperature (LCST) of the micelles was pH-dependent. In PBS (pH 7.4), it was 38.0ºC, while it was 36.2ºC in pH 6.6. Particle size and dug release from micelles were pH-dependent. The micelles were stable in PBS (pH 7.4) at 37°C, but deformed in an acidic environment, leading to fast release. DOX-loaded folate-conjugated micelles perhaps were taken up rapidly by cells *via* endocytosis. The *in vitro* studies have proved that the DOX-loaded micelles killed cancer cells efficiently. The DOX-loaded micelles had a longer circulation time in the blood, and yielded greater concentration in the tumors

when compared to free DOX. The enhanced accumulation of DOX in the tumors using the micelles may result in a higher for cancer therapy.

CHAPTER SEVEN

CONCLUSIONS AND RECOMMENDATIONS FOR FUTURE WORK

Conclusions

In this study, poly(*N*-isopropylacrylamide) (PNIPAAm) was blocked with PLA or PLGA or polyfatty acid to form amphiphilic block copolymers. These block copolymers were utilized to make thermo-responsive microspheres and micelles for controlled delivery of proteins and anticancer drugs.

Firstly, PNIPAAm-*b*-PLA microspheres containing bovine serum albumin (BSA, as a model protein) were fabricated and investigated. It was found that BSA was well entrapped within the PNIPAAm-*b*-PLA microspheres. Under the optimized fabrication conditions, more than 90% encapsulation efficiency of BSA was achieved. The microspheres were erodible in the *in vitro* medium, and polymer degradation occurred in the PLA block. The erosion of microspheres was dependent on their morphology. The more porous the microspheres, the faster was the erosion. A PVA concentration of 0.2% (w/v) in the internal aqueous phase yielded microspheres with an inter-connected porous structure, resulting in fast matrix erosion and sustained BSA release. This is mainly because a higher PVA concentration made the first emulsion more stable, leading to higher encapsulation efficiency and a more porous internal structure. The microspheres made from PNIPAAm-*b*-PLA with a higher portion of PNIPAAm provided faster BSA release. In addition, BSA release was slower at 37^{o}C (above the LCST) than at a temperature below the LCST. One reasonable explanation is that microspheres were more hydrophilic below the LCST and underwent significant swelling. Thus, water molecules diffused into micropsheres more easily, leading to faster BSA release below the LCST. The results indicate that the PNIPAAm-*b*-PLA microsppheres not only

provided a mild environment for BSA but also improved protein release pattern compared to unmodified PNIPAAm or PLA microspheres.

However, a major problem with such microspheres is the non-specific uptake by the reticuloendothelial system (RES) (Kwon and Kataoka, 1995). Temperature sensitive polymeric micelles were developed in this study to overcome this problem. Temperature sensitive block copolymers with different compositions and lengths of PLGA block were synthesized, and used to develop thermo-responsive polymer micelles that had enhanced vascular permeability and retention in tumor tissues compared to healthy tissue. The micelles prepared from the block copolymer had a very low CAC value ranging from 25 mg/L to 4 mg/L. In addition, the CAC value was similar in both aqueous solution and PBS buffer. DOX and paclitaxel were encapsulated into the micelles by a membrane dialysis method. The Polymer D provided a favorable hydrophilic/hydrophobic balance for high drug loading. The TEM morphologies showed that micelles were spherical and had a uniform distribution, which is consistent with the particle size analysis. The LCST of the micelles in PBS was 39.0ºC. In particular, it was determined by the shell instead of the core. The micelles were stable in both PBS and PBS containing 10% fetal bovine serum at 37ºC. Moreover, the hydration-dehydration process was reversible. Drug release from micelles was responsive to external temperature changes. Drug release was much faster above the LCST than at body temperature. This is because the hydrophilic shell became aggregated above the LCST. The aggregated shell could induce the deformation of the inner core structure, resulting in fast drug release. However, when the temperature is below the LCST, the hydrated shell stabilizes the drug loaded in the core.

Therefore, only a small amount of the drug was released. The polymers did not cause significant cytotoxicity against the cells, indicating that they are biocompatible. Drug-loaded micelles were internalized through an endocytosis pathway. Drug-loaded micelles showed higher cytotoxicity against cells at a temperature above the LCST. The IC_{50} of drug-loaded micelles also depends on drugs and cells. The results indicate that reversible and thermo-responsive micelles can be used to deliver anticancer drugs timely to surface cancers by modulating local temperature at cancers.

Since deep organs or tumors may not be easily accessible to temperature sensitive micelles (Soppimath et al., 2005), another strategy to targeting drugs to tumor tissues is to use pH-triggered temperature sensitive carriers. A new polymer, folate-conjugated poly(*N*-isopropylacrylamide-*co*- *N, N*-dimethylacrylamid-*co*-methacrylate)-*b*-PUA was synthesized and utilized to fabricate core-shell micelles for targeted delivery of DOX. DOX was loaded into the micelles by a membrane dialysis method with actual drug loading level of 2.5%. The morphologies of the micelles are spherical (examined by TEM). The mean diameters of the empty and DOX-loaded micelles were 92.8 nm and 98.5 nm respectively. The lower critical solution temperature (LCST) of the micelles was pH-dependent, being 38.0ºC in PBS (pH 7.4) but 36.2ºC in pH 6.6. Particle size and dug release from micelles were pH-dependent. It was found that the micelles were stable in PBS (pH 7.4) at 37°C, but deformed in an acidic environment, triggering the release of enclosed drug molecules. Confocal images showed that DOX-loaded folate-conjugated micelles were taken up rapidly by cells *via* endocytosis. The *in vitro* studies have proved that the DOX-loaded micelles killed cancer cells more efficiently. The *in vivo* studies

showed increased circulation time of DOX administrated in the micelles. This is possibly due to slower release in the blood and thus slower elimination of DOX. DOX micelles also led to less distribution in heart and lung, decreasing the cardiotoxicity of DOX. In particular, the enhanced accumulation in tumors and longer circulation of DOX using DOX-loaded micelles may result in a higher efficacy for cancer therapy.

The novelty of this work is to improve control over the drug release rate through the design of environmental sensitive drug delivery systems. Drug release from these systems is triggered at the desired site of action by changes in temperature or pH. Moreover, micelles self-assembling from a novel multifunctional block copolymer (folate-conjugated Poly(NIPAAm-*co*-DMAAm-*co*-MAm)-*b*-PUA) were developed. These micelles may provide a good carrier for delivering anticancer drugs to deep tumour tissues (slightly acidic) or for intracellular drug delivery (escaping from the endosomes-a low pH environment and thus entering the cytosols) without external heating.

The results obtained from this work provide an optimal process for developing biodegradable and environmental-responsive polymer drug carriers with high drug loading level. It was also demonstrated that both protein-loaded microspheres and anticancer drug-loaded micelles showed a clear thermo-responsive behavior for drug release. In addition, drug-loaded micelles showed higher cytotoxicity against cancer cells at a temperature above the LCST. The thermo-responsive micelles may make a good candidate for the treatment of surface cancers by localized hypothermia. More

importantly, DOX-loaded folate-conjugated temperature and pH sensitive micelles would make a promising carrier for intracellular delivery of anticancer drugs.

Recommendations for future work

In the first part of this study, it was demonstrated that PNIPAAm-*b*-PLA (1:5, 0.2%) microspheres were able to provide a sustained release of BSA, which was faster at a temperature below the LCST. Although such microspheres provided many attractive features such as high encapsulation efficiency and favorable release pattern, initial burst release of proteins from PNIPAAm-*b*-PLA microspheres still existed. This initial burst may cause side effects in body. Therefore, the initial burst should be minimized in future work by adjusting polymer composition. In addition, the bioactivity of released proteins is not fully understood yet. The degradation of microspheres leads to release of acidic oligomers, which create acidic microenvironments, making proteins prone to structure disruption or denaturation. However, proteins must maintain their three-dimensional structure in order to function properly. Thus, it would be of interest to know the bioactivity of proteins in microspheres and of the proteins released. Although HPLC gives some information on the integrity of proteins, more analyses such as SDS-PAGE and ELISA should be done in future work.

The results in the second part of this study show that thermo-responsive micelles, incorporated with anticancer drugs, displayed thermo-responsive behavior for drug release. However, such a system suffered from the disadvantage of not being easily accessible to deep organs or tumors. An alternative approach to targeting drugs to tumor

tissues is to use pH sensitive carriers. Although DOX-loaded micelles showed a similar cytotoxicity as free DOX, the *in vitro* cytotoxicity against culture medium with different pH values should be done to test the pH-dependent cytotoxicity. In addition, the confocal image alone is not enough to elucidate the mechanisms of cellular uptake of micelles. The integrity of the cell membrane should be examined using the trypan blue method. Furthermore, although initial *in vivo* studies show that pH triggered temperature sensitive micelles might target drugs to specific tissues or cell compartments without external heating, further modification of micelle surface is necessary to reduce accumulation in the liver and the spleen. Finally, a better understanding of *in vivo* pharmacokinetics of DOX-loaded micelles, toxicology and bioavailability of drug would be of interest for future *in vivo* studies before clinical trials.

REFERENCES

Abuchowski, A., Es, T. V., Palczuk, N.C., Davis, F.F., Alteration of immunological properties of bovine serum albumin by covalent attachment of polyethylene glycol, J. Biol. Chem. 252 (1977) 3578-3581.

Allen T.M., Cullis P.R., Drug delivery systems: Entering the mainstream, Science 303 (2004) 1818-1822.

Allen, A., Maysinger, D., Eisenberg, A., Nano-engineering block copolymer aggregates for drug delivery, Colloids and surfaces B: Biointerfaces 16 (1999) 3-27.

Alonso, M.J., Cohen, S., Park, T.G., Gupta, R.K., Siber, G.R., Langer, R., Determinants of release rate of tetanus vaccine from polyester microspheres, Pharm. Res. 10 (1993) 945-953.

Bader, H., Ringsdorf, H., Schmidt, B., Water moluble polymers in medicine, Angew. Makromol. Chem. 123/124(1984) 457-485.

Bae, Y., Fukushima, S., Harada, A., Kataoka, K., Design of environment-sensitive supramolecular assemblies for intracellular drug delivery: polymeric micelles that are responsive to intracellular pH change, Angew. Chem. Int. Ed. 42 (2003) 4640-4643.

Baldwin, S.P., Saltzman, W.M., Materials for protein delivery in tissue engineering, Advanced drug delivery reviews 33 (1998) 71-86.

Barrat, G., Couarraze, G., Couvreur, P., Dubernet, C., Fattal, E., Gref, R., Lavarre, D., Legrand, P., Ponchel, G., Vauthier, C., Polymeric micro- and nanoparticles as drug carriers, Polymeric biomaterials second edition, revised and expanded (edited by Severian Dumitriu), Marcel dekker Inc., New York. Basel (2002) 753-754.

Belbella, A., Vauthiew, C., Fessi, H., Devissaguet, J. P., Puisieux, F, In vitro degradation of nanospheres from poly(D,L-lactides) of different molecular weights and polydispersities, International J. Pharmaceutics 129 (1996) 95-102.

Bittner B, Witt C, Mader K, Kissel T., Degradation and protein release properties of microspheres prepared from biodegradable poly(lactide-co-glycolide) and ABA triblock copolymers: influence of buffer media on polymer erosion and bovine serum albumin release, J. Control. Rel. 60 (1999) 297-309.

Boury F., Marchais H., Proust J. E., Benoit J. P., Bovine serum albumin release from poly(α-hydroxy acid) microspheres: effects of polymer molecular weight and surface properties, J. Control. Rel. 45 (1997) 75-86

Braxel, C. S., Peppas, N. A., Pulsatile local delivery of thrombolytic and antithrombotic agents using poly(N-isoacrylamide-co-methacrylic acid) hydrogels, J. Control. Rel. 39 (1996) 57-64.

Brigger, I., Dubernet, C., Couvreur, P., Nanoparticles in cancer therapy and diagnosis, Advanced drug delivery reviews 54 (2002) 631-651.

Brornberg, L.E., Ron, E.S., temperature responsive gels and thermogelling polymer matrices for protein and peptide delivery, Advanced drug delivery reviews 31 (1998) 197-221.

Brownlee, M., Cerami, A., A glucose-controlled insulin-delivery system: semisynthetic insulin bound to lectin, Science 206 (1979) 1190-1191.

Burersroda, F.V., Schedl, L., Gopferich A. Why degradable polymers undergo surface erosion or bulk erosion, Biomaterials 23 (2002) 4221-4231.

Cammas, S., Suzuki, K., Thermo-responsive polymer nanoparticles with a core-shell micelle structure as site-specific drug carriers, J. Control. Rel. 48 (1997) 157-164.

Chaw, C.S., Chooi, K.W., Liu, X.M., Tan, C.W., Wang, L., Yang, Y.Y., Thermally responsive core-shell nanoparticles self-assembled from cholesteryl end-capped and grafted polyacrylamides: drug incorporation and in vitro release. Biomaterials 25 (2004) 4297-4308.

Chen, G., Hoffman, A. S., Grafted copolymers that exhibit temperature-induced phase transitions over a wide range of pH, Nature 373(1995) 49-52.

Chen, J.P., Yang, H.J., Hoffman, A.S., Polymer-protein conjugates. I. Effect of protein conjugation on the cloud point of poly (N-isopropylacrylamide), Biomaterials 11 (1990) 625-630.

Chia, H.H., Yang, Y.Y., Chung, T.S., Ng S., Heller J., Auto-catalyzed poly(ortho ester) microspheres: a study of their erosion and drug release mechanism. J. Control. Rel. 75 (2001) 11-25.

Chourasia, M.K., Jain, S.K., Polysaccharides for colon targeted drug delivery, Drug Delivery 11 (2004) 129-148.

Chung, J.E., Yokoyama, M., Okano, T., Reversibly thermo-responsive alkyl-terminated poly(N-isopropylacrylamide) core-shell micellar structures. Colloids Surfaces B: Biointerface 9 (1997) 37-48.

Chung, J. E., Yokoyama, M., Okano, T., Inner core segment design for drug delivery control of thermo-responsive polymeric micelles, J. Control. Rel. 65 (2000) 93-103.

Chung, J.E., Yokoyama, M., Yamato, M., Aoyagi, T., Sakurai, Y., Okano, T., Thermo-responsive drug delivery from polymeric micelles constructed using block copolymers of

poly(N-isopropylacrylamide) and poly(butylmethacrylate). J. Control. Rel. 62 (1999) 115-127.

Cleland, J. L., Duenas, E. T., Park, A., Daugherty, A., Kahn, J., Kowalski, J., Cuthbertson, A., Development of poly-(D,L-lactide--coglycolide) microsphere formulations containing recombinant human vascular endothelial growth factor to promote local angiogenesis. J. Control. Rel. 72 (2001) 13-24.

Cohen, S., Yoshioka, T., Lucarelli, M., Hwang, L. H., Langer, R., Controlled delivery systems for proteins based on poly(lactic/glycolic acid) microspheres. Pharm. Res. 8 (1991) 713-720.

Couvreur P, Puisieux F.N., nano-, microparticles for the delivery of polypeptides and proteins. Adv. Drug Deliv. Syst. 10 (1993) 141–162.

Crotts G., Park, T. G., Stability and release of bovine serum albumin encapsulated within poly(D,L-lactide-co-glycolide) microspheres, J. Control. Rel. 44 (1997) 123-134.

Crotts, G., Sah, H., Park, T. G., Adsorption determines in vitro protein release rate from biodegradable microspheres: quantitative analysis of surface area during degradation. J. Control. Rel. 47 (1997) 101-111.

Crowns J., Creaven P., Greco W. et al., Initial clinical (phase 1) trial of TLC D-99 (doxorubicin encapsulated in lipsomes), Cancer Research 53 (1993) 2796-2802.

Davis S.S., Illum L., Polymeric Microspheres as Drug Carriers, Biomaterials 9 (1988) 111-115.

Deng, L., Mrksich, M., Whitesides, G. M., Self-Assembled Monolayers of alkanethiolates presenting tri(propylene sulfoxide) groups resist the adsorption of protein**,** J. Am. Chem. Soc. 118 (1996) 5136-5137.

Domb, A.J., Nudelman, R., In vivo and in vitro elimination of aliphatic polyanhydrides, Biomaterials 16 (1995) 319-323.

Dubois, P., Jacobs, C., Jerome, R., Teyssie, P., Macromolecular engineering of polylactones and polylactides. 4. Mechanism and kinetics of lactide homopolymerization by aluminum isopropoxide, Macromolecules 24 (1991) 2266-2270.

Dumitriu. S., Polymeric biomaterials, Marcel dekker, Inc., Newyork.Basel (2002) 32-39.

Edelman, E.R., Langer, R., Optimization of release from magnetically controlled polymeric drug release devices, Biomaterials 14 (1993) 621-626.

Einmahal, S., Deshpande A.A., Tabatabay, C., Gurny, R., Mucosal drug delivery, intravitreal, Encyclopedia of controlled drug delivery (1999) 572-573.

Feil, H., Bae, Y. H., Jan, F.J., Kim, S. W., Effect of comonomer hydrophilicity and ionization on the lower critical solution temperature of N-isopropylacrylamide copolymers Macromolecules 26 (1993) 2496-2500.

Feng, S.S., Chien, S., Chemotherapeutic engineering: Application and further development of chemical engineering principles for chemotherapy of cancer and other diseases, Chemical Engineering Science 58 (2003) 4087-4114.

Feng, S.S., Mu, L., Win, K.Y., Huang, G., Nanoparticles of biodegradable polymers for clinical administration of paclitaxel, Curr Med Chem. 11 (2004) 413-424.

Fu, K., Pack, D. W., Klibanov, A. M., Langer, R., Visual evidence of acidic environment within degrading poly(lactic-co-glycolic acid) (PLGA) microspheres. Pharm. Res. 17 (2000) 100-106.

Gadelle, F., Koros, W.J., Schechter, R.S., Solubilization of aromatic solutes in block copolymers. Macromolecules 28 (1995) 4883-4892.

Gao Z, Lukyanov A.N., Singhal, A., Torchilin, V.P., Diacylpolymer micelles as nanocarriers for poorly soluble anticancer drugs, Nano Letter 2 (2002) 979-982.

Gao, Z., Lukyanov, A.N., Chakilan, A.R., Torchilin, V.P., PEG-PE/Phosphatidylcholine mixed immunomicelles specifically deliver encapsulated taxol to tumor cells of different origin and promote their efficient killing, Journal of drug targeting 11 (2003) 87-92.

Ginde, R.M., Gupta, R.K., In vitro chemical degradation of poly(glycolic acid) pellets and fibers, J. applied polymer science 33 (1987) 2411-2429.

Giunchedi, P., Conti, B., Scalia, S., In vitro degradation study of polyester microspheres by a new HPLC method for monomer release determination. J. Control. Rel. 56 (1998) 53-62.

Gombotz, W.R., Pettit, D.K., Biodegradable polymers for protein and peptide drug delivery. Bioconjug Chem. 6 (1995) 332-351.

Govender T, Stolnik S, Garnett MC, Illum L, Davis SS., PLGA nanoparticles prepared by nanoprecipitation: drug loading and release studies of a water soluble drug, J. Control. Rel. 57 (1999) 71-85.

Greenwald, R.B., Choe, Y.H., McGuire, J., Conover, C.D., Effective drug delivery by PEGylated drug conjugates, Advanced drug delivery reviews 55 (2003) 217-250.

Greenwald, R.B., Gilbert, C.W., Pendri, A., Conover, C.D., Xia, J., Martinez, A., Drug delivery systems: Water soluble taxol 2-poly(ethylene glycol) ester prodrugs-design and in vivo effectiveness, J. Med. Chem. 39 (1996) 424-431.

Gref, R., Minamitake, Y., Peracchia, M.T., Trubetskoy, V., Torchilin, V., Langer, R., Biodegradable long-circulating polymeric nanospheres, Science 263 (1994) 1600-1603.

Guo, X., Szokajr, C.S., Chemical approaches to triggerable lipid vesicles for drug and gene delivery, Acc. Chem. Res. 36 (2003) 335-341.

Haag, R., Supramolecular drug delivery systems based on polymeric core-shell architectures, Angrew. Chem. Int. Ed., 43 (2004) 278-282.

Hagan, S.A., Coombes, A.G.A., Garnett, M.C., Dunn, S.E., Davies, M.C., Illum, L., Davis, S.S., Harding S. E., Purkiss S., Gellert P. R., Polylactide-Poly(ethylene glycol) Copolymers as Drug Delivery Systems. 1. Characterization of Water Dispersible Micelle-Forming Systems, Langmuir 12 (1996) 2153-2161.

Heller, J., Barr, J., Ng, S.Y., Abdellauoi, K.S., Gurny, R., Poly(ortho esters): synthesis, characterization, properties and uses, Advanced drug delivery reviews 54 (2002) 1015-1039.

Heller, J., Barr, J., Poly(ortho esters)-from concept to reality, Biomacromolecules 5 (2004) 1625-1632.

Heller J., Gurny, R., Poly (ortho esters), Encyclopedia of controlled drug delivery (1999) 852-874.

Heskins, M., Guillet, J.E., Solution properties of poly(N-isopropylacrylamide), J. macromol. Sci. chem. A2, 9 (1968) 1441-1455.

Hsieh, S.T., Langer, R., Folkman, J., Magnetic modulation of release of macromolecules from polymers, Proceedings of the National Academy of Sciences of the United States of American 78 (1981) 1863-1867.

Huh, K.M., Lee, S.C., Cho, Y.W., Lee, J., Jeong, J.H., Park, K., Hydrotropic polymer micelle system for delivery of paclitaxel, J. Control. Rel. 101 (2005) 59-68.

Inomata, H., Goto, S., Saito, S., Phase transition of N-substituted acrylamidegels, Macromolecules 23 (1990) 4887 – 4888.

Inouse, T., Chen, G., An AB block copolymer of oligo(methyl methacrylate) and poly(acrylic acid) for micellar delivery of hydrophobic drugs, Journal J. Control. Rel. 51 (1998) 221-229.

Ito, Y., Casolaro, M., Kono, K., Imanishi, Y., An insulin-releasing system that is responsive to glucose, J. Control. Rel. 10 (1989) 195-203.

Jeong, B., Bae, Y. H., and Kim, S. W., Drug release from biodegradable injectable thermosensitive hydrogel of PEG–PLGA–PEG triblock copolymers, J. Control. Rel. 63 (2000) 155–163.

Jeong, J.H., Park, T.G., Novel polymer-DNA hybrid polymeric micelles composed of hydrophobic poly(D,L-lactic-co-glycolic acid) and hydrophilic oligonucleotides. Bioconjugation Chemistry 12 (2001) 917-923.

Jette, K.K., Law, D., Schmitt, E.A., Kwon, G.S., Preparation and drug loading of poly(ethylene glycol)-block-poly(epsilon-caprolactone) micelles through the evaporation of a cosolvent azeotrope, Pharm Res. 21 (2004) 1184-1191.

Jian, R., Shah, N.H., Malick, A.W., Rhodes, C.T., Controlled drug delivery by biodegradable poly(ester) devices: different preparative approaches. Drug delivery Ind. Pharm.24 (1998) 703-727.

Jiang, W., Gupta, R.K., Deshpande, M.C., Schwendeman, S.P., Biodegradable poly(lactic-co-glycolic acid) microparticles for injectable delivery of vaccine antigens, Adv Drug Deliv Rev. 57 (2005) 391-410.

Jiang, W.L., Schwendeman, S.P., Stabilization and controlled release of bovine serum albumin encapsulated in poly(D,L-lactide) and poly(ethylene glycol) microsphere blends. Pharmaceutical Research 18 (2001) 878-885.

Johnson, R.E., Lanaski, L.A., Gupta, V., Griffin, M.J., Gaud, H.T., Needham, T.E., Hossein, Z., Stability of atriopeptin III in poly(D,L-lactide-co-glycolide) microspheres, J. Control. Rel. 17 (1991) 61-68.

Jones, M.C., Leroux, J.C., Polymeric micelles – a new generation of colloidal drug carriers , European J. of pharmaceutics and Biopharmaceutics 48 (1999) 101-111.

Kaneko, Y., Nakamura, S., Synthesis and swelling-deswelling kinetics of poly(N-isopropylacrylamide) hydrogels grafted with LCST modulated polymers, Biomater Sci Polym Ed. 10 (1999) 1079-1091.

Kaotaoka, K., Matsumot, T., Yokoyama, M., Doxorubicin-loaded poly(ethylene glycol)-poly(β-benzyl-L-aspartate) copolymer micelles: their pharmaceutical characteristics and biological significance, J. Control. Rel. 64 (2000) 143-153.

Kim, C., Lee, S.C., Kang, S.W., Synthesis and the micellar characteristics of poly(ethylene oxide)-deoxycholic acid conjugates. Langmuir 16 (2000) 4792-4797.

Kim, H.K., Park, T.G., Microencapsulation of human growth hormone within biodegradable polyester microspheres: protein aggregation stability and incomplete release mechanism. Biotechnol. Bioeng. 65 (1999) 659-667.

Kim, S.Y., Lee, Y.M., Taxol-loaded block copolymer nanospheres composed of methoxy poly(ethylene glycol) and poly(ε-caprolactone), Biomaterials 22 (2001) 1697-1704.

Kim, S.Y., Shin, I.G., Lee, Y.M., Cho, C.S., Sung, Y.K., Methoxy poly(ethylene glycol) and epsilon-caprolactone amphiphilic block copolymeric micelle containing indomethacin. II. Micelle formation and drug release behaviours, J. Control. Rel. 51 (1998) 13-22.

Kissel, T., Brich, Z., Bantle, S., Lancranjan, I., Nimmerfall, P.V., Parenteral depot-systems on the basis of biodegradable polyesters, J. Control. Rel.16 (1991) 27- 41.

Kissel, T., Li, Y. X., Volland, C., Gurich, S., Konenerg, R., Parental protein delivery systems using biodegradable polyesters of ABA block structure, containing hydrophobic poly(lactide-co-glycolide) A blocks and hydrophilic poly(ethylene oxide) B blocks, J. Controlled Release 39 (1996) 315-326.

Kohn, F.H., Van Omnen, J.G., Feijen, J., The mechanisms of the ring-opening polymerization of lactide and glycolide, Europen polymer Journal 19 (1983) 1081-1088.

Kohori, F., Sakai, K., Aoyagi, T., Okano, T., Preparation and characterization of thermally responsive block copolymers comprising poly(*N*-isopropylamide)-*b*-poly(D,L-lactide). J. Control. Rel. 55 (1998) 87-98.

Kohori, F., Sakai, K., Aoyagi, T., Yokoyama, M., Yamato, M., Sakurai, Y., Okano, T., Control of adriamycin cytotoxic activity using thermally responsive polymeric micelles composed of poly(*N*-isopropylacrylamide-*co*-*N,N*-dimethylacrylamide)-b-poly(D,L-lactide). J. Control. Rel. 16 (1999) 195-205.

Kost, J., Horbett, T.A., Ratner, B.D., Singh, M., Glucose-sensitive membranes containing glucose oxidase: activity, swelling, and permeability studies. J Biomed Mater Res. 19 (1985) 1117-1133.

Kost, J., Langer, R., Responsive polymeric delivery systems, Advance drug delivery Reviews 6 (1991) 19-50.

Kost, J., Langer, R., Responsive polymeric delivery systems, Advanced drug delivery reviews 46 (2001) 125-148.

Kostanski, J.W., Thanoo, B.C., DeLuca, P.P., Preparation, characterization, and in vitro evaluation of 1- and 4-month controlled release orntide PLA and PLGA microspheres. Pharm. Dev. Technol. 5 (2000) 585-596.

Krewson, D., Mak, R.B., Saltzman, M.W., Stabilization of nerve growth factor in polymers and in tissues, J. Biomater. Sci. 8 (1996) 103-117.

Kristein, D., Brasselmann, H., Vacik. J., Kopecek, J., influence of medium and matrix composition on diffusivities in charged membranes, Biotech. Bioeng. 27 (1985) 1382-1384.

Kumar, N., Langer, R.S., Domb, A.J., Polyanhydrides: an overview, Advanced drug delivery reviews 54 (2002) 889-910.

Kumar, N., Ravikumar, N.V., Dornb, A.J., Biodegradable block copolymers, Advanced drug delivery reviews 53(2001)23-44.

Kurcok, P., Penczek, J., Franek, J., Jedlinski, Z., Anionic polymerization of lactones. 14. Anionic block copolymerization of δ-valerolactone and L-lactide initiated with potassium methoxide, Macromolecules 25 (1992) 2285-2289.

Kwon, G.S., Kataoka, K., Block copolymer micelles as long circulating drug vehicles, Advanced Drug Delivery Reviews 16 (1995) 295-309.

Lam, X.M., Duenas, E.T., Daugherty, A.L., Levin, N., Cleland, J.L., Sustained release of recombinant human insulin-like growth factor-I for treatment of diabetes, J. Control. Rel. 67 (2000) 281-292.

Langer, R., Drug delivery and targeting, Science 392 (1998) 5-10.

Lee, E.S., Na, K., Bae, Y.H., Polymeric micelle for tumor pH and folate-mediated targeting, J. Control. Rel. 91 (2003) 103-113.

Lee, J.H., Jung, S.W., Kim, I.S., Polymeric nanoparticles composed of fatty acids and poly(ethylene glycol) as a drug carrier, International J. of Pharmaceutics 251(2003) 23-32.

Lee, S. C., Kim, C., Kwon, I. C., Chung, H., Jeong, S.Y., Polymeric micelles of poly(2-ethyl-2-oxazoline)-block-poly(ε-caprolactone) copolymer as a carrier for paclitaxel, J. Control. Rel. 89(2003) 437-446.

Lee, V.H., Changing needs in drug delivery in the era of peptide and protein drugs, in: V.H.L. Lee(Ed.), Peptide and protein drug delivery, Marcel Dekker, New york (1991) 1-56.

Lehmann K.O.R., Bossler H.M., Dreher D.K., Controlled Drug Release From Small Particles Encapsulated with Acrylic Resin, Niol Macromol. Monogr. 5, Polym. Delivery Sys. (1979) 111-119.

Leong, K.W., Langer, R., Polymeric controlled drug delivery, Advanced drug delivery reviews 1 (1987) 199-233.

Li, S., Vert, M., Scott, G., Gilead, D., Degradable polymers-Principles and applications, Ghapman and Hall, London (1995) 43-87.

Li, S.M., Vert, M., Biodegradable polymers: polyesters, Encyclopedia of controlled drug delivery (1999) 71-93.

Li, Y., Pei, Y., Zhang, X., Gu, Z., Zhou, Z., Yuan, W., Zhou, J., Gao, X., PEGylated PLGA nanoparticles as protein carriers: synthesis, preparation and biodistribution in rats, J. Control. Rel. 71 (2001) 203-211.

Liggins, R,T,, Burt, H.M., Paclitaxel loaded poly(L-lactic acid) microspheres: properties of microspheres made with low molecular weight polymers, Int. J Pharm. 222 (2001)19-33.

Lisa, B.P., Polymers in Controlled Drug Delivery, http://www.devicelink.com/mpb/archive/97/11/003.html.

Liu S.Q., Yang Y.Y., Tong Y.W., Preparation and characterization of temperature-sensitive poly(*N*-isopropylacrylamide)-*b*-poly(D.L-lactide) microspheres for protein delivery, Biomacromolecules 4 (2003) 1784-1793

Lu Z., Yeh T.K., Tsai M., Au J.L., Wientjes MG., Paclitaxel-loaded gelatin nanoparticles for intravesical bladder cancer therapy, Clin Cancer Res. 22 (2004) 7677-7684.

Lu, Y., Low, P.S., Immunotherapy of folate receptor-expressing tumors: review of recent advances and future prospects, J. Control. Rel. 91 (2003) 17-29.

Luo, L.B., Tam, J., Maysinger, D.M., Eisenberg, A., Cellular internalization of poly(ethylene oxide)-*b*-poly(ε-caprolactone) diblock copolymer micelles, Bioconjugate Chemistry 139 (2002) 1259-1265.

Lynn, D.M., Amiji, M.M., Langer, R., pH-responsive polymer microspheres: Rapid release of encapsulated material within the range of intracellular pH, Angew. Chem. Int. Ed. 40 (2001) 1707-1710.

Mao H.Q., Kadiyala I., Leong K.W., Zhao Z., Dang W.B., Biodegradable polymers: Poly(phosphoester)s, Encyclopedia of controlled drug delivery (1999) 45-60.

Mathiowitz E., Kreitz M.R., Peppas L.B., Microencapsulation, Encyclopedia of controlled drug delivery (1999) 493-553.

Matsumura, Y., Maeda, H., A new concept for macromolecular therapeutics in cancer chemotherapy: mechanism of tumoritopic accumulation of proteins and the antitumor agent smancs, Cancer Research 46 (1986) 6387-6392.

Meinel, L., Illi, O. E., Zapf, J., Malfanti, M., Merkle, H. P., Gander, B., Stabilizing insulin-like growth factor-I in poly(D,L-lactide-co-glycolide) microspheres, J. Control. Rel. 70 (2001) 193-202.

Miller, R.A., Brady, J.M., Cutright, D.E., Degradation rates of oral resorbable implants (polylactates and polyglycolates): rate modification with changes in PLA/PGA copolymer ratios, J. of Biomedical. Material Research 11 (1977) 711-719.

Mitragotri, S., Blankschtein, D., Langer, R., Ultrasound-mediated transdermal protein delivery, Science 269 (1995) 850-853.

Miyazaki, S., Nakayama, A., Oda, M., Takada, M., Attwood, D., Chitosan and sodium alginate based bioadhesive tablets for intraoral drug delivery, Biol.Pharm. Bull. 17 (1994) 745-747.

Nagarajan R, Ganesh K. Block copolymer self-assembly in selective solvents: spherical micelles with segregated cores, J. Chem. Phys. 90 (1989) 5843-5856.

Nakanishi, T., Fukushima, S., Okamoto, K., Kataok, K., Development of the polymer micelle carrier system for doxorubicin, J. of Controlled Release 74 (2001) 295-302.

Narasimhan, B., Mallapragada, Peppas, N.A., Release kinetics, data interpretation, Encclopedia of controlled drug delivery (1999) 921-935

Nasongkla, N., Shuai, X.T., Ai, H., Weinberg, B.D., Pink, J., Boothman, D.A., Gao J.M., Crgd-Functionalized polymer micelles for targeted Doxorubicin delivery, Angew. Chem. Int. Ed. 43 (2004) 6323-6327.

Ng, S.Y., Vandamme, T., Tayor, M.S., Heller, J**.,** Synthesis and Erosion Studies of Self-Catalyzed Poly(ortho ester)s, macromolecules 30 (1997) 770-772.

Nijenhuis, A.J., Grijpma, D.W., Pennings, A.J., Lewis acid catalyzed polymerization of L-lactide. Kinetics and mechanism of the bulk polymerization, Macromolecules 25 (1992) 6419-6424.

Nucci, M.L., Shorr, R., Abuchowski, A., The therapeutic value of poly(ethylene glycol)-modified proteins, Adv Drug Deliver Rev 6 (1991) 133-151.

Patrick couvreur, Maria Jose Blanco-prieto, Francis Puisieux, Bernard Roques, Elias Fattal, Multiple emulsion technology for the design of microspheres containing peptides and oligopeptides, Advanced drug delivery reviews 28 (1997) 85-96.

Peracchia M.T., Gref R., Minamitake Y., Domb A., Lotan N., Langer, R., PEG-coated nanospheres from amphiphilic diblock and multiblock copolymers: Investigation of their drug encapsulation and release characteristics, J. Control. Rel. 46 (1997) 223-231.

Pistel, K. F., Breitenbach, A., Zange-Volland, R., Kissel, T., Brush-like branched biodegradable polyesters, part III - Protein release from microspheres of poly(vinyl alcohol)-graft-poly(D,L-lactic-co-glycolic acid), J. Control. Rel. 73 (2001) 7-20.

Potineni A, Lynn DM, Langer R, Amiji MM, Poly(ethylene oxide)-modified poly(beta-amino ester) nanoparticles as a pH-sensitive biodegradable system for paclitaxel delivery, J. Control. Rel. 86 (2003) 223-234.

Puri N., Jones A.B., Kou J.H., Wyandt C.M., Release of bovine serium albumin from preformed porous microspheres of poly(L-lactide acid), J. microencapsulation, 17 (2000) 207-214.

Quellec, P., Gref, R., Perrin, L., Dellacherie, E., Sommer, F., Verbavatz, J.M., Alonso, M.J., Protein encapsulation within PEG-coated nanospheres, Part I. Physico-chemical characterization, J. Biomed. Mater. Res. 42 (1998) 45-54.

Rahman N.A., Mathiowitz E., Localization of bovine serum albumin in double-walled microspheres, J. Control. Rel. 94 (2004) 163-175.

Robinson J.R., Lee H.L., Controlled drug delivery: fundaments and applications, second edition, Marcel Dekker Inc., New York (1990) 3-61.

Savic R, Luo L, Eisenberg A, Maysinger D., Micellar nanocontainers distribute to defined cytoplasmic organelles, Science 300 (2003) 615-618.

Sawahata, K., Hara, M., Yasunaga, H. Osada, Y., Electrically controlled drug delivery system using polyelectrolyte gels, J. Control. Rel. 14 (1990) 253–262.

Shao, P. G., Bailey, L. C., Porcine insulin biodegradable polyester microspheres: stability and in vitro release characteristics, Pharm. Dev. Technol. 5 (2000) 1-9.

Shao, P. G., Bailey, L. C., Stabilization of pH-induced degradation of porcine insulin in biodegradable polyester microspheres, Pharm. Dev. Technol. 4 (1999) 633-642.

Shiah J.G., Dvorak M., Kopeckova P., Sun Y., Peterson C.M., Kopecek J., Biodistribution and antitumour efficacy of long-circulating N-(2-

hydroxypropyl)methacrylamide copolymer-doxorubicin conjugates in nude mice, Eur J Cancer, 37 (2001)131-139.

Shiah J.G., Sun Y., Peterson C.M., Straight R.C., Kopecek J., Antitumor activity of N-(2-hydroxypropyl) methacrylamide copolymer-Mesochlorine e6 and adriamycin conjugates in combination treatments, Clin Cancer Res. 6 (2000) 1008-1015.

Shive, M. S., Anderson, J. M., Biodegradation and biocompatibility of PLA and PLGA microspheres, Adv. Drug Deliv. Rev. 28 (1997) 5-24.

Shuai, X.T., Ai, H., Nasongkla N., Kim, S., Gao, J.M., Micellar carriers based on block copolymers of poly(ε-caprolactone) and poly(ethylene glycol) for doxorubicin delivery, J. Control. Rel. 98 (2004) 415-426.

Shuai, X.T., Ai, H., Nasongkla, N., Kim, S., Gao, J., Micellar carriers based on block copolymers of poly(ε-caprolactone) and poly(ethylene glycol) for doxorubicin delivery, J. Control. Rel. 98 (2004) 415-426.

Shuai, X.T., Merdan, T., Schaper, A.K., Xi, F., Kissel, T., Core-cross-linked polymeric micelles as paclitaxel carriers, Bioconjugate Chem. 15 (2004) 441-448.

Siegel, R.A., Falamarzian, M., Firestone, B.A., Moxley, B.C., pH-controlled release from hydrophobic/polyelectrolyte copolymer hydrogels, J. Control. Rel. 8 (1988) 179–182.

Sinha, V.R., Khosla, L., Bioabsorbable polymers for implantable therapeutic systems, Drug Dev Ind Pharm. 24 (1998) 1129-1138.

Sinha, V.R., Trehan, A., Biodegradable microspheres for protein delivery, J. Control. Rel. 90 (2003) 261-280.

Soppimath K. S., Tan C. W., Yang Y. Y., pH-Triggered Thermally Responsive Polymer Core-shell Nanoparticles for Drug Delivery, Advanced Materials 17 (2005) 318-323.

Stanislaw S., Stanislaw P., Macroions and Macroion Pairs in the Anionic Polymerization of β-Propiolactone (β-PL), Macromolecules 13 (1980) 229-233.

Stannett, V.T., Koros, W.J., Paul, D.R., Lonsdale, H.K., Baker, R.W., Recent Advances in Membrane Science and Technology, Adv. Polym. Sci. 32 (1979) 69-121.

Sturesson, C., Carlfors, J., Incorporation of protein in PLG-microspheres with retention of bioactivity, J. Control. Rel. 67 (2000) 171-178.

Suzuki, A., Tanaka, T., Phase transition in polymer gels induced by visible light, Nature 346 (1990) 345–347.

Talmadse, J.E., The pharmaceutical and delivery of therapeutic polypeptides and proteins, Advanced drug delivery review 10 (1993) 247-299.

Tokuhiro, T., Amiya, T., Mamada, A., Tanaka, T., NMR study of poly(N-isopropylacrylamide) gels near phase transition, Macromolecules 24 (1991) 2936 – 2943.

Toncheva V, Schacht E, Ng SY, Barr J, Heller J., Use of block copolymers of poly(ortho esters) and poly (ethylene glycol) micellar carriers as potential tumour targeting systems, Drug Target 11 (2003) 345-353.

Torchilin VP. Structure and design of polymeric surfactant-based drug delivery systems, J. Control. Rel. 73 (2001) 137-172.

Uhrich, K.E., Cannizzaro, S.M., Langer, R.S., Shakesheff, K.M., Polymeric systems for controlled drug release, Chem. Rev. 99 (1999) 3181-3198.

Van, A.L., McGuire, T., Langer, R., Small scale systems for in vivo drug delivery, Nature biotechnology 21 (2003) 1185-1191.

Weert, M., Hoechstetter, J., Hennink, W. E., Crommelin, D. J., The effect of a water/organic solvent interface on the structural stability of lysozyme, J. Control. Rel. 68 (2000) 351-359.

Winzenburg, G., Schmidt, C., Fuchs, S., Kissel, T., Biodegradable polymers and their potential use in parenteral veterinary drug delivery systems, Advanced drug delivery reviews 56 (2004) 1453-1466.

Wong, J.Y., Langer, R., Ingber, D.E., Electrically conducting polymers can noninvasively control the shape and growth of mammalian cells, Proceedings of the National Academy of Sciences of the United States of American 91 (1994) 3201-3204.

Wu, X.S, Wang, N., Synthesis, characterization, biodegradation, and drug delivery application of biodegradable lactic/glycolic acid polymers, Part II: biodegradation, J Biomater Sci Polym Ed. 12 (2001) 21-34.

Yang Y.Y., Chia H.H., Chung T.S., Effect of preparation temperature on the characteristics and release profiles of PLGA microspheres containing protein fabricated by double-emulsion solvent extraction/evaporation method, J. Control. Rel. 69 (2000) 81-96.

Yang Y.Y., Shi, M., Goh, S.H., Moochhala, S.M., Ng, S., Heller, J., POE/PLGA composite microspheres: formation and in vitro behavior of double walled microspheres, J. Control. Rel. 88 (2003) 201-13.

Yang Y.Y., Wan J.P., Chung T.S., Pallathadka P.K., Ng S., Heller J., POE-PEG-POE triblock copolymeric microspheres containing protein, I. Preparation and characterization, J. Control. Rel. 75 (2001) 115-28.

Yang, Y. Y., Chung, T. S., Ng, N. P., Morphology, drug distribution, and in vitro release profiles of biodegradable polymeric microspheres containing protein fabricated by double-emulsion solvent extraction/evaporation method, Biomaterials 22 (2001) 231-241.

Yang, Y.Y., Wan, J.P., Chung, T.S., POE-PEG-POE triblock copolymeric microspheres containing protein, I: Preparation and characterization. J. Control. Rel. 75 (2001) 115-128.

Yang, Y.Y., Chung, T.S., Bai, X.L., Chan, W.K., Effect of preparation conditions on morphology and release profiles of biodegradable polymeric microspheres containing protein fabricated by double emulsion method, Chemical Engineering Science 55 (2000) 2223-2236.

Yasugi K., Nagasaki Y., Kato M., Kataoka M., Preparation and characterization of polymer micelles from poly(ethylene glycol)-poly(D,L-lactide) block copolymers as potential drug carrier, J. Control. Rel. 55 (1998) 87-98.

Yeh, M.K., Jenkins, P.G., Davis, S.S., Coombes, A.G.A., Improving the delivery capacity of microparticle systems using blends of poly(DL-lactide-co-glycolide) and poly(ethylene glycol), J. Control. Rel. 37 (1995) 1-9.

Yokoyama, M., Miyauchi, M., Yamada, N., Okano, T., Sakurai, Y., Kataoka, K., Inoue, S., Characterization and anticancer activity of the micelle-forming polymeric anticancer drug adriamycin-conjugated poly(ethylene glycol)-poly(aspartic acid) block copolymer, Cancer Res. 50 (1990) 1693-700.

Yokoyama, M., Okano, T., Targetable drug carriers: present status and a future perspective, Advance drug delivery Reviews 21 (1996) 77-80.

Yoo, H.S., Oh, J.E., Lee, K.H., Park, T.G., Biodegradable nanoparticles containing doxorubicin-PLGA conjugate for sustained release, Pharm Res. 16 (1999) 1114-1118.

Yoo, H.S., Park, T.G. (2004), Folate-receptor-targeted delivery of doxorubicin nano-aggregates stabilized by doxorubicin-PEG-folate conjugate, J. Control. Rel. 100 (2004) 247-256.

Yoo, H.S., Park, T.G., In vitro and in vivo anti-tumor activities of nanoparticles based on doxorubicin-PLGA conjugates, Polymer preparation 41 (2000) 992-993.

Yoo, H.S., Park, T.G., Folate receptor targeted biodegradable polymeric doxorubicin micelles, J. Control. Rel. 96 (2004) 273-283.

Yoshida, R., Sakai, K., Okano, T., Sakurai, Y.J., Modulating the phase transition temperature and thermo-sensitivity in *N*-isopropylacrylamide copolymer gels, J. Biomater. Sci. Polymer Ed. 6 (1994) 585-598.

You H.B., Ick, C.K., Stimuli-Sensitive polymers for modulated drug release, Biorelated polymers and gels: controlled release and application, Academic press, USA (1998) 93-133.

Zhang, L, Eisenberg, A., Multiple morphologies of "crew-out' aggregates of polystyrene-b-poly(acrylic acid) block copolymers, Science 268(1995)1728-1731.

Zhang, X., Jackson, J.K., Burt, H.M., Development of amphiphilic diblock copolymers as micellar carriers of taxol, International Journal of Pharmaceutics 132 (1996) 195-206.

Zhang, X.Z., Yang, Y.Y., Chung, T.S., Ma, K.X., Fabrication and characterization of fast response poly(*N*-isopropylacrylamide) hydrogels, Langmuir 17 (2001) 6094-6099.

APENDICES

LIST OF PAPERS FINISHED DURING PHD STUDY

1. **Liu, S.Q.,** Yang, Y.Y., Tong, Y.W., Preparation and characterization of temperature-sensitive poly(*N*-isopropylacrylamide)-*b*-poly(D.L-lactide) microspheres for protein delivery, Biomacromolecules 4 (2003)1784-1793.

2. Wu, J.Y., **Liu, S.Q.,** Yang, Y.Y., Heng, W.S., Evaluating Proteins Release from, and their Interactions with, Thermosensitive Poly (*N*- isopropylacrylamide) Hydrogels, Journal of Controlled Release 102(2005)361-372.

3. **Liu, S.Q.,** Tong, Y.W., Yang, Y.Y., Incorporation and *in vitro* release of doxorubicin in thermally sensitive micelles with varying compositions, Biomaterials 26(2005)5064-5074.

4. **Liu, S.Q.,** Tong, Y.W., Yang, Y.Y., Thermally sensitive micelles self-assembled from poly(*N*-isopropylacrylamide-*co*-*N,N*-dimethylacrylamide)-*b*-poly(D,L-lactide-*co*-glycolide) for controlled delivery of paclitaxel, Mol. Biosyst. 2(2005)158-165

5. Wei, J.S., Zeng, H.B., **Liu, S.Q.**, Wang, X.G., Tay, E.H., Yang, Y.Y., Temperature-and pH-sensitive core-shell nanoparticles self-assembled from poly(*N*-isopropylacrylamide-*co*-acrylic acid-*co*-cholesteryl acrylate) for intracellular delivery of anticancer drugs, Front Biosci. 10 (2005)3058-3067.

6. **Liu, S.Q.,** Gao, S.J., Tong, Y.W., Yang, Y.Y., pH sensitive Micelles for targeted drug delivery**,** To be submitted to Journal of Controlled Release.